Bulletin of the Geological Survey of Japan, vol, 39 (5), p. 269-365, 1988 551.242/.46/.782 (265.54)

Geological structure of the Japan Sea and its tectonic implications

Kensaku TAMAKI*

TAMAKI, K. (1988) Geological structure of the Japan Sea and its tectonic implications. *Bull. Geol. Surv. Japan,* vol. 39 (5), p. 269-365.

Abstract: Extensive and new marine geological and geophysical data of the Japan Sea have been compiled into geological maps. The tectonic evolution of the Japan Sea has been examined based on observation and interpretation of its geological structure.

The ages of formation of the basins in the Japan Sea are estimated from sediment stratigraphy, basement depth, and heat flow data. They are from 30 to 15 Ma for the Japan Basin, 30 to 10 Ma for the Yamato Basin, and nearly comparable age ranges for the Tartary Trough and the Tsushima Basin.

Topographic highs in the Japan Sea are classified into four groups; continental fragments, rifted continental fragments, tectonic ridges, and volcanic seamounts. Continental fragments are large topographic features and composed of older rocks including those of Precambrian age. Rifted continental fragments are distributed at midwater depth, primarily along the basin margins because of their transitional structures between continental and oceanic crusts. Tectonic ridges exist along the eastern margin of the Japan Sea where they have been elevated by convergence since latest Pliocene. Volcanic seamounts are abundant in the basins.

Two types of back-arc spreading are proposed; a single rift type and multi rift type. The multi rift type best fits the observed structures of the Japan Sea. Large tensional stresses over a broad volcanic zone in the former island arc caused a multi rift system. Some of the rifts developed into multi back-arc spreading systems while others became aborted rifts. The broad volcanic zone of the Japanese island arcs overprinted the activity of back-arc spreading, due to a shallow subduction angle. Arc volcanism during the Japan Sea opening produced a thick accumulation of volcaniclastic sediments and abundant seamounts and knolls within the basins. This multi back-arc spreading system resulted in the fragmentation of the continental crust and isolation of continental fragments within the Japan Sea.

The large tensional stresses necessary for the above evolution are possible only by retreat of the continental plate. The back-arc continental plate of the Japan Sea, the Amurian Block, is postulated to have retreated northward due to the India-Eurasia collision and associated lithospheric deformation in East Asia. The northward movement of the block generated the Stanovoy Range along its northern margin by collision with Siberia and a pull-apart basin of the Baikal Rift along its western margin.

The Okushiri and Sado Ridges along the eastern margin of the Japan Sea are bounded by thrust faults on either or both sides. These thrust faults have

*Marine Geology Department (presently at Ocean Research Institute, University of Tokyo)

been active since latest Pliocene time. The ridges are formed by thrust movements associated with the uplift of the edge of the hanging side over the footwall. Lithospheric convergence is evident along these thrust zones on the basis of the occurrence of thrust faults and their corresponding earthquakes. The convergent stress is again inferred to be due to the India–Eurasia collision and associated intra-plate or inter microplate movements in East Asia. The eastward movement of the Amurian Plate have caused Baikal extension along its western margin and Japan Sea convergence along its eastern margin.

The tectonic evolution of the Japan Sea is summarized in two significant tectonic stages.

1) Divergent tectonics over the Japanese island arcs caused back-arc spreading of the Japan Sea from 30 to 10 Ma. The spreading system was initiated from a multi rift system within a broad arc volcanic zone. Through the development of the spreading system, many continental fragments are left within the basins. Overprinting of arc volcanism on the back-arc basin resulted in an abundance of volcanic seamounts and a thick accumulation of volcaniclastics in the basins.

2) Lithospheric convergence along the eastern margin of the Japan Sea since latest Pliocene time produced the uplifted and thrust faulted Okushiri and Sado Ridges.

1. Introduction

Most of the island arcs in the Western Pacific are associated with marginal seas or back-arc basins. The Japan Sea is one of the back-arc basins of the Western Pacific. Present geometry shows that the Japan Sea is situated between the Eurasia Continent and the islands of Sakhalin, Hokkaido, Honshu, and others.

The back-arc basins of the Western Pacific have been studied intensively since the 1960's, and, in particular, results of the Deep Sea Drilling Project and the identification of geomagnetic anomaly lineations have presented effective constraints for the age determination of the back-arc basins such as the Shikoku Basin, the Parece Vela Basin, the West Philippine Basin, and the South China Sea. The age of the Japan Sea, together with the Kuril Basin, however, is still enigma and controversial. It is because four deep sea drilling sites in the Japan Sea could not reached the basement (KARIG, INGLE *et al.*, 1973) and the magnetic anomaly lineations of the Japan Sea are weak and complicated (ISEZAKI and UYEDA, 1973).

The tectonic evolution of the Japan Sea has a close relation to the tectonics of the Japanese Islands, and its ambiguity has caused divergent models of tectonic evolution of the Japanese Islands and adjacent areas. Although it is still difficult to constrain the age of the Japan Sea from the data presently available, a better understanding of the geology and tectonics of the Japan Sea is indispensable for the study of the geological evolution of the Japanese Islands and the Western Pacific.

In this paper, the author presents new and extensive marine geological and geophysical data of the Japan Sea and discuss its geological structure and tectonics. The substantial improvement of this paper over previous works is the stratigraphic correlation of the sedimentary sequence of the Japan Sea on the basis of the synthetic analyses of seismic profiles and age estimated from bottom sampling data. The stratigraphic constraints deduced are used effectively, in

this paper, for the discussion of the tectonic evolution of the Japan Sea.

1.1 Bathymetry of the Japan Sea

The Japan Sea shows a depressional topographic feature (Fig. 1 and 2). A 200 m contour line surrounding the Japan Sea shows the closed depressional feature of the Japan Sea. The Japan Sea is characterized by a complicated sea floor topography with many topographic expressions of ridges, rises, banks, and seamounts. It makes the Japan Sea the most topographically complicated marginal basin of the world.

Physiographic nomenclatures adopted in this paper are basically those of LUDWIG *et al.* (1975) and GNIBIDENKO (1979). The author, however, used tentative nomenclature in some cases such as the Ullung Plateau and the Tsushima Deep Sea Channel.

There are four major topographic depressions and two major topographic highs in the Japan Sea. The four depressions are the Japan Basin, the Yamato Basin, the Tsushima Basin, and the Tartary Trough. The two largest highs are the Yamato Rise in the center of the Japan Sea and the Korea Plateau in the western part of the Japan Sea. Many other topographic highs and depressions are distributed in the Japan Sea.

In the southwestern Japan Sea, the topography is rather complicated with many topographic highs and depressions. The topographic highs are the Yamato Rise, the Korea Plateau, the Ullung Plateau, the Kita-Oki Bank, the Oki Bank, and the Oki Ridge. Several basins and troughs are developed among the topographic highs. They are the Yamato Basin, the Tsushima Basin, the Genzan Trough, and the Oki Trough.

Physiographic contrasts between the continental slope along the Eurasia Continent and that along the eastern margin of the Japan Sea are remarkable ; that is, the former is very simple and generally smooth without ruggedness, while the latter is very complicated with many ridges and troughs trending north-south. The ridges along the eastern margin of the Japan Sea are the Okushiri Ridge and the Sado Ridge. Many troughs are distributed in the area east of the Okushiri and Sado Ridges. Some of them are, from the north, the Shiribeshi Trough, the Okushiri Trough, the Nishitsugaru Trough, and the Mogami Trough. The Musashi Bank and the Oshima Plateau also lie along the eastern margin of the Japan Sea. This topographic contrast between the eastern and western margins of the Japan Sea suggests neotectonic deformation along the eastern margin, which will be discussed later in detail.

Japan Basin

The Japan Basin is the largest depression in the Japan Sea. It is located in the central part of the Japan Sea and trends ENE. The width of the Japan Basin is 200 to 300 km and its length is about 700 km. The eastern half of the basin is the deepest part of the Japan Sea. The water depth of the basin ranges from 3500 to 3700 m. The greatest water depth of the Japan Sea is 3742 m and is observed in the easternmost area. The Japan Basin is for the most part characterized by a smooth and flat sea floor which forms the abyssal plain due to the deposition of distal turbidites.

Several large deep sea channels and canyons flow into the abyssal plain. They are the Toyama Deep Sea Channel from Honshu, the Tsushima Deep Sea Channel from the Tsushima Strait

("Tsushima Deep Sea Channel" is tentative naming in this text), the Genzan Canyon from the Korea Peninsula, and the Tartary Trough from Sikhote-Alin. Several smaller Channels are observed on the continental slopes off Sikhote-Alin and Japanese Islands. One of them is the Mogami Channel off northeast Honshu. The Japan Basin is the present depositional center of the Japan Sea.

There are several seamounts in the Japan Basin. The larger ones are named but smaller ones are unnamed. The largest one among them is the Siberia Seamount off Nakhodka of Sikhote-Alin. The seamount is about 2000 m high above the surrounding basin floor. The next largest seamount is the Vityaz Seamount which is located just on the boundary between the Japan Basin and the Tartary Trough. The seamount is 2000 m high above the basin floor and higher than the Siberia Seamount.

The other large seamounts in the Japan Basin are the Bogorov Seamount and the Gabass Seamounts. The Bogorov Seamount is isolated in the eastern Japan Basin. The Seamount, 2300 m high above the basin floor, is elongated and trends north-south with a length of 70 km and a width of 20 km. The Gabass Seamount is located in the southwestern part of the Japan Basin. The Seamount is about 1500 m high above the basin floor. Several other unnamed seamounts are observed in the Japan Basin. A seamount north of the Oki Bank is prominent among them.

Yamato Basin

The Yamato Basin is developed in the southern part of the Japan Sea, and extends from off the Shimane Peninsula to off Oga Peninsula of Honshu. The Basin trends northeasterly. Its width is 200 to 100 km. The Yamato Basin has two separated abyssal plains with a flat and smooth sea floor. The water depth of the deeper abyssal plain in the west central part of the basin is about 3000 m, which is about 500 m less than that of the abyssal plain of the Japan Basin. The shallower abyssal plain lies at a depth of about 2700 m and is in the eastern part of the Yamato Basin. The northeastern part of the Yamato Basin is shallower than the central part of the Basin, showing a water depth of 2500 m and is characterized by the presence of the meandering Toyama Deep Sea Channel. The channel comes from the Toyama Canyon in the Toyama Trough, runs across the northeastern part of the Yamato Basin, and extends into the Japan Basin.

A seamount chain with a ENE-WSW trend is located near the axis of the Yamato Basin. The author tentatively calls it "Yamato seamount chain". The largest seamount in it is the Yamato Seamount which is located in the western part. The Seamount is about 2000 m high above the basin floor. The Matsu Seamount with a height of about 1000 m is in the eastern end of the chain.

Tartary Trough

The Tartary Trough, the second largest basin in the Japan Sea, appears as a north-northeasterly elongated depression between Sikhote-Alin and the Sakhalin-Hokkaido Islands. The water depth of the Tartary Trough is generally shallower than those of the other three major basins. The trough bottom deepens from north to south and attains a maximum depth of 3500 m at the junction with the Japan Sea. The Tartary Canyon is developed along the axis of the Trough, as a discontinuous feature.

Figure 2 3-D topographic map of the whole Japan Sea. The data used for processing are GEBCO digital bathymetric data of JOCD and GSJ digital bathymetric data. Processing system is SIGMA of Geological Survey of Japan.

Tsushima Basin

The Tsushima Basin situated on the southwestern corner of the Japan Sea is the smallest of the four major basins. The dimension of the basin is 200 km EW × 150 km NS. The basin floor deepens to the north, from 1000 m to 2300 m. The basin opens northeastwards and joins to the Japan Basin through a passage between the Oki Bank and the Ullung Plateau. The Tsushima Deep Sea Channel is developed at the axis of this passage.

Four seamounts are arranged in a WNW trend at the northern part of the Tsushima Basin. Two of them are elevated above sea level with a height greater than 2000 m above the sea floor and make Ullung Island and Takeshima Island.

1.2 Previous works

Numerous studies on the marine geology and geophysics of the Japan Sea have been previously done. Most of them have been made by Russian and Japanese scientists. Several works have been done by American scientists. The studies can be largely divided into three categories : geological structure, bottom sampling, and geophysics.

Geological structure

Synthetic works on the marine geological structure of the entire Japan Sea were done by HILDE and WAGEMAN (1973) and LUDWIG *et al.* (1975). HILDE and WAGEMAN carried out regional seismic reflection surveys of the Japan Sea for the first time and presented an outline of the geological structure. They suggested rifting and spreading as the origin of the Japan Sea. They proposed two spreading stages of the Japan Sea ; the first stage is spreading of the Japan Basin and the Tsushima Basin during Mesozoic or early Tertiary time and the second stage is spreading of the Yamato basin during about Early Miocene time. Their discussion on the age, however, as they have mentioned, is ambiguous due to the lack of data on age assignment of the marine sediments and rocks. They pointed out that the sediments of the Japan Basin thicken from west to east and that there is rough, uneven basement along western margin which they supposed to be a fossil spreading center.

LUDWIG *et al.* (1975) presented high quality seismic reflection data and sono-buoy refraction record. They studied the crustal structure of the Japan Basin, the Yamato Basin, and the Yamato Rise on the basis of sixty-five sono-buoy refraction/reflection records and extensive seismic reflection coverage. They concluded that the Japan Basin and the Yamato Basin are underlain by oceanic crusts. It was emphasized that the smooth basement of the Japan Basin and the Yamato Basin has a 3.5 km/sec refraction velocity and that this velocity is unique to the Japan Sea.

Two other synthetic works were done by MELANKHOLINA and KOVYLIN (1977) and GNIBIDENKO (1979), although they have not presented the original results of their survey cruises. Melankholina and Kovylin compiled a simple tectonic province map of the Japan Sea. Similar works have been done by other Russian scientists (e.g., BERSENEV and LELIKOV, 1979 ; MARKOV *et al.*, 1979 ; IVANOV *et al.*, 1981). GNIBIDENKO (1979) made a detailed sediment isopach map of the entire Japan Sea, although the original data were not presented. Most of the Russian scientists do not agree with the sea floor spreading origin of the Japan Sea, but consider that the oceanization of the continental crust generated the oceanic crust of the Japan Sea. The ages of the oceanic crust estimated by them are

rather old; e.g., Paleozoic (MELANKHOLINA and KOVYLIN, 1977), Early Mesozoic (GNIBIDENKO, 1979), etc. KOBAYASHI (1985) also discussed the general geological and geophysical aspect of the Japan Sea.

Many works on the geological structures of local areas of the Japan Sea by seismic methods have been done by Japanese scientists. HOTTA (1967) carried out the first seismic reflection survey of the Japan Sea at the Yamato Basin and the Sado Ridge. MURAUCHI *et al.* (1970) and HOTTA (1971), successively, presented seismic profiles of the Oki Bank and the Tsushima Basin, and the Okushiri Ridge and the Musashi Bank, respectively. Although the seismic penetration of these profiles was weak, the distribution of the sedimentary layer in the eastern and southern margins of the Japan Sea was studied preceding the work of HILDE and WAGEMAN (1973). Many detailed seismic profiling surveys at the continental shelves and slopes along the Japanese Islands have been carried out by the Hydrographic Department of Japan in the 1970's (SATO, 1971; SAKURAI and SATO, 1971; SAKURAI *et al.*, 1971; SAKURAI *et al.*, 1972; SATO *et al.*, 1973; KATSURA and KITAHARA, 1977; TOZAKI *et al.*, 1978). These surveys presented detailed data on the topography and geological structure of the slopes along the Japanese Islands. INOUE (1982) discussed the marine geological structure of the southwestern corner of the Japan Sea on the basis of the synthetic study of land and marine geology.

The recent works of several Japanese oil companies are outstanding. Although the studied areas are restricted to the continental shelf along the Japanese Islands, their high quality and deep penetration of seismic profiles, together with boring data for oil prospecting, have presented important stratigraphic information (MINAMI, 1979; TANAKA, 1979; SUZUKI, 1979; TANAKA and OGUSA, 1981).

The Geological Survey of Japan carried out extensive marine geological surveys in the late 1970's which include seismic profiling, Sono-buoy refraction measurements, bottom sampling, geomagnetic measurements, and gravity measurements (HONZA ed., 1978ab; HONZA ed., 1979). The work of this paper is based mainly on the data obtained by these surveys. The surveyed area covers most of the Japan Sea excluding the area along the coast of Sikhote-Alin. The data have been compiled into three marine geological maps (HONZA *et al.*, 1979; TAMAKI *et al.*, 1979a; TAMAKI *et al.*, 1981a), which have revealed the detailed marine geology of the Japan Sea for the first time.

Bottom sampling

Many bottom sampling surveys by dredge hauls have been done during this half of the century mainly by Japanese and Russian scientists. In the early stages of investigation the data were concentrated on the Yamato Rise, the Kita-Oki Bank, and the Oki Ridge (TSUYA, 1932; NIINO, 1933, 1935, and 1942; SATO and ONO, 1964; HOSHINO and HONMA, 1966). IWABUCHI (1968) presented detailed bottom sampling data on the Sado Ridge, the Yamato Rise, and their surrounding areas.

The Geological Survey of Japan carried out extensive bottom sampling surveys by dredge and coring methods (HONZA ed., 1978ab; HONZA ed., 1979). Bottom sampling by piston and gravity cores was carried out for stratigraphic correlation of seismic profile data. KOIZUMI (1979) presented age data for the numerous bottom sediment samples including the data of the Geological Survey of Japan on the basis of diatom

assemblage. The assigned ages by Koizumi have presented an important information for the stratigraphic correlation of seismic profiles in this paper.

Other important data on bottom sampling are the results of the Deep Sea Drilling Projects (KARIG, INGLE *et al.*, 1975). Four sites were drilled in the Japan Sea during the Glomar Challenger cruise Leg 31. Site 299 is in the northeastern part of the Yamato Basin, Sites 300 and 301 are in the Japan Basin north of the Yamato Rise, and Site 302 is on the eastern margin of the Yamato Rise. Sites 299, 300 and 301 did not reach the basement rocks. Sites 299 and 301, however, penetrated half to one third of the sedimentary layer and have presented important data for the stratigraphy of the basin sediments.

Thirty-five radiometric age determinations of the sampled rocks by the K-Ar and Rb-Sr methods have been done by Japanese and Russian scientists (SHIMAZU, 1968; UENO *et al.*, 1971; OZIMA *et al.*, 1972; LELIKOV and BERSENEV, 1973; SAHNO and VASILIEV, 1974; VASILIEV, 1975; YUASA *et al.*, 1978; HONZA ed., 1978 a; GNIBIDENKO, 1979). The age-determined rocks are volcanic, intrusive, and metamorphic rocks sampled from the Yamato Rise, the Kita-Oki Bank, the Korea Plateau, the Ullung Plateau, the Musashi Bank, the Bogorov Seamount, the Gabass Seamount, and a few seamounts in the Yamato Basin. The data are referred to in detail in this paper.

Geophysics

There have been many works on the geophysical surveys of the Japan Sea in terms of geomagnetics, gravity, heat flow, crustal study, and earthquake research.

Geomagnetic anomaly lineations are important for the age assignment of back-arc basins. ISEZAKI and UYEDA (1973) suggested the presence of weak magnetic anomaly lineations trending N 60°E in the Japan Sea, although they could not identify the age of the lineations due to weak amplitudes less than 300 nT p-p and the lack of pronounced linearity. ISEZAKI (1975) postulated two spreading centers on the basis of the correlation of the magnetic anomaly peaks; one is in the Japan Basin and the other is along eastern half of the Yamato Basin. ISEZAKI (1979) further suggested that the age of a fossil spreading center of the Japan Basin might be 30.6 Ma with great ambiguity. Thus, the results strongly suggest the sea floor spreading origin of the Japan Sea. The age of the spreading, however, is still controversial.

Gravity data in the Japan Sea was compiled by STROYEV (1971), TOMODA (1973), TOMODA and FUJIMOTO (1981), and ISHIHARA (1983). The Japan Sea is considered to be isostatically compensated.

Heat flow measurements of the Japan Sea have been done actively from the 1960's (YASUI *et al.* 1967; UYEDA and VAQUIER, 1968; YOSHII, 1972). The heat flow of the Japan Sea is remarkably high compared to that of the Western Pacific Basin. The average heat flow of the Japan Basin is 2.23 ± 0.52 HFU (YASUI *et al,* 1967) and that of the Yamato Basin is 2.5 HFU. The high heat flow of the Japan Sea has been discussed by many authors (e.g., KOBAYASHI and NOMURA, 1972; KONO and AMANO, 1977).

Extensive crustal studies of the Japan Sea by seismic refraction methods have been done by many Russian scientists (e.g., TUEZOV, 1969; BIKKENIA *et al.*, 1968; TUEZOV, 1971; RODNIKOV and KHAIN, 1971). The results have shown that the Japan Basin does not have a granitic

layer and that the Yamato Basin has a thin granitic layer. MURAUCHI (1972), however, suggested that both the Japan Basin and the Yamato Basin have oceanic crust and that the crust of the Yamato Basin is thicker than that of the Japan Basin, The Tsushima Basin also appears to have oceanic crust according to LUDWIG *et al.* (1975). BERSENEV *et al.* (1970) postulated that suboceanic crust lies beneath the axis of the Tartary Trough. Then, four major basins and troughs of the Japan Sea are inferred to be underlain by oceanic to suboceanic crust.

Distribution and focal mechanisms of the earthquakes present critical imformation for recent tectonics. FUKAO and FURUMOTO (1975) investigated source mechanisms of large earthquakes along the eastern margin of the Japan Sea and suggested that the lithosphere of the Japan Sea is detached from the northern Japan Arc by large reverse faults. This suggestion is important for the neotectonics of the Japan Sea. The

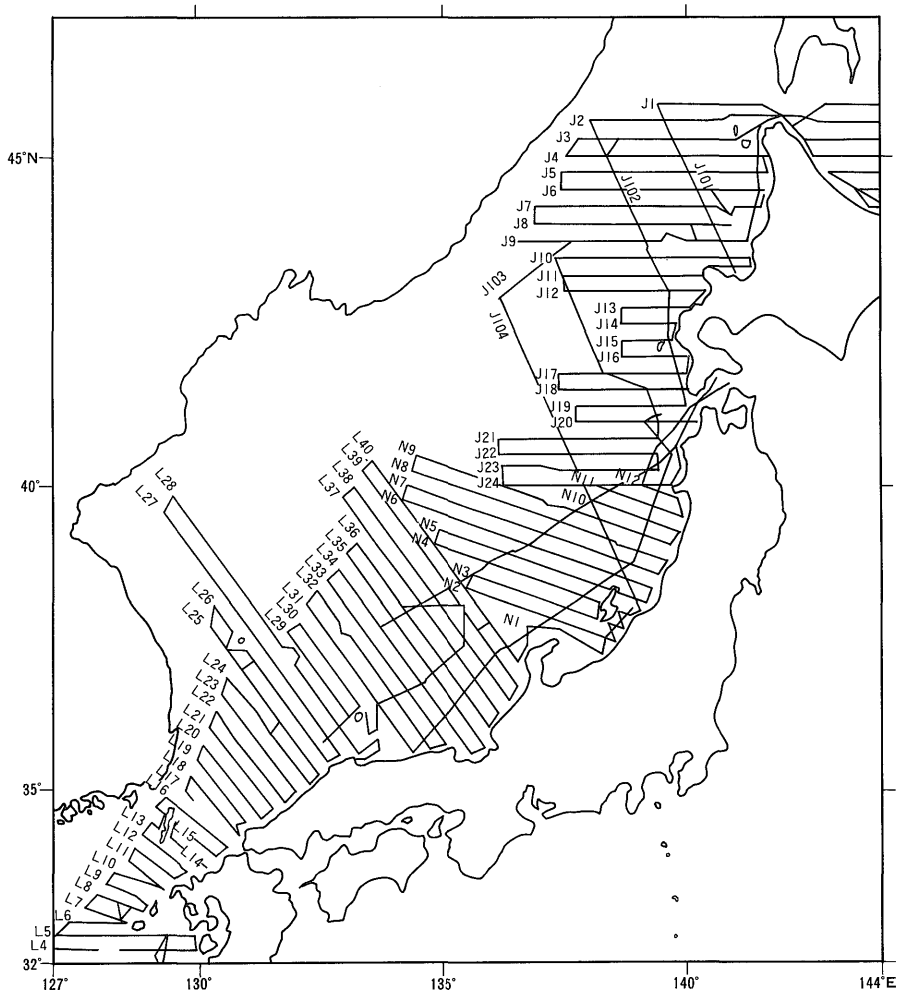

Figure 3 Ship's track chart with line numbers of GH 77-2, GH 77-3, GH 78-2 and GH 78-3 cruises.

thickness of the lithosphere of the Japan Sea was estimated to be 30 km by surface wave analyses of earthquakes (ABE and KANAMORI, 1970).

1.3 Data used in this study

The data used in this paper obtained by the Geological Survey of Japan during four research cruise from 1977 to 1978. The four research cruises are GH 77-2, GH 77-3, GH 78-2, and GH 78-3 cruises of R/V Hakurei-maru. The cruises were the first systematic marine geological and geophysical surveys of the Japan Sea. The surveys consist of seismic profiling, sono-buoy refraction measurements, geomagnetic measurements, gravity measurements, and bottom sampling.

Track lines for geophysical surveys are shown in Figure 3. The intervals of the traverse lines are every 15 nautical miles. The ship speed during the survery was maintained at 10 knots. Position fixing of the ship was done every 30 minutes by a combination of satellite navigation (NNSS) and Loran C. Along these tracks, seismic profiling data, geomagnetic data, and gravity data were obtained. Three sono-buoy refraction measurements were carried out in the Tsushima Basin, the Mogami Trough, and the Tartary Trough.

The apparatus for bottom sampling are the dredge, gravity corer (core length : 2 m), and piston corer (core length : 8 m). The dredge was used for recovering rocks from the outcrops at the sea floor, the gravity corer for consolidated sediments, and the piston corer for soft sediments. The gravity corer was effective for recovering consolidated sediments underlain by superficial soft sediments less than 2 m in thickness. The ages of the sedimentary rocks and the consolidated sediments were determined by the analyses of diatom assemblages (KOIZUMI, 1979) and pollen assemblages (HONZA ed., 1979). The age assignment data presented important constraints for the submarine stratigraphic correlations.

Outlines of these surveys were presented in three cruise reports (HONZA ed., 1978 ab ; HONZA ed., 1979). Synthetic studies of seismic profiles and bottom sampling data were summarized into three marine geological maps of the Geological Survey of Japan, Marine Geology Map Series (HONZA *et al.*, 1979 ; TAMAKI *et al.*, 1979 a ; TAMAKI *et al.*, 1981 a).

2. Description of Geological Structure of the Japan Sea

2.1 Condition of seismic profiling

Seismic reflection profiles are fundamental data source in this study. Seismic profiles, which present visual subbottom sections, are most important for the study of marine geological structures. Seismic profiling data used in this study were obtained by the continuous seismic reflection survey method. Airguns were used as the sound source. The equipment and conditions during the research cruises GH 77-2, GH 77-3, GH 78-2, and GH 78-3 are listed in Table 1. The seismic recording system achieves high sensitivity (high signal to noise ratio) by using hydrostreamers which are manufactured on board during the survey. The high sensitivity of hydrostreamer was maintained by disassembling hydrostreamer and replacing the hydrophone elements frequently. A seismic profiling system of high sensitivity makes it possible to conduct a high speed survey (10-12 knots) without suppressing quality of the record. The towing system of airgun sound sources is specially design-

Table 1 Equipments and conditions of seismic reflection survey during GH 77-2, GH 77-3, GH 78-2, and GH 78-3 cruises.

1)	Equipment	
	Air Gun	Bolt Par Air Gun 1900 B×2
	Compressor	Norwalk APS-120 (120 S.C.F.M.)
	Receiver	Hydrostreamer GSJ-4 II-78 (with 78 elements of Geo Space MP 18-200)
	Amplifier	Geo Space 111 Amplifier
	Recorder	Raytheon UGR-196 B
2)	Condition	
	Total volume of air gun	270 to 300 in^3 (4425 to 4916 cm^3)
	Pressure	1500 p.s.i. (105 kg/cm^3)
	Shot interval	10 sec.
	AGC of amplifier	off
	Filter range	16 to 98 Hz
	Record range	4 sec.
	Ship speed	10 knots
	Hydrostreamer	towed 150 m behind the ship

ed for high speed surveys. The high speed seismic profiling method improved efficiency in the survey and made it possible to gather much more data in a limited amount of time.

The profiles obtained by the seismic reflection method are displayed with a vertical scale of two-way acoustic travel time in seconds. Two-way acoustic travel time in seconds is used for the discussions of sediment thickness and basement depth on the profiles in this paper. The vertical exaggeration of the seismic profiles is about 20 due to the seismic recording system.

2.2 Outline of the geological structure

There are several sedimentary basins and many topographic highs in the Japan Sea. The geology of these basins and topographic highs is closely related to the tectonics of the Japan Sea. The understanding of these basins and highs is fundamental for the discussion of the tectonics of the Japan Sea. In this section, the author introduces the overall view of the geological structure of the Japan Sea which includes these basins and topographic highs. In the next section the author describes the detail of each basin and topographic high. The overall view of the Japan Sea is described with some typical seimic sections, compiled geological maps, sediment isopach maps, and basement isodepth map as below.

Typical seismic profiles of the Japan Sea

About 70 seismic reflection transects were obtained by GH 77-2, GH 77-3, GH 78-2 and GH 78-3 cruises. Twelve typical seismic profiles with interpretative line drawings are shown in Figures 4 to 15. These seismic profiles show the general structural view of the Japan Sea from the south to the north.

Figures 4 and 5 show the structure of the Tsushima Basin and the continental shelf off San-in. The acoustic basement of the Tsushima Basin cannot be detected by the single channel seismic reflection system because of the thick and highly reflective sediments of the basin. The sediment thickness of the basin is great-

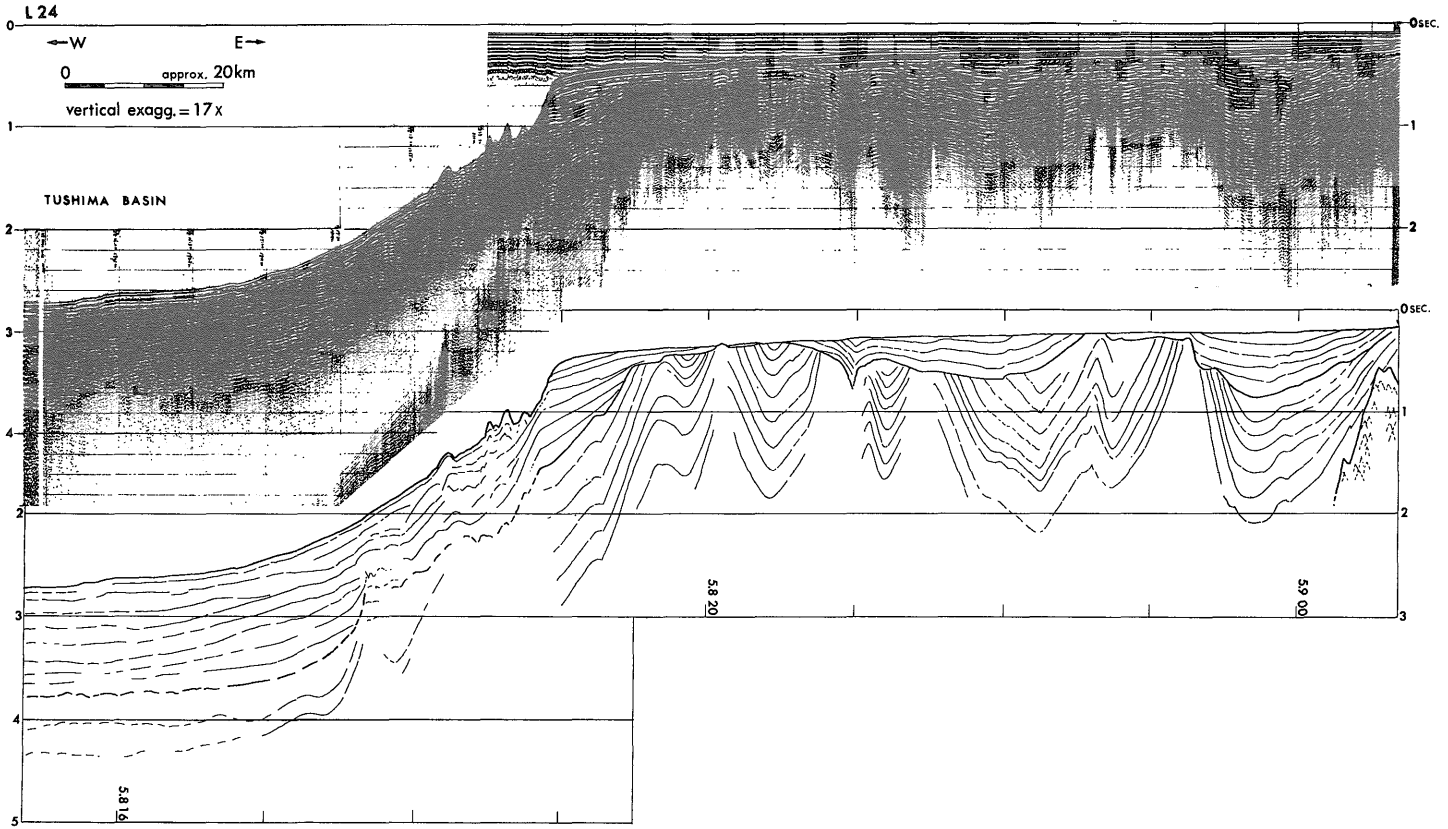

Figure 4 Seismic reflection profile and interpretation of Line L 24.

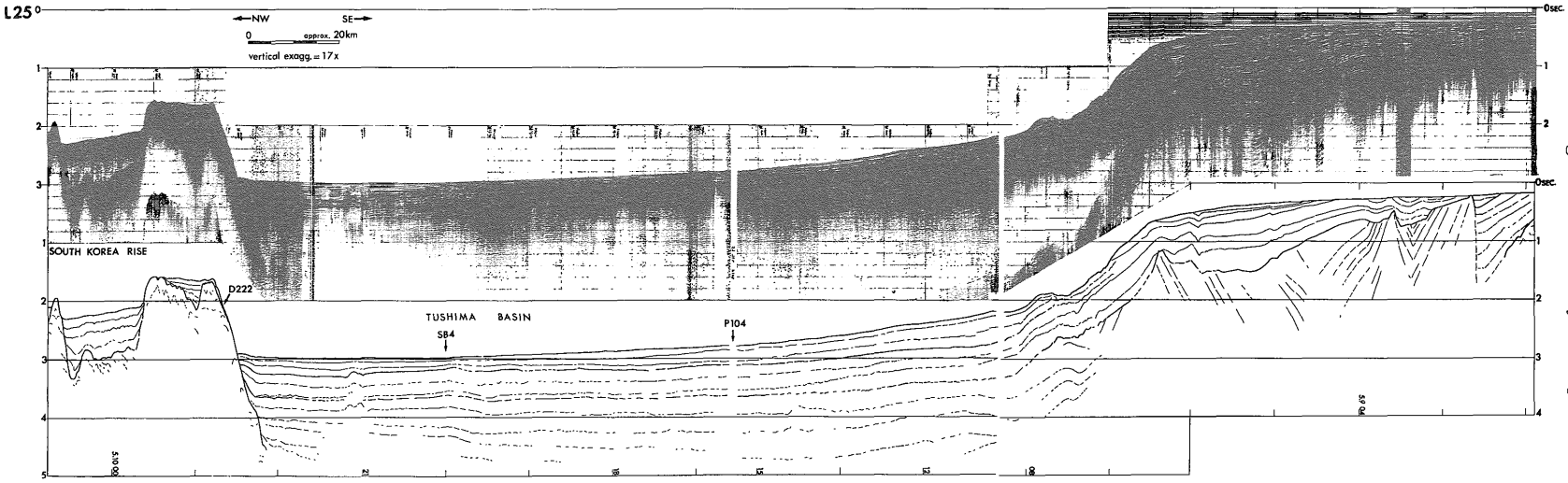

Figure 5 Seismic reflection profile and interpretation of Line L 25.

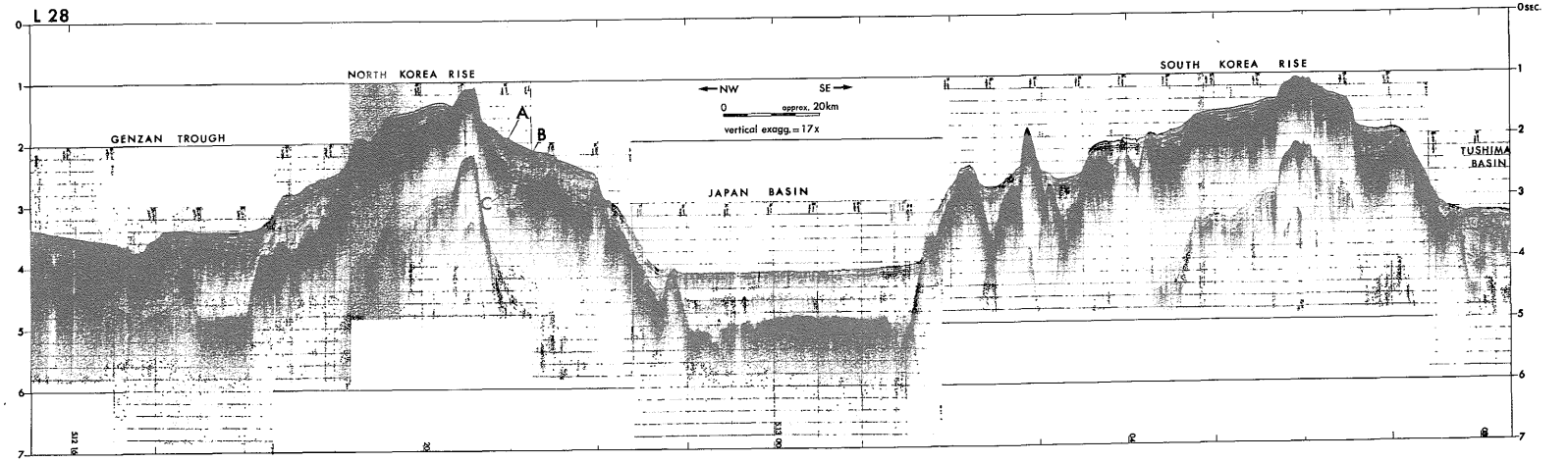

Figure 6 Seismic reflection profile and interpretation of Line L 28.

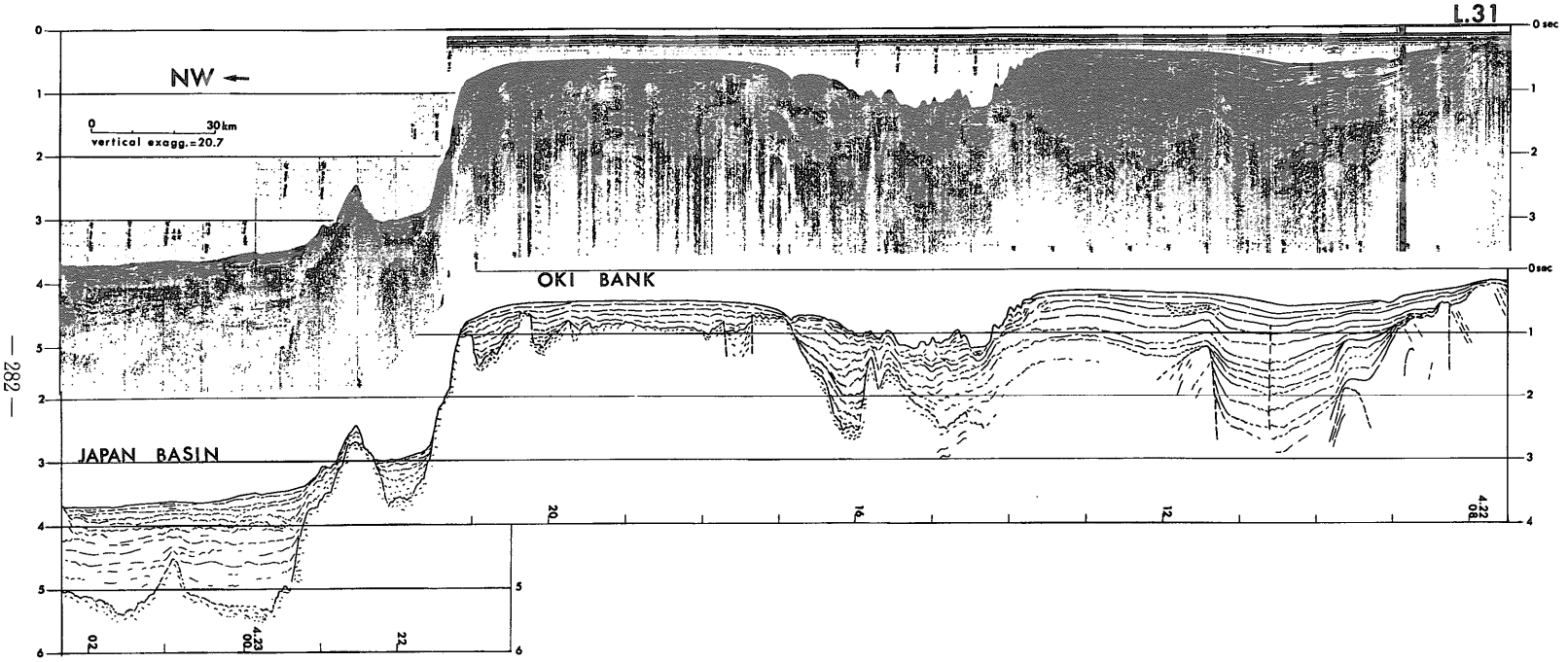

Figure 7 Seismic reflection profile and interpretation of Line L 31.

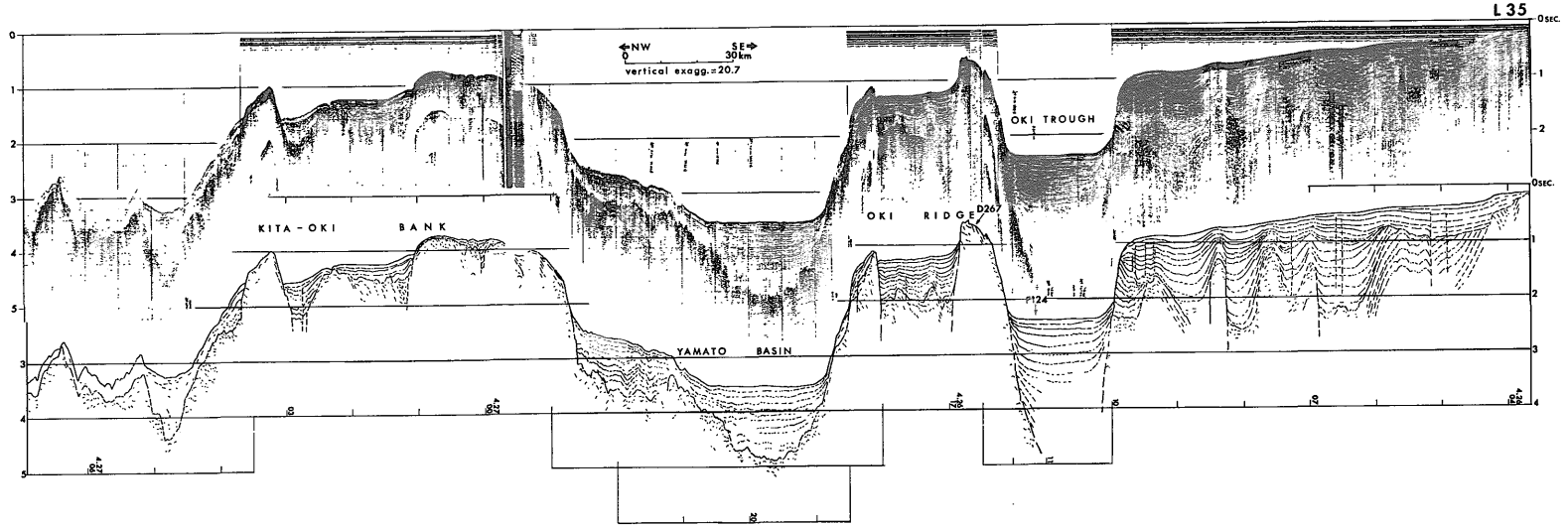

Figure 8 Seismic reflection profile and interpretation of Line L 35.

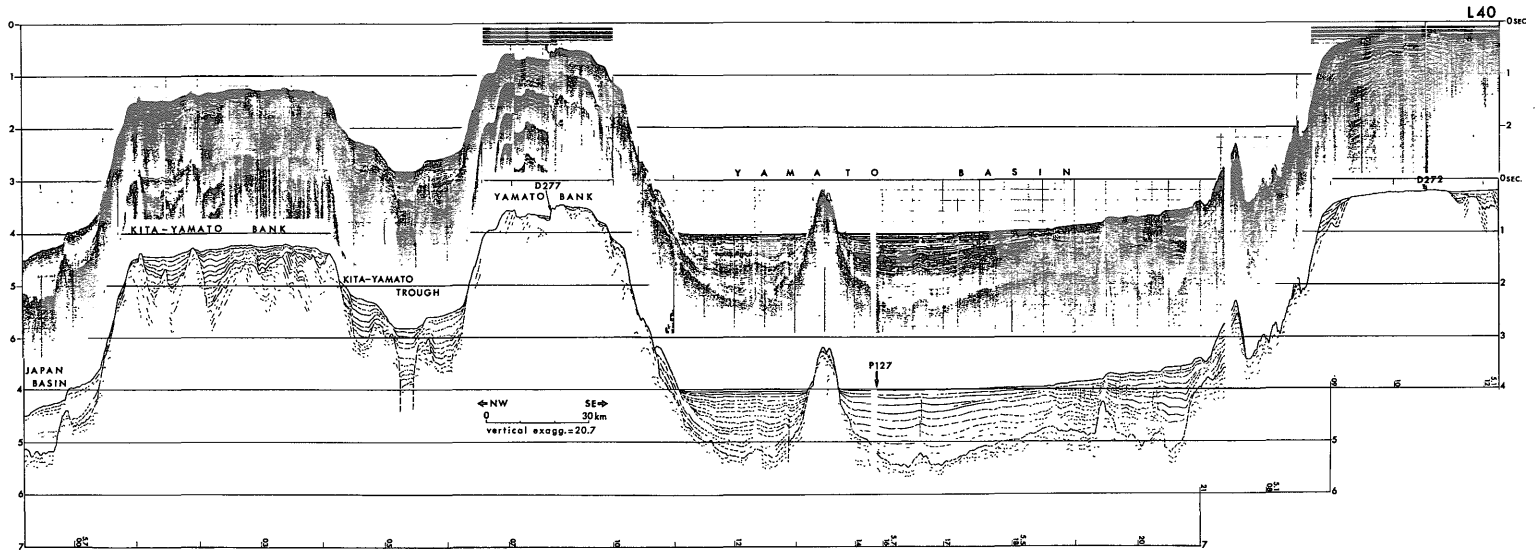

Figure 9 Seismic reflection profile and interpretation of Line L 40.

er than 2.0 seconds. A remarkable unconformity is observed in the sedimentary sequence of the continental shelf off San-in.

Figure 6 shows the transect of the South Korea Rise (the Ullung Rise), the southwestern end of the Japan Basin, the North Korea Rise, and the Genzan Trough. High reflectivity of the sediments in the Genzan Trough is prominent in association with the development of the Genzan Canyon. Both Korea Rises have rough topography on the basement with sediment drape of thickness less than 0.5 second.

Figure 7 shows the profile of the Oki Bank. The profile suggests that the Oki Bank consists of an isolated basement high with a thin sedimentary cover. The sedimentary cover makes the bank appear to be continuous to the continental shelf topographically.

Figures 8, 9, and 10 show the profile of the Yamato Basin, the Yamato Rise, and other topographic highs. Sediments with the thickness of 1.5 seconds are observed in the Yamato Basin. They are divided into upper and lower parts. The upper part is acoustically stratified and the lower part is acoustically transparent. The Oki Ridge, the Kita-Oki Ridge, the Yamato Rise, and the Takuyo Bank are covered by a rather thin layer of sediments with a thickness of less than 0.5 seconds. The Yamato Bank is free of sediments on the summit. A typical profile of the Toyama Deep Sea Channel is shown in Figure 10. The Sado Ridge and the Takuyo Bank are characterized by a blocked basements (Fig. 10). The blocked feature of the basements should be closely related to the origin of the both topographic highs. Smaller basins such as the Mogami Trough are developed along the eastern margin of the Japan Sea (Fig. 10).

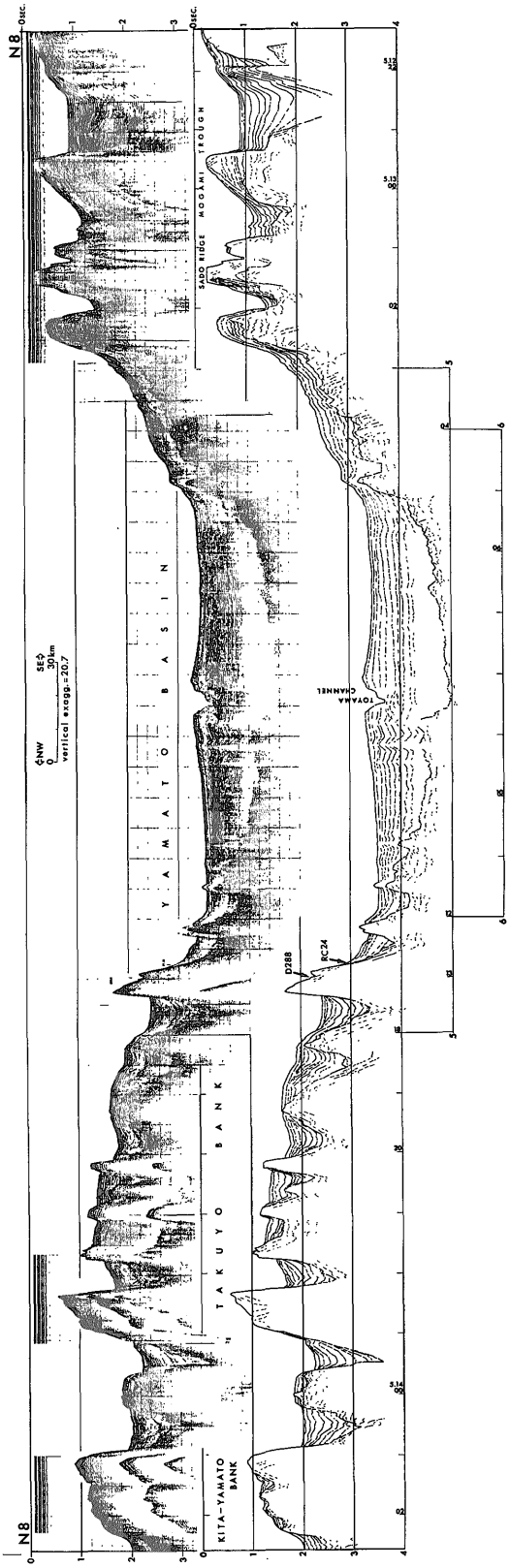

Figure 10 Seismic reflection profile and interpretation of Line N 8.

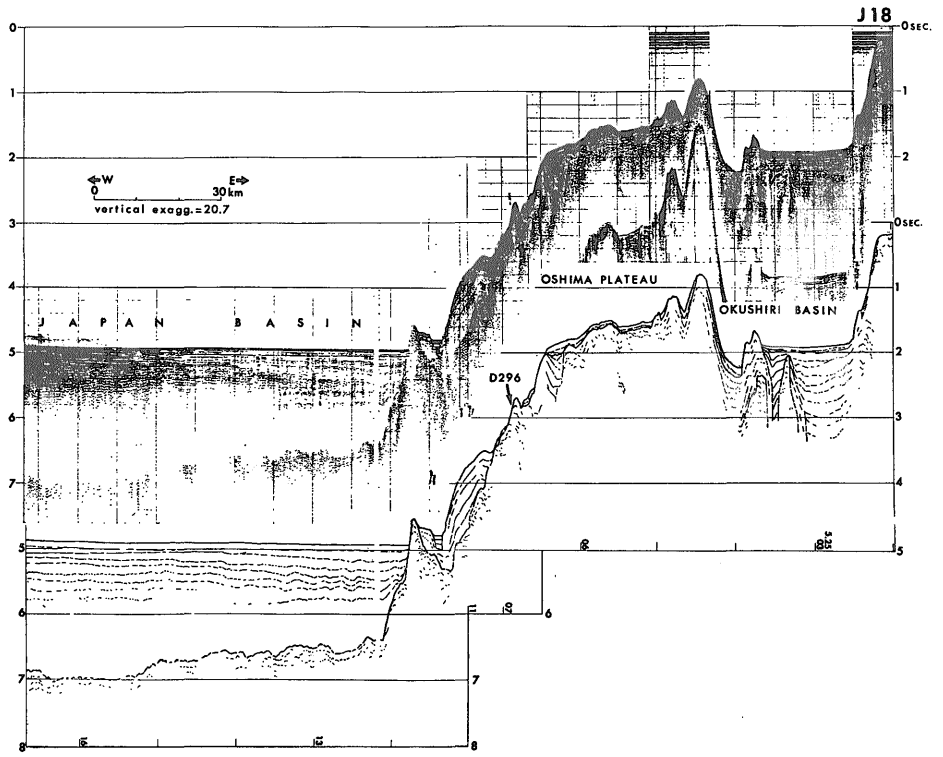

Figure 11 Seismic reflection profile and interpretation of Line J 18.

Figures 11 and 12 show the eastern margin of the Japan Basin. The sediment thickness of the Japan Basin is much thicker than that of the Yamato Basin, The thickness exceeds 2.0 seconds on Line J 18 (Fig. 11). The sediments of the Japan Basin are also acoustically stratified in its upper part and transparent in its lower part as is in the Yamato Basin and other basins. The basement depth of the Japan Basin decreases landward as shown in Line J 10 (Fig.12). The continental slope on Line J 10 north of Okushiri Island shows complicated topography. The complicated topography is the general feature of the eastern margin of the Japan Sea.

Figures 13, 14, and 15 show the transects of the northern part of the Japan Basin. The Tartary Trough along the Sikhote-Alin coast also has a thick layer of sediments which exceeds 2.0 seconds on Line J 2 (Fig. 15). In the southern part of the trough, the basement is blocked and the sea bottom is rough due to the development of the Tartary Canyon on Lines J 6 and J 8 (Figs. 13 and 14). The sediments of the Tartary Trough also show stratification in the upper part and transparency in the lower part. The northern end of the Japan Basin is observed on Line J 8. The sediments in the northern Japan Basin is acoustically more transparent and thinner, with the thickness of about 1 second, compared to the southern main part of the Japan Basin. Two topographic highs, the Vityaz Rise and the Okushiri Ridge, are observed on both sides of the Japan Basin on Line J 8. The Vityaz Rise is free of sediments on its summit, but the Okushiri Ridge is covered by sediments with a

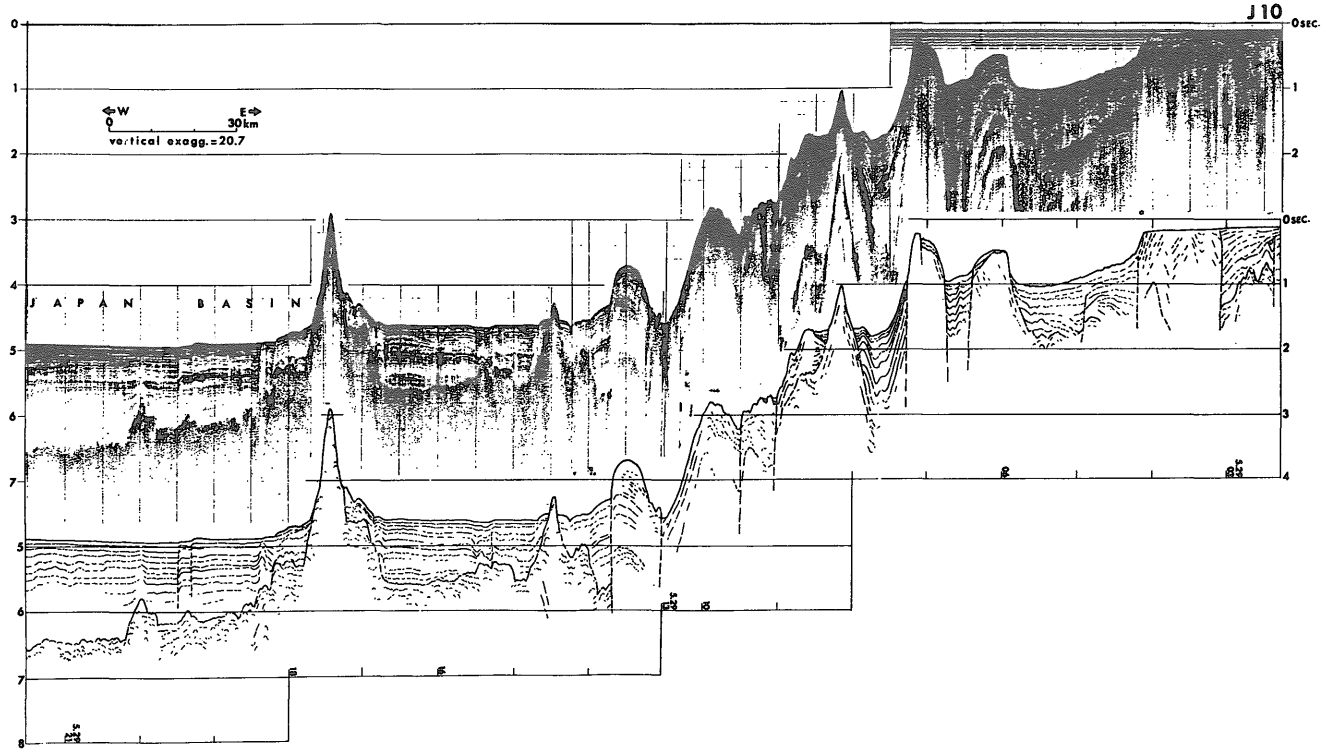

Figure 12 Seismic reflection profile and interpretation of Line J 10.

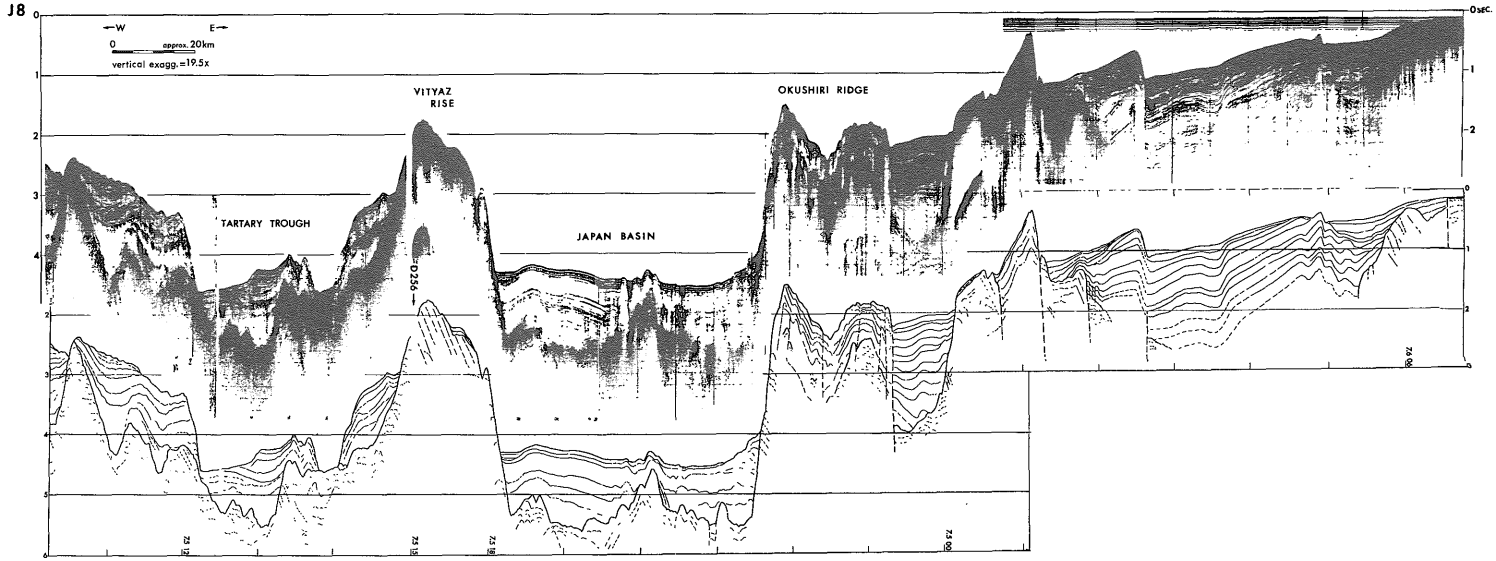

Figure 13 Seismic reflection profile and interpretation of Line J 8.

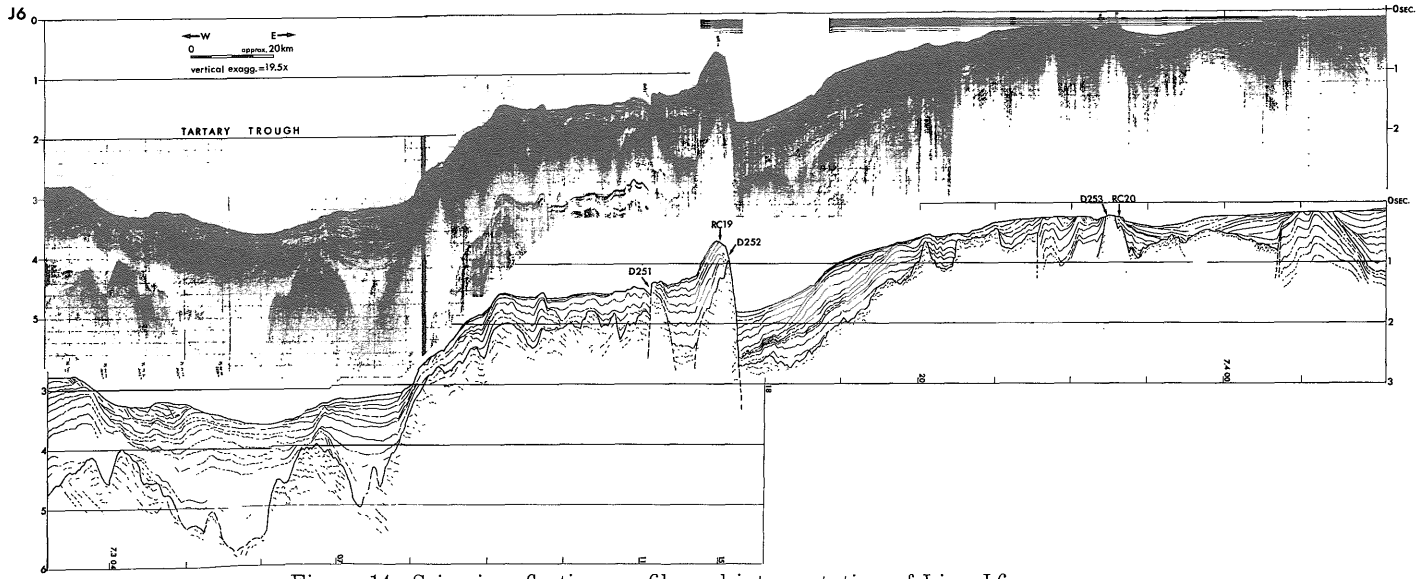

Figure 14 Seismic reflection profile and interpretation of Line J 6.

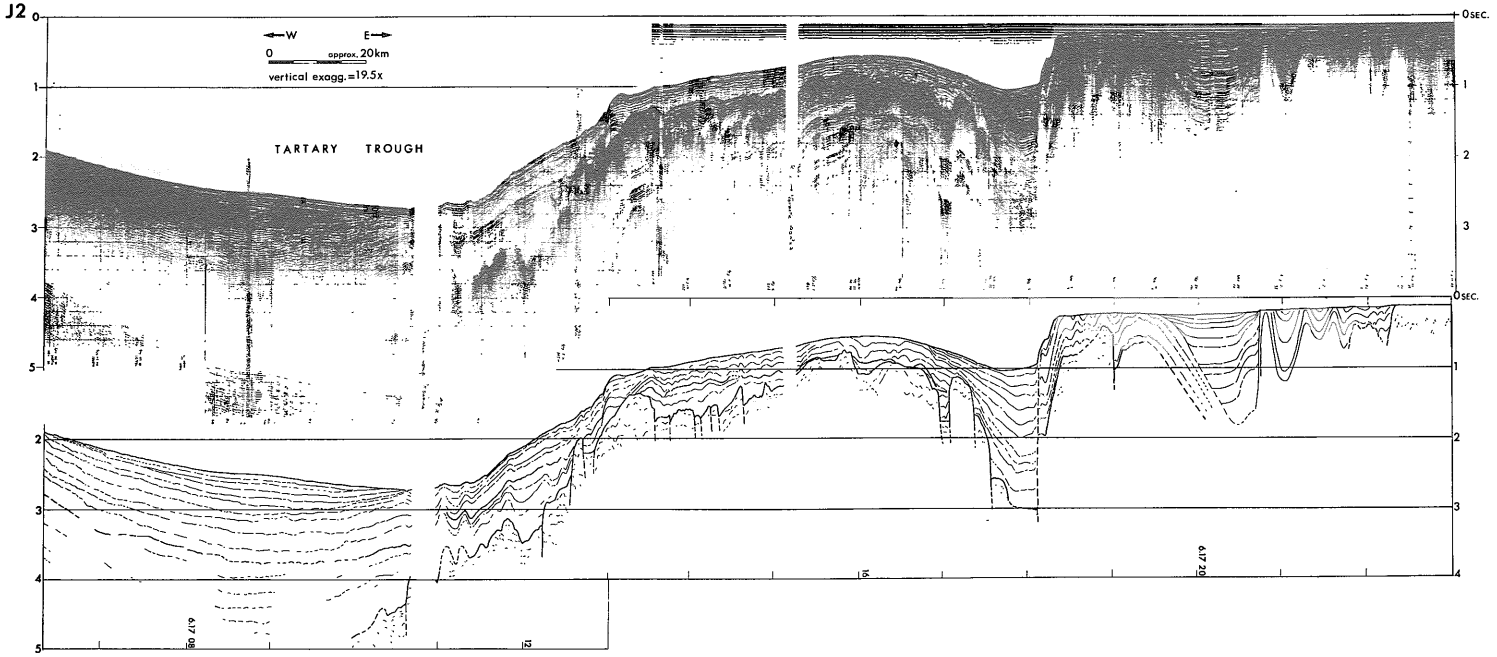

Figure 15 Seismic reflection profile and interpretation of Line J 2.

thickness of 1.0 second. The difference should be due to the difference in the history of each topographic high. Several small basins are observed on the eastern slope area. The basement on the eastern slope area shows a rather rugged topography.

Geological map of the Japan Sea

Three geological maps of the Japan Sea were compiled by HONZA *et al.* (1979), TAMAKI *et al.* (1979 a), and TAMAKI *et al.* (1981 a) based on the compilation of seismic profiles, bottom sampling data, deep sea drilling results, and other published geological and geophysical data.

Figure 16 is a geological map of the Japan Sea compiled by INOUE and HONZA (1982) from the three geological maps of HONZA *et al.* (1979), TAMAKI *et al.* (1979 a), and TAMAKI *et al.* (1981 a). The twelve geological sections are shown in Figure 16 also based on the above three maps. The geological sections on Figure 16 are almost identical with the seismic profiles shown in Figures 4–15. The sedimentary sequence is divided into four units in the basin and slope area. They are Quaternary, Pliocene, Miocene sediments, and Miocene volcanic sediments.

The Pliocene to Late Miocene sediments are observed on the Okushiri Ridge and the continental slope area off Hokkaido. They are cut by many faults. The faults are mostly NS trending. Syncline and anticline axes are also mostly NS trending. The wide distribution of Miocene volcanic sediments is observed in the eastern continental slope area.

The Neogene–Quaternary volcanic rocks are distributed on the continental shelf and slope area in the northern Japan Sea with minor distribution. The distribution of pre-Neogene strata in the submarine area is observed on the Musashi Bank and the Soya Strait. The basement rocks in the basin area are unknown with the lack of bottom sampling data of solid rocks and deep sea drilling data which reached the basement.

The Pliocene and the Miocene sediments are prominent on the Sado Ridge. The outcrops are formed with some structural movement as is in the Okushiri Ridge. The faults observed are mostly NNE–SSW trending and syncline and anticline axes in the area have mostly the same trend. The Pliocene and the Miocene sediments are observed along the topographic highs such as the Yamato Rise, the Kita-Oki Bank, the Oki Ridge, and the Hakusanse Bank.

Wide distribution of volcanic rocks are observed in the central part of the Japan Sea. Age assignment of the volcanic rocks range from the Tertiary to the Quaternary. Granitic rocks are widely distributed on the Kita-Yamato Bank and the Kita-Oki Bank. The Yamato Bank is mainly composed of volcanic rocks while the Kita-Yamato Bank is composed of the granitic rocks. The pre-Tertiary sedimentary rocks are observed only on the northern end of the Oki Bank. Some parts of the basement rocks are described as unknown due to very scarce information.

The continental slope and basin areas are wholly covered by Quaternary sediments in the southern part of the Japan Sea. An outstanding unconformity on the continental shelf (Figs. 4 and 5) lies under the Quaternary or Plio-earliest Pleistocene sediments. Many faults are traced on the continental shelf, trending parallel or subparallel to the coast line. Slumping structure of the Quaternary sediments is distinct in the southern margin of the Tsushima Basin.

Isopach maps of the Japan Sea

Several isopach maps of sediments of the Japan Sea have been published. HILDE and WAGEMAN (1973), LUDWIG *et al.* (1975) and MOROZOWSKI and HAYES (1978) presented isopach map of the deep sea basin area. TAMAKI *et al.* (1979 a) and TAMAKI *et al.* (1981 a) also presented a detailed isopach map of the whole Yamato Basin and a part of the Japan Basin. ISHIWADA and OGAWA (1976) and SUZUKI (1979) presented isopach maps of the continental shelf and slope area along the Japanese Isalands. ISHIWADA *et al.* (1984) compiled all these isopach maps with some of unpublished data of the Geological Survey of Japan (Fig 17). GNIBIDENKO (1979) also showed the overall isopach map of the Japan Sea.

Figure 17 shows the distribution of sediments in the Japan Sea. The major deep sea sedimentary basins are the

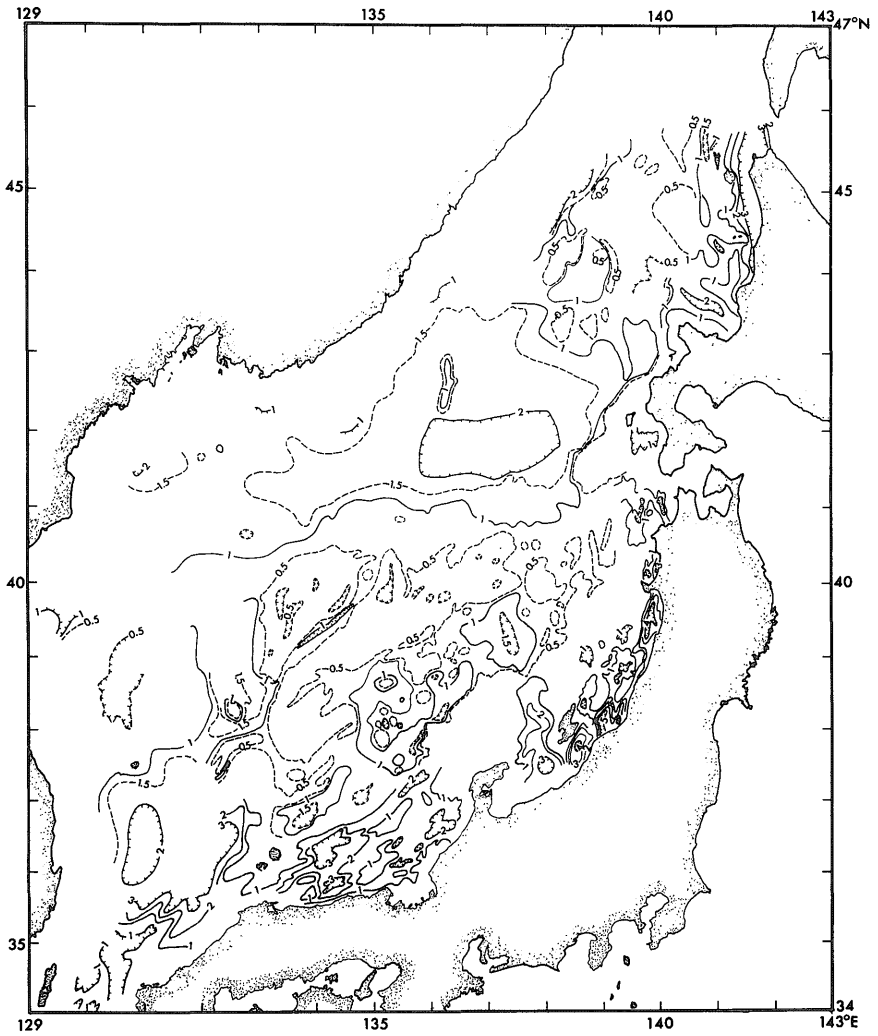

Figure 17 Isopach map of the whole Japan Sea after ISHIWADA *et al.* (1984). Contours are in second of two-way acoustic travel time.

Japan Basin, the Yamato Basin, the Tartary Trough, and the Tsushima Basin, which are presently under active deposition. The thickest sedimentary fill in the Japan Sea, however, is not observed in these deep sea basins but placed on the continental shelf of the Northeast Japan (Tohoku) Arc. The sediment thickness off Niigata exceeds 5.0 seconds which is the largest of the Japan Sea in our available data.

The sediments are generally thicker in the central part of the Japan Basin and an isopach contour of 2.0 seconds shows E-W extension in the north of the Yamato Bank. The thickest sediment accumulation of 2.3 seconds is observed in the center of the basin south of the Bogorov Seamount (MOROZOWSKI and HAYES, 1978).

The sediment thickness of the Yamato Basin is less than that of the Japan Basin. The maximum sediment thickness observed in the Yamato Basin is 1.6 seconds (TAMAKI *et al.*, 1979 b), which is about 1.0 second less than that of the Japan Basin. Isopach contours of the Yamato Basin complicated with many seamounts and subbottom basement relieves. The Yamato Basin is generally separated into two sedimentary basins ; the northeastern basin and the southwestern one.

The Tsushima Basin has a sediment thickness over than 2.0 seconds in thickness. The sedimentary structure and high reflectivity of the sediments show that slumping and sliding deposits are main constituents of the sediments in the basin. The prevalence of slumping in the Tsushima Basin may suggest rapid subsidence of the basin.

The sediment thickness of the Tartary Trough exceeds 2.0 seconds. The southern part of the Tartary Trough is dissected by the Tartary Canyon. Deposition in the Tartary Trough appears to be saturated and the excess sediments are fed into the Japan Basin through the Tartary Canyon.

There are many small sedimentary basins observed on the continental shelves along the west coast of the Japanese Islands. The sediment thickness is generally larger than that of the deep sea basin and at maximum exceeds 5.0 seconds. These basins are continuous onto the shore area. The litho- and biostratigraphy of the basins shows that the sedimentary basins were formed in the deep sea since early Middle Miocene (ISHIWADA *et al.*, 1984).

The sediments on the topographic highs are rather thin with a thickness of less than 0.5 seconds. The shin deposition on the topographic highs show that the main part of the sedimentation in the Japan Sea is due to the turbidites which are deposited only in the basin area. Some part on the Okushiri Ridge, however, is overlain by sediments with a thickness of 1.0 second. The thick sedimentation on the Okushiri Ridge is due to the recent uplift of the ridge by the compressional tectonics since latest Pliocene as discussed on detail in Chapter 3. The Okushiri Ridge was uplifted with the basin turbidites on it.

Isobase map of the Japan Sea

Figure 18 shows a contour map of the depth of the acoustic basement of the Japan Sea by TAMAKI *et al.* (1981 a). The map covers a part of the Japan Sea including the whole Yamato Basin and a part of the Japan Basin. This is the first isobase map on the Japan Sea.

The isobase map clearly shows the configuration of the Yamato Basin. The Yamato Basin trends NE with a general width of about 110 km and a maximum width of 150 km in its southwestern part.

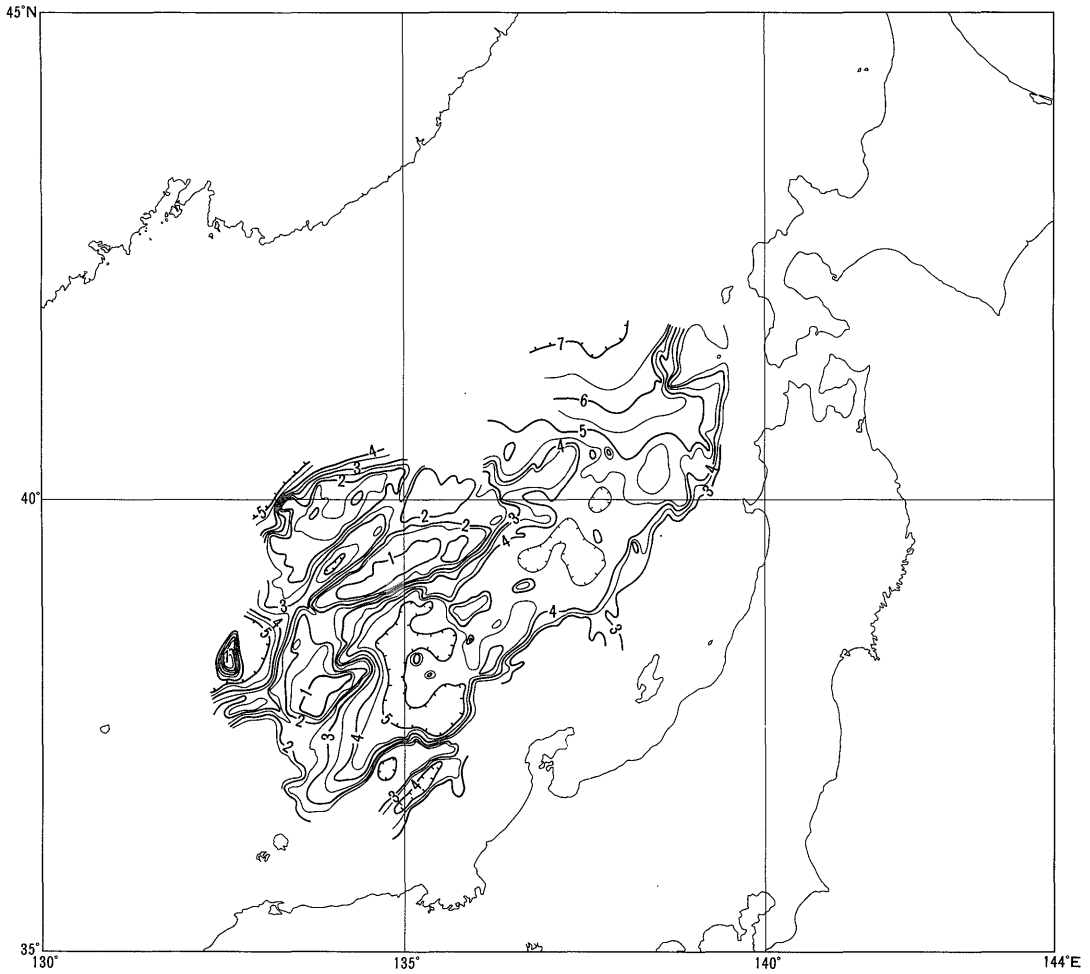

Figure 18 Isobase map of the Japan Sea after TAMAKI *et al.* (1981 a). Contours are in second of two-way acoustic travel time.

The southwestern part of the basin shows deep basement depth greater than 5.0 seconds.

The basement depth of the Japan Sea exceeds 7.0 seconds in the central part. The difference of the basement depth between the Japan Basin and the Yamato Basin is remarkable. If the acoustic basement represents oceanic crust, the greater depth of the Japan Basin should indicate that the Japan Basin is older than the Yamato Basin. The relationship between the age and the basement depth of the both basins is discussed in detail in Chapter 3.

Another characteristics of the basement depth of the Japan Sea is that the central part of the Japan Basin is generally deeper than its marginal area. This feature is also shown on the sediment isopach map. The sediment thickness of the Japan Basin is also greater in the central part than in the marginal part. Simple application of the age-depth relationship of the oceanic crust suggests that the central part of the

Japan Basin is older than the marginal part of the basin. If this is the case, such feature, younger in the margin and older in the center, is unrealistic in the back-arc basin which generally has a spreading center in the center of the basin. This discrepancy is also discussed in Chapter 3.

2.3 Geological structure of basins and troughs

Japan Basin

The Japan Basin is the largest basin in the Japan Sea and occupies about two-third of the whole Japan Sea. Two of the typical seismic profiles of the Japan Sea are shown in Figures 11 and 19.

The maximum sediment thickness of the Japan Basin reaches 2.2 seconds on the seismic profiles (Fig. 19). The sediment thickness generally exceeds 1.5 seconds on the central part of the Japan Basin (Fig. 17). The sedimentary sequence of the Japan Basin is divided into two acoustic units ; the upper stratified layer and the lower transparent layer. The stratified layer shows a rather uniform thickness of 1.0 second over the entire basin area while the thickness of the transparent layer is variable from less than 1.0 to 1.5 seconds. The variation of sediment thickness is due to the variation of the lower transparent layer. The sedimentary layers onlap to the continental slope of the Japanese Islands (Fig. 11).

The stratified layer and the transparent layer show conformable relation in the basin area, whereas they show disconformable relation around the Yamato Rise. The disconformity is shown in the manner that the transparent layer is continuous on to the Yamato Rise while the stratified layer onlaps to the transparent layer (Fig. 20). This unconformity suggests a different depositional manner of both sedimentary layers. The sea bottom of the Japan Basin, corresponding to the upper surface of the stratified layer, is generally smooth and flat. Such sea bottom topography is general features of the abyssal plain. The stratified layer is deposited in the topographic low and onlaps to the slopes. The sedimentary manner like this also suggests that the stratified layer is a turbidity layer. The stratification of the stratified layer represents the distal turbidites facies of the submarine fan. The turbidities were fed to deep sea basins through several large submarine canyons and channels such as the Toyama Deep Sea Channel.

The sedimentary structure of the transparent layer is different from that of the turbidity layer. The transparent layer drapes the basement topography. Acoustic transparency of the layer indicates the uniform nature of the sedimentary layer. Such sedimentary manner appears to be the results of the sedimentation of pelagic sediments rather than terrigenous turbidites.

The sedimentary layers onlap to the continental slope of the Japanese Islands and no major unconformable relation is observed there (Fig. 19) while the unconformity between the stratified layer and the transparent layer is well observed around the Yamato Rise (Fig. 20). The unique unconformity around the Yamato Rise suggests the tectonic movement of the Yamato Rise, in terms of uplift or subsidence, which is different from that of the Japanese Islands.

A deep sea drilling site, Site 301, is located in the Japan Basin north of the Kita-Yamato Bank. The hole stopped at the depth of 497 m below the sea bottom, the mid part of the entire sedi-

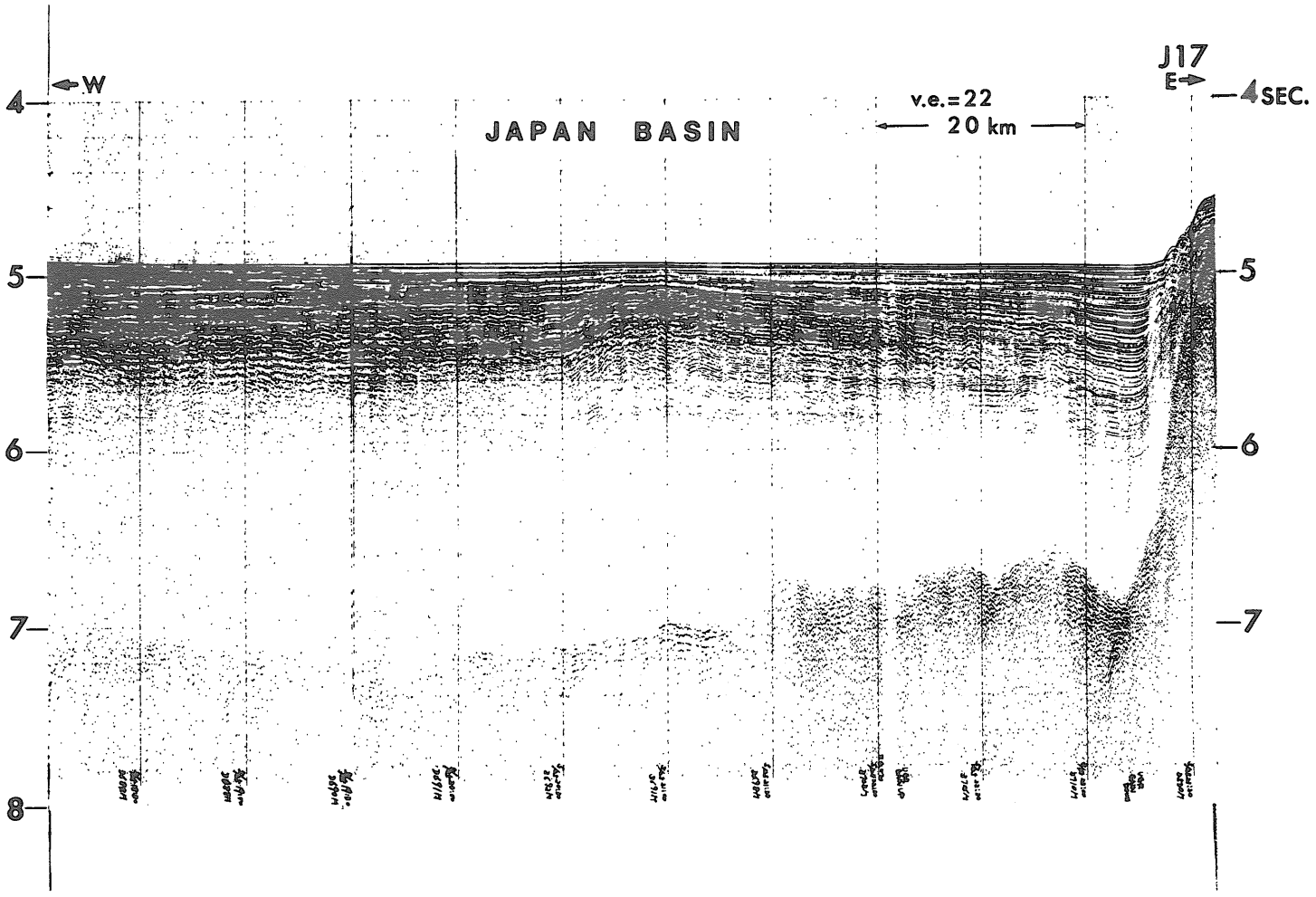

Figure 19 Seismic reflection profile of the eastern part of the Japan Basin on Line J 17.

mentary layer and did not reach the basement (KARIG and INGLE, Jr. *et al.*, 1975). The drilling data at this site, however, present important information for the sediment stratigraphy of the Japan Basin. The drilling hole almost reached the boundary between the stratified layer and the transparent layer which is not generally sharp. The upper 250 meters of the drilling sample is silty clay and the lower half of the hole is diatomaceous clay. The age of the bottom of the hole is 4 Ma according to the analysis of the diatom fossil by KOIZUMI (1979). The upper stratified layer generally shows a uniform thickness in the main part of the basin area. Thus, the boundary between the stratified layer and the transparent layer is generally correlated to 4 Ma in the Early Pliocene according to the results of Site 301.

Yamato Basin

The sediment thickness of the Yamato Basin is less than that of the Japan Basin. The sedimentary sequence of the basin is also divided into two units in its central part as is in the Japan Basin (Fig. 21). The upper layer is stratified and the lower layer is transparent. The upper stratified layer is generally thicker than the lower transparent layer in the Yamato Basin while, in the Japan Basin, the stratified layer is much thinner than the transparent layer. The thickness of the stratified layer is variable from 0.6

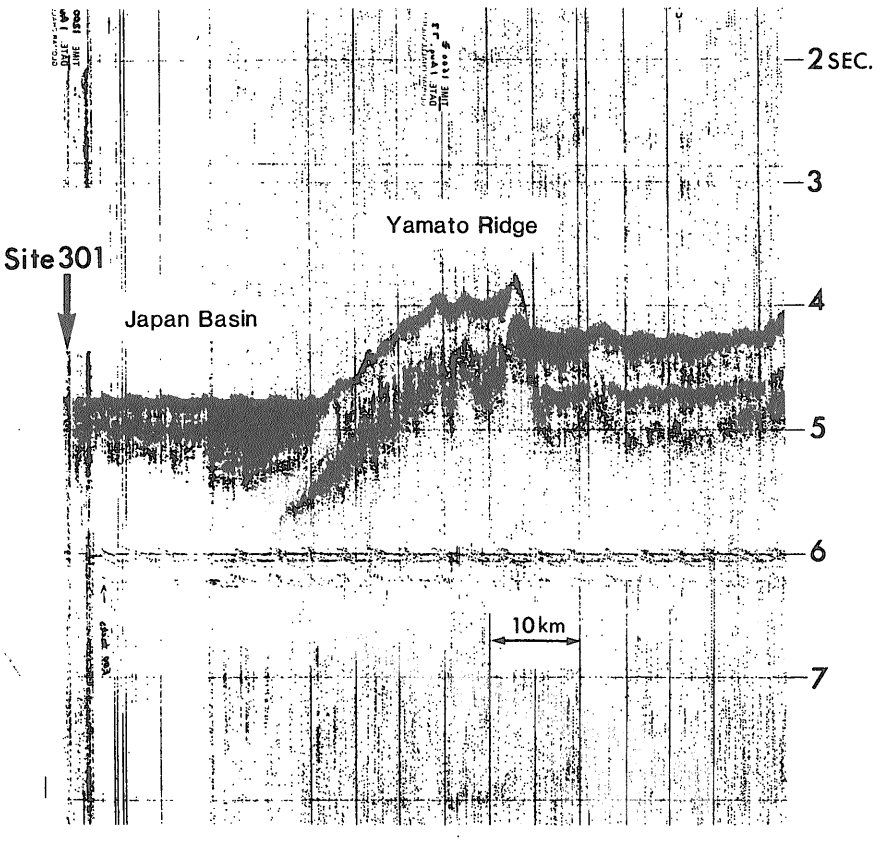

Figure 20 Seismic reflection profile on the Yamato Rise and the Japan Basin. An arrow shows the DSDP drilling Site 301. The profile data is of DSDP cruise Leg 31.

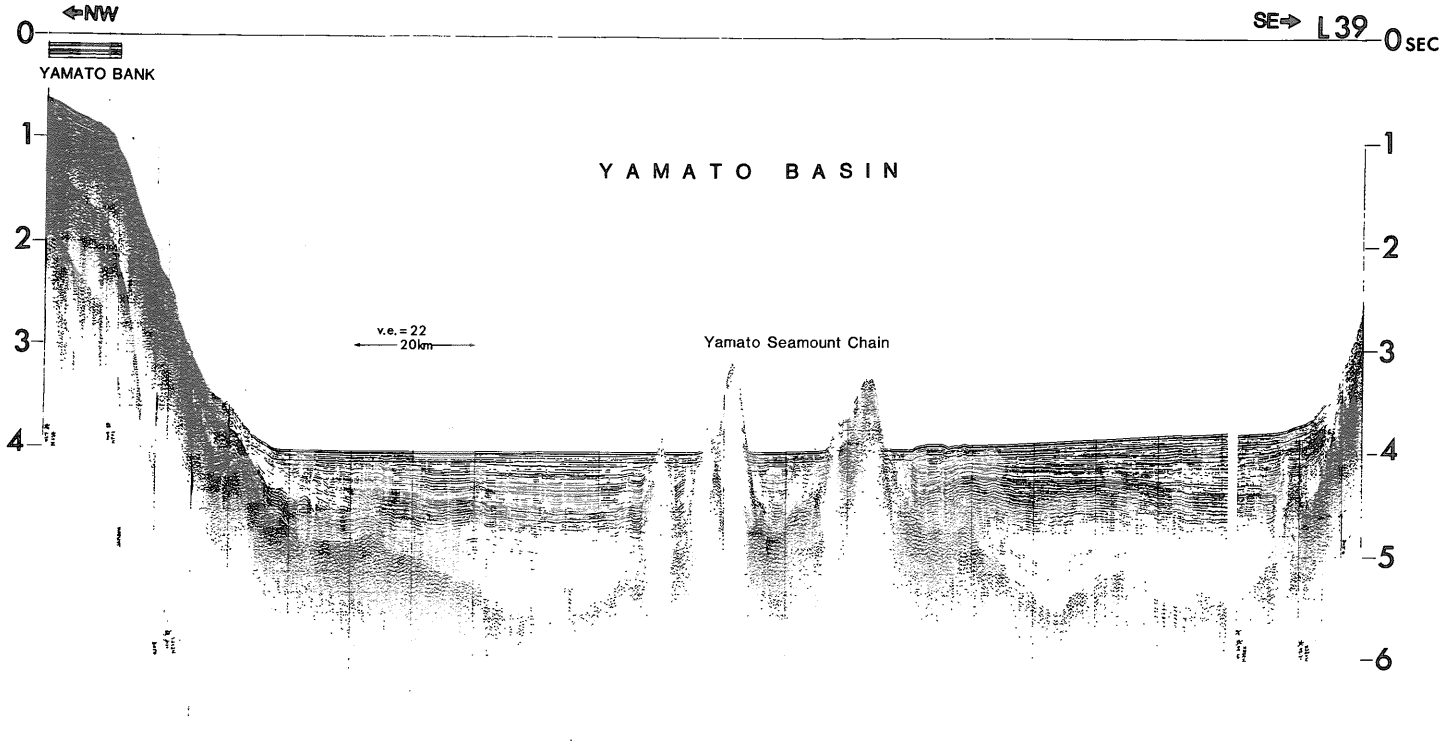

Figure 21 Seismic profile of the Yamato Basin and the Yamato Seamount Chain on Line L 39.

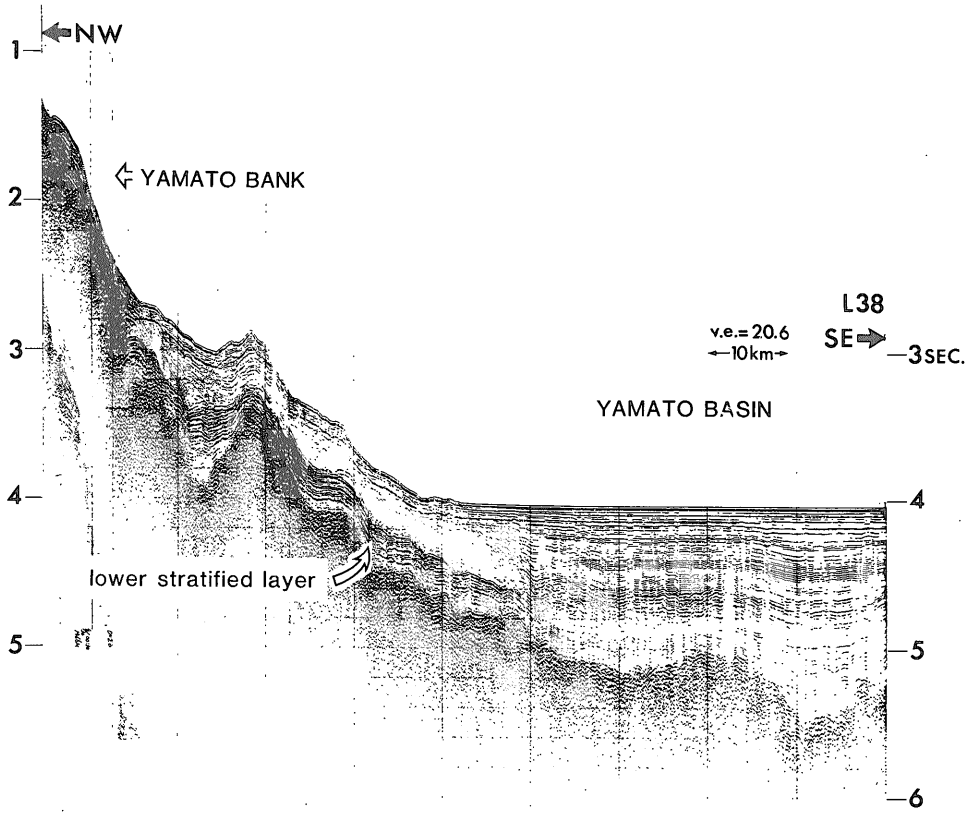

Figure 22 Seismic profile of the western margin of the Yamato Basin Line L 38.

to 1.0 second. The variable thickness of the upper stratified layer of the Yamato Basin is due to the development of a deep sea submarine fan and the Toyama Deep Sea Channel in the northeastern part of the basin (Fig. 10).

Another stratified layer which underlies the transparent layer is distributed in the margin of the basins (Fig. 22). The author calls this layer the lower stratified layer in this paper. The lower stratified layer is observed in the basin margin and it is traced onto the slopes of the Yamato Rise and the Sado Ridge. The thickness of the layer is less than 0.3 seconds. The lower stratified layer seems to change to transparent towards the central part of the basin. This change of facies from the margin to the center of the basin suggests that the lower stratified layer is correlated to the lowermost part of the transparent layer in the central part of the basin. It should be noted that the distribution of the lower stratified layer is limited only in the marginal area of the basin. The lower stratified layer is also observed at the northern end of the Yamato Basin as shown in Figure 23.

The sea bottom topography of the Yamato Basin shows a typical abyssal plain with a flat and smooth surface in the southern half of the basin (Figs. 9 and 21). The feature shows the depositional environment of distal turbidites as is in the Japan Basin. The Yamato Basin has two abyssal plains. The larger one is located in the southwestern part of the Yamato Basin and has the water depth of about 3000 m. The smaller one

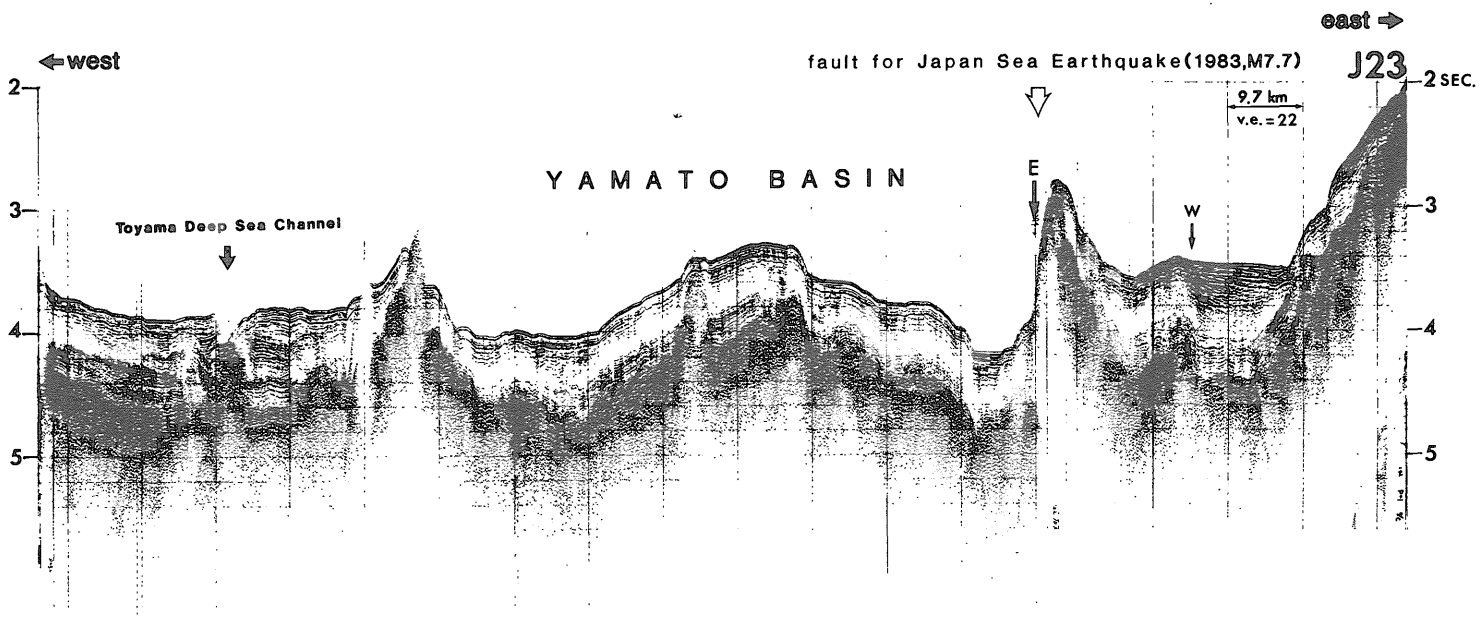

Figure 23 Seismic profile of the northern end of the Yamato Basin on Line J 23.

is located in the central part of the basin and shows a shallower water depth of about 2700 m. These two separated abyssal plains are inferred to have different provenances.

The northeastern part of the Yamato Basin is characterized by the development of a submarine fan (Fig. 10). The submarine fan is developed just off the Toyama Trough. The Toyama Deep Sea Channel cuts and meanders through the deep sea fan. The Toyama Deep Sea Channel extends into the Japan Basin. These features suggest the following sedimentary history in the area. The deep sea fan was formed off the Toyama Trough by sediment transportation from the Toyama submarine canyon at the first stage. After the saturation of the submarine fan, the fan was eroded by the Toyama Deep Sea Channel. Now the depression of the channel reaches 300 m with a width of about 10 km, and the main depositional area is shifted into the Japan Basin. Some of overflowed sediments from the channel may be deposited in the shallower abyssal plain of the Yamato Basin.

The Yamato Basin is characterized by the abundant distribution of seamounts and knolls in contrast with the other basins in the Japan Sea. The seamounts and knolls are concentrated in the axial central part of the basin. There are two seamount chains. One is just along the central line of the Yamato Basin trending NE. The other crosses the basin trending ENE. Both seamount chains cross each other at the north of the Hakusanse Bank. The author calls the former one the Central Yamato Seamount Chain (Fig. 21) and the latter one the Yamato Seamount Chain.

Two deep sea drilling sites, Sites 299 and 302, are located in the Yamato Basin. Site 299 is located in the northeastern part of the Yamato Basin. The hole did not reach the basement layer and stopped at the depth of 532 m below the sea bottom, the mid part of the entire sedimentary layer (KARIG and INGLE, Jr. *et al.*, 1975). The drilling hole almost reached the boundary between the upper stratified layer and the lower transparent layer which is not generally sharp. The drilling samples are clay, silty clay and sandy clay. The age of the bottom of the hole is 3.5 Ma according to the analysis of the diatom fossil by KOIZUMI (1979). Site 302 is located at the northern margin of the Yamato Basin. The hole penetrated the lower stratified layer and reached the basement at a depth of 531.5 m below the sea bottom. The upper two-thirds of the core, which is correlated to the transparent layer, is composed of mostly diatomaceous clay with the age of post Pliocene. The lower stratified layer is composed of clay of upper Miocene age. The basement rocks appear to be correlated to the Green Tuff (SHIMAZU, 1979). The composite analysis of seismic profiles with these two DSDP holes presents an important information for the stratigraphy of the Yamato Basin as discussed in Chapter 3.1.

Tartary Trough

The sediments of the Tartary Trough are highly stratified in the upper part and transparent in the lower part. The maximum sediment thickness exceeds 2.3 seconds at the west of the Soya Strait (Fig. 15), where the basement could not be detected on our seismic profiler records. The upper stratified sediments increase their reflectivity to the north and to the west. This phenomena suggest that the sediments are supplied from the northern end of the trough and the continent to the west of the trough.

An erosional feature by the Tartary Trough is prevailed in the southern area of the trough (Figs. 13 and 14). The Tartary Canyon is shown on a typical profile on Line J 8 (Fig. 13) with a canyon dissected to the depth of 500 m. The topographic correlation from profile to profile, however, is poor, which indicates a complicated depositional environment in the southern area of the trough. The thickness of the upper stratified sediments is generally 1.0 second with a variable range of 0.8 to 1.2 seconds. The thickness of the lower transparent sediments is variable from 0 to more than 1.4 seconds. The sediments are thicker in the depression. The transparent sediments are intercalated by a stratified horizon in some places (Fig. 14).

The basement morphology is rugged with a depth of 4 to 5.6 seconds where the basement is detected. The basement at an axial deep is observed with the depth exceeding 5 sec. The rugged basement morphology may be due to or show a relic of the initial rifting of the Tartary Trough.

A sono-buoy refraction measurement at Station SB 7 was carried out in the trough at the west of Rishiri Island (Honza *et al.*, 1978). The results show that the sonic velocity of the basement is 3.6 km/sec with a thickness of 1.72 km. The basement velocity of about 3.5 km/sec, which is slower than 4.5 km/sec of the normal oceanic basement, is also observed in the Japan Basin and the Yamato Basin.

Broad basement highs are observed along the eastern margin of the Trough as typically shown on Line J 2 (Fig. 15). The upper stratified sediments of the trough continue eastward onto the basement high, while the thin lower transparent sediments are observed only in the depressions on the basement highs. This feature suggests that the subsidence of the basement highs has occurred after the deposition of the lower sediments.

The age of the sedimentary sequence of the trough can be estimated from the outcrops on the Okushiri Ridge as shown on section JS 2 of Figure 16. The lower part of the sediments is unknown because of the lack of any boring data and outcrops.

Tsushima Basin

The Tsushima Basin has a smooth floor gently tilting upward to the south. The basement cannot be detected except around the Ullung Rise. The deepest reflector observed in the sediments is 2.2 seconds below the sea floor on the foot of the continental slope off San-in.

The sedimentary sequence is divided into three units. The upper unit is a non-deformed stratified layer with high frequency reflection and it forms a small abyssal plain south of Ullung Island. This unit is presumably composed of turbidites. Its maximum thickness is 0.3 second.

The middle unit is a stratified and highly reverberant layer which is weakly deformed in the basin and strongly deformed on the foot of the continental slope. The middle unit is overlain slightly unconformably by the upper unit. The thickness of the middle unit increases southward and the maximum thickness is 1.4 seconds on the foot of the continental slope off San-in. This southward thickening of the middle unit is due to the southward tilting of the sea floor. The middle unit is correlated to the upper sedimentary unit of the continental shelf off San-in whereas, northward, it abuts onto the basement of the Ullung Rise. A reverberant layer similar to this unit is also observed in the Hidaka Trough off the Pacific coast of

southwestern Hokkaido (TAMAKI *et al.* 1977).

The lower unit is a transparent layer with weak reflectors which are almost evenly deposited. The middle unit lies slightly unconformably on the lower unit. The thickness of the lower unit is supposed to exceed 1.0 second although the bottom of the unit cannot be detected. The lower unit might also be continuous with the lower sedimentary unit on the continental shelf whereas it abuts onto the Ullung Rise.

Submarine sliding and slumping structures are common in the southern margin of the basin and appear as small ridges or swells on the profiles L 24 and 25 (Figs. 4 and 5). The rapid accumulation of coarse materials associated with such active slumping or sliding compose the highly reflective upper sedimentary unit. The rapid accumulation of the sediments in the Tsushima Basin may indicate the rapid subsidence or excess sediment feed to the basin from the San-in coast. The deposition of the reverberant layer in the Tsushima Basin may be related to some kind of tectonic movement of the basin and the surrounding area.

Genzan Trough

The Genzan Trough, one of large sedimentary basins in the Japan Sea, is located in the western part of the Japan Sea. The trough lies between the Korea Rise and the continent. The trough trends NE. There has been very little description and discussion of the Genzan Trough in previous works. Two seismic profiles of the trough were obtained during the GH 77-2 cruise.

The thickness of the sedimentary sequence ranges from 0.5 to 1.4 seconds in the Genzan Trough. The basement topography is rugged in the northern part in contrast with that in the southern part, and decreases in depth toward north (Fig. 6). The northern sedimentary sequence is highly reflective in comparison with the southern sedimentary sequence. These features suggest that the terrigenous sediments derived from the north form the northern reflective sedimentary sequence.

A prominent channel is observed on the foot of the continental slope and the features suggests its activity. The channel has the width of 5 km and a relative depth of 150 m on Line L 28 (Fig. 6).

The upper half of the sedimentary layer of the Genzan Trough is stratified and the lower part is transparent as is in other basins. The stratification of the upper stratified layer is complicated suggesting the change of the depositional environment through time.

Mogami Trough

The Mogami Trough lies alnog the eastern margin of the Japan Sea from off Niigata to the Oga Peninsula. The width of the trough is 40 km and its length exceeds 200 km with the trend of NNE-SSW. The trough is developed between the Sado Ridge and the northern Honshu.

A profile of the Mogami Trough is shown on Line N 8 (Fig. 10). The bottom of the Mogami trough is not simple due to the presence of several banks and a channel. The sedimentary layer in the trough is wholly stratified with a maximum thickness exceeding 1.5 seconds. Several banks in the trough are overlain by thick sediments with a thickness of over 0.5 second. The NNE trending faults occur on either side of the banks. Such thick accumulation of the sediments on the banks indicates their recent uplift along the faults with the overlying sediments on them. The lower half of the

sedimentary layer in the trough is considered to be Miocene age based on comparison with the shore geology as is shown in geological section JS 6 of Figure 16.

Oki Trough

The Oki Trough is located in the southern part of the Japan Sea east of the Oki Islands off San-in. The trough has the width of about 35 km and the length of 200 km with the trend of NE. The Oki Trough lies along the southern margin of the Oki Ridge.

The Oki Trough is filled by rather thick sediments with a thickness exceeding 2.0 seconds (Line L 35, Fig. 8). The upper sequence of the sediments is stratified with a thickness of about 1.0 second. The lower sequence of sediments is transparent. The whole sediments are undisturbed. The sediments in the trough about the Oki Ridge in the northwest, while to the southeast the feature is not simple. The sediments generally continue to the sedimentary layer on the continental slopes, but the sediments abut to the basement or lower sedimentary layer on the continental slope in some areas. The Sea floor of the Oki Trough is smooth and flat and appears to show the deposition of distal turbidites. The age of sedimentary layer of the Oki Trough is Pliocene to Quaternary according to TANAKA and OGUSA (1981).

Shiribeshi, Okushiri, and Nishitsugaru Troughs

The Shiribeshi, the Okushiri, and the Nishitsugaru Troughs are developed along the eastern side of the Okushiri Ridge in the eastern Japan Sea. The basins show a north-south elongated structure. Each basin has a width of 20 km and a length of 70 to 80 km. The sediment thickness of the basins exceeds 1.0 second and in some basins reaches 2.0 seconds or more. The sediments are stratified in the upper part. The basins are characterized by a flat and smooth sea floor suggesting the deposition of the distal turbidites. The origin of these basins is discussed in Chapter 3.4.

2.4 Geological structure of ridges, banks, and seamounts

Yamato Rise

The Yamato Rise is the largest topographic high in the Japan Sea. The rise is divided into three topographic units ; the Yamato Bank, the Kita-Yamato Bank, and the Takuyo Bank (Fig. 1). The topographic depression between the Yamato Bank and the Kita-Yamato Bank is called the Kita-Yamato Trough. The width of the Yamato Rise is 180 km and its length is 300 km. The height of the rise above the surrounding sea floor exceeds 2500 m. The rise trends NE to NEE.

The Yamato Bank forms an NEE trending, ridge-like feature with a flat summit, on which basement is widely exposed (Fig. 9). This flat summit is interpreted as a wave cut terrace formed when the upper parts of the Bank were near the sea level. The feature suggests that the subsidence of the ridge occurred in association with the subsidence of the surrounding basin floor with time. The Yamato Bank is composed mainly of volcanic rocks (Fig. 16). The volcanic rocks are basalts and andesites. Many basalts and andesites are dated by the K-Ar age determination method (Tables 2 and 3). Most of them are of the Eocene-Oligocene to the Early Miocene in age (20 to 46 Ma). An age of 76 Ma for basalt is reported by VASILIEV (1975). Some of volcanic rocks on the Yamato Bank appear to be Late Cretaceous.

Table 2 Absolute age of the rocks recovered by the bottom sampling. Age determination by Japanese scientists.

locality	site no.	rock	age (Ma)	method	reference
Hakusanse	HSA	andesite	007.7 ±0.81	K-Ar	UENO *et al.* (1971)
Kita Oki Bank	D 266	granite	141.6	K-Ar	GSJ unpublished
Kita Yamato Bank		granodiorite	197	K-Ar	SHIMAZU (1968, MS)
Korea Plateau	D 223-7	granite	126.8 ±6.3	K-Ar	HONZA ed. (1978)
Matsu Seamount	MASA	andesite	004.16 ±0.16	K-Ar	UENO *et al.* (1971)
Meiyou No. 2 Smt	MESA		013	K-Ar	OZIMA *et al.* (1972)
Musashi Bank	D 248	welded tuff	077.8 ±3.9	K-Ar	YUASA *et al.* (1978)
Nishitakuyou Bank		granodiorite	227	Rb/Sr	OZIMA *et al.* (1972)
Takuyou Bank		granite	220	K-Ar	SHIMAZU (1968, MS)
Yamato Bank	YS 7-1	andesite	019.3 ±0.5	K-Ar	UENO *et al.* (1971)
Yamato Bank	YS 1-2	basalt	021.6 ±0.5	K-Ar	UENO *et al.* (1971)

Table 3 Absolute age of the rocks recovered by the bottom sampling. Age determination by Russian scientists.

locality	site no.	rock	age (Ma)	method	reference
Bogorov Seamount		basalt	18	K-Ar	SAHNO & VASILIEV (1974)
Gabass Seamount		granite	110	K-Ar	LELIKOV *et al.* (1975)
Kita Yamato Bank		granite	136	K-Ar	VASILIEV *et al.* (1975)
Kita Yamato Bank		granite	128	K-Ar	VASILIEV *et al.* (1975)
Kita Yamato Bank		granite	110	K-Ar	VASILIEV *et al.* (1975)
Kita Yamato Bank		granite	156	K-Ar	VASILIEV *et al.* (1975)
Korea Plateau		gneiss	2231	Rb/Sr	LELIKOV *et al.* (1975)
Korea Plateau		gneiss	2097	Rb/Sr	LELIKOV *et al.* (1975)
Korea Plateau		gneiss	1983	Rb/Sr	LELIKOV *et al.* (1975)
Korea Plateau		gneiss	2729	Rb/Sr	LELIKOV *et al.* (1975)
Korea Plateau		gneiss	2139	Rb/Sr	LELIKOV *et al.* (1975)
Slope off Primore		granite	60	K-Ar	LELIKOV *et al.* (1975)
Slope off Primore		granite	76	K-Ar	LELIKOV *et al.* (1975)
Slope off Primore		granite	90	K-Ar	LELIKOV *et al.* (1975)
Ullung Plateau		granitoids	102	K-Ar	LELIKOV *et al.* (1975)
Ullung Plateau		granitoids	110	K-Ar	LELIKOV *et al.* (1975)
Yamato Bank		basalt	76	K-Ar	VASILIEV (1975)
Yamato Bank		basalt	28.5 to 35.6	K-Ar	GNIBIDENKO (1979)
Yamato Bank		basalt & andesite	23 to 46	K-Ar	GNIBIDENKO (1979)
Yamato Rise		granitoids	270	K-Ar	LELIKOV *et al.* (1975)
Yamato Rise		granitoids	310	K-Ar	LELIKOV *et al.* (1975)
Yamato Rise		granitoids	220	K-Ar	LELIKOV *et al.* (1975)
Yamato Rise		granitoids	178	K-Ar	LELIKOV *et al.* (1975)
Yamato Rise		granitoids	194	K-Ar	LELIKOV *et al.* (1975)

The Kita-Yamato Bank forms a plateau like feature with a weak trend of NE. The basement morphology is rugged on the summit (Fig. 9). The basement is overlain by densely stratified sedimentary layer with the thickness of

around 0.5 second. The sedimentary layer abuts the basement. The boundary between the sedimentary layer and the basement is difficult to recognize in places because of the dense stratification of the sedimentary layer. The Kita-Yamato Bank is mostly composed of granitic rocks (Fig. 16). Several granites and granodiorites are also dated by the K-Ar Age determination method (Tables 2 and 3). The dated age ranges from 110 to 197 Ma (Jurassic to Early Cretaceous).

The Takuyo Bank shows a rugged basement morphology (Fig. 10). Sediments with a thickness of 1.0 second are deposited in the depressions among the basement highs. The northern part of the bank is composed of granitic rocks while the southern part is composed of volcanic rocks (Fig. 16). It has the same characteristics as the Yamato Rise as the northern area is composed of granitic rocks while the southern part is characterized by the wide distribution of the volcanic rocks. Radiometric age of granite from the Takuyo Bank is reported to be 220 Ma (Late Triassic) by SHIMAZU (1968) (Table 2).

The Kita-Yamoto Trough shows an elongated basement depression trending NE. The feature on the seismic profile (Fig. 9) suggests that the depression was formed by the graben-like movement bounded by normal faults on both sides. The faults are well traced from profile to profile. The sediment thickness in the trough exceeds 1.0 second in the central graben.

Oki Bank, Oki Ridge, and Kita-Oki Bank

The Oki Bank, the Oki Ridge, and the Kita-Oki Bank are located off San-in in the southern part of the Japan Sea. They are isolated topographic highs at the southwestern end of the Yamato Basin.

The Oki Bank shows spur feature extending northward off Oki Islands. Seismic profiles of the Oki Bank (Fig. 7) show a plateau like feature of the basement. The basement plateau is isolated from the continental shelf area. Well stratified sediments with a thickness of 0.5 second are deposited on the basement. The sediments buried the basement depression between the basement high of the Oki Bank and the continental shelf with a thickness of 1.5 second. Such sediment accumulation has made the topographic connection of the Oki Bank and the continental shelf area. Phyllite is sampled from the basement outcrops of the northern cliff of the Oki Bank.

The Oki Ridge is clearly NE trending. The width of the Oki Ridge is about 50 km and its length is about 150 km. Oki Island are located just southern extension of the Oki ridge. The Oki Trough lies just south of the Oki Ridge as a trapped sedimentary basin behind the ridge.

The mid part of the Oki Ridge has a prominent depression of the basement as is well shown on Line L 35 (Fig. 8). The depression has the same trend with the ridge. The stratified sediments with the thickness of 0.7 to 0.8 seconds are accumulated in the basement depression. The basement depression is bounded by fault scarps. The structural feature on the seismic profile suggests that the depression is a graben bounded by normal faults on both sides. The deformation of the sediment fill in the depression is weak and it does not suggest any recent activity of the faults.

Northern part and southern part of the Oki Ridge have exposed basement. Many volcanic rocks were dredged from the ridge during GH 78-2 cruise. They

are welded tuff, tuff breccia, andesite, basalt, and dolerite (YUASA *et al.*, 1979). There is no radiometric age data on the ridge.

The Kita-Oki bank is located between the Yamato Rise and the Oki Bank. Its width is 80 km and its length is 130 km with a trend of NE. The Kita-Oki Bank shows a rough basement morphology with highs and depressions (Fig. 8). The basement highs are almost free of sediments while the basement depressions are filled with stratified sediments with a thickness more than 1.0 second which are less opaque than the sediments of the Kita-Yamato and Oki Banks. The thickness of the sediments on the bank is generally less than 0.5 second. Fault like structures are observed in some places in the basement of the bank. The northern part of the bank is composed of granitic rocks while the southern part is characterized by the distribution of volcanic rocks (Fig. 16). The separated distribution of the granitic rocks and the volcanic rocks in the northern part and the southern part are the same as in the Yamato Rise. An radiometric age of 141.6 Ma (Early cretaceous) for the granite is known on the Kita-Oki Bank (Table 2). This age is comparable to the age of the granitic rocks of the Kita-Yamato Bank.

Korea Plateau and Ullung Rise

The Korea Plateau and the Ullung Rise are located in the southwestern part of the Japan Sea just east of the Korea Peninsula. The Korea Plateau is the second largest topographic high in the Japan Sea. The width of the Korea Plateau is 100 km and the length is 250 km with the trend of NE. The Ullung Rise has a round configuration with a diameter of about 100 km. The typical seismic profiles of both topographic highs are shown in Line L 28 (Fig. 6).

A sedimentary sequence with a maximum thickness of 1.1 seconds is observed on the Korea Plateau and the Ullung Rise. The sedimentary sequence is divided into three units bounded by disconformities. The upper unit (A on Figure 6) is a transparent or weakly stratified layer with a thickness less than 0.1 second and is occasionally absent. The middle unit (B on Figure 6) with a maximum thickness less than 0.6 second forms the main part of the sedimentary sequence. The upper part of the unit is stratified and its lower part is transparent of very weakly stratified. The lower unit of the sedimentary sequence (C on Figure 6) is observed in the basement depressions on the rise and plateaus. The unit is composed of an upper stratified layer and a lower transparent layer which is absent where the unit is thin. The maximum thickness of the unit is 0.6 second.

The basements of the plateau and rise are composed of granitic rocks and gneiss. The gneiss is restricted to the Korea Plateau. The absolute age of the gneiss by the Rb/Sr dating method is 1,983 to 2,729 Ma (Precambrian) (Table 3). Such old Precambrian rocks suggest the Korea Rise is closely related to the shield of the Korean Peninsula.

Okushiri Ridge

The Okushiri Ridge is an outstanding topographic feature in the northeastern margin of the Japan Sea. The ridge shows nearly NS trending. The ridge is not a single continuous ridge but is composed of en-echelon arrangement of several small ridges. The ridge is traced from the west of Rishiri Island to off the Oga Peninsula. Its overall length reaches 450 km. Its width is not greater than 50 km. The maximum relative height over

the sea floor of the Japan Basin exceeds 2500 m. The width and height of the ridge increases to the north.

The Okushiri Ridge is covered by rather thick sediments which reach 1.0 second. The sediment thickness of 1.0 second on the ridge is extraordinarily thick for such narrow ridges. The sediments, at the middle part of the ridge, are continuous with the sediments of the Japan Basin with appreciable thinning of the upper most part. The ridge is commonly associated with fault scarps on either or both sides. The sedimentary sequence crops out at the scarps of the Okushiri Ridge. Bottom samples from the scarps indicate that the sediments of the ridge are mainly composed of Late Miocene to Pliocene sediments with a thin or no Quaternary sediments. The sampling data are restricted in the northern part of the ridge. The acoustic basement of the northern Okushiri Ridge is composed of Early-Middle Miocene siltstones and sandstones. The age determination of the siltstone is based on diatom (SAWAMURA 1978 MS) and pollen assemblages of the samples of GH 77-3 cruise. The geological structure of the Okushiri Ridge is discussed in detail in Chapter 3.4.

Sado Ridge

The Sado Ridge lies in the eastern

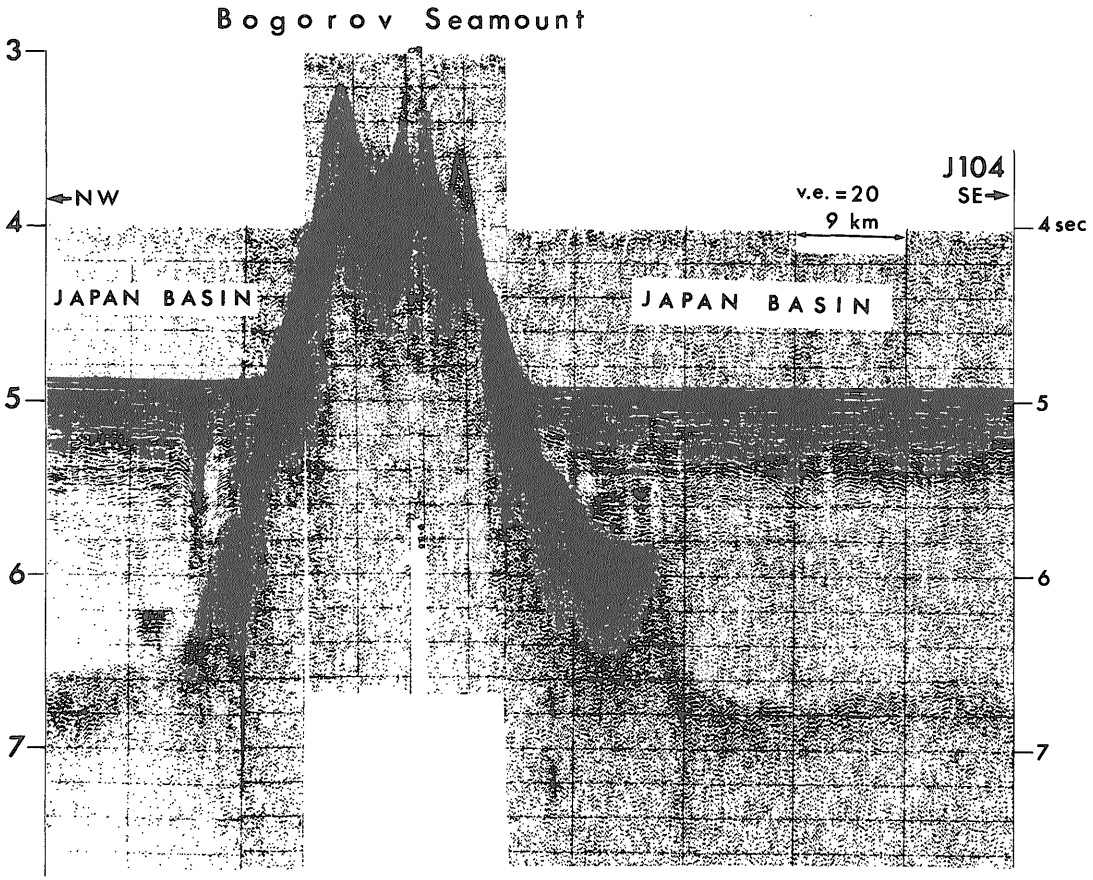

Figure 24 Seismic profile of the Bogorov Seamount in the Japan Basin on Line J 104.

margin of the Japan Sea parallel to Northeast Japan. The Sado ridge is not a single ridge, but is composed of many small ridges. The small ridges are in a row with the width of 80 km. Each ridge has a width of about 10 km and a length less than 50 km with the general trend of NNE. These small ridges stand on a broad topographic rise (Fig. 10). The small ridges are bounded by faults on their either or both sides. The ridges are commonly bounded by faults on its eastern side but occasionally on both sides. The faults are discussed in detail in Chapter 3.4.

The sediment thickness on the small ridge is generally less than 0.5 second. The sediments are mostly composed of Pliocene and Miocene sediments without Quaternary deposits on the ridges. The basement is composed generally of volcanic rocks. No radiometric ages are reported on the Sado Ridge.

Bogorov Seamount

The Bogorov Seamount is one of the largest topographic high in the Japan Basin. The Bogorov Seamount is isolated in the central part of the Japan Basin. The basement of the Bogorov Seamount is not covered by an appreciable amount of sediments in the subsea area (Fig. 24). The sediments of the Japan Basin abut to the basement of the Bogorov Seamount. Some Russian scientists identified the Bogorov Seamount as a Cretaceous basement (MELANKHOLINA and KOVYLIN, 1977; GNIBIDENKO 1979). SAHNO and VASILIEV (1974), however, reported the occurrence of basalt with the K-Ar age of 18 Ma (Table 3). The volcanic activity of such age in the central part of the Japan Sea should be noted in discussing the spreading tectonics.

3. Discussion

The origin of the Japan Sea in controversial despite of the abundant geological and geophysical data on the area. The author described the geological structure of the Japan Sea in Chapter 2. The geological structure is the most essential data for discussing the tectonics of the area. The author discusses several principal problems of the Japan Sea, based on the observation of the geological structure. The principal problems are the age of the basins (when was the Japan Sea formed?), the origin of the topographic highs which are closely related to the spreading tectonics of the Japan Sea, the tectonics of back-arc spreading (review and the case of the Japan Sea), and the recent crustal movement along eastern margin of the Japan Sea. Through these discussions, the author summarizes the tectonic evolution of the Japan Sea since its earliest stage of development.

3.1 Age of the basins

The age of formation of the Japan Sea is critical for the tectonics of Japanese Islands. However, until recently it was a controversial subject. Usually, the most important information for the age of back-arc basins are gotten from the deep sea boring and the identification of magnetic anomaly lineations. As discussed in Chapter 1.1, these information is very weak in the Japan Sea.

The plate tectonics show that the formation of oceanic basins such as the Japan Basin and the Yamato Basin is caused by the sea floor spreading process which is analogous to the process along the mid-oceanic ridges. This means that the formation age of the Japan Sea is represented by the age of the oceanic

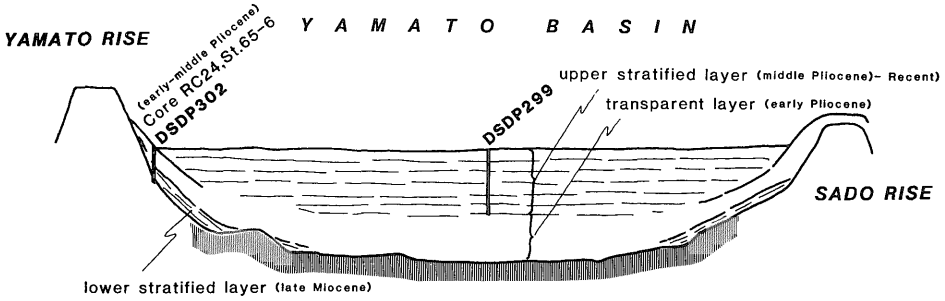

Figure 25 Summary cartoon of stratigraphy of the Yamato Basin.

basement of the Japan Basin, the Yamato Basin, and along with the other oceanic basins in the Japan Sea. Then, in this section, the author discusses the age of the oceanic basement of the Japan, the Yamato, and other significant oceanic basins in the Japan Sea.

Age of Yamato Basin

There are two deep sea drilling sites in the Yamato Basin; Site 299 in the center of the basin and Site 302 in the margin. There are many outcrops of the lower sedimentary sequence of the Yamato Basin along the surrounding topographic highs such as the Yamato Rise and the Sado Ridge. The results of two deep sea drilling sites together with the bottom sampling data from the surrounding outcrops present information effective for estimating the age of the acoustic basement of the Yamato Basin, even though the hole of Site 299 in the basin did not reach the basement. The principle of the age estimation of the Yamato Basin based on such data are summarized in a drawing shown in Figure 25.

The hole of Site 299 stopped at the bottom of the upper stratified layer and the age of the bottom of the hole was estimated to be 3.5 Ma by diatom analyses as described in Chapter 2.3. The hole did not penetrate into the transparent layer, but outcrops of the transparent layer are common on the southern slope of the Yamato Rise. Piston and gravity cores from the southern slope of the Yamato Rise such as sites RC 24 and St. 656 recovered older sediments with the age of 4 to 5 Ma. Site 302 penetrated the transparent layer and the lower stratified layer. According to these results, the age of the lower stratified layer is older than 5 Ma, presumably extending to 10 Ma. Site 302 reached the acoustic basement. SHIMAZU (1979) identified the basement rock at Site 302 as possibly Green Tuff, but the radiometric age was not given.

The lower stratified layer of Late Miocene age (5 Ma to 10 Ma) is not distributed in the central part of the basin, but is distributed only in the marginal area of the Yamato Basin. It is not easy to trace the lower stratified layer into the central basin area. The layer appears to change into the transparent layer towards the central part of the basin. The age of the bottom of the lower stratified layer is not determined at this time, but it appears not to be older than 10 Ma. The age of the bottom of the transparent layer at the central part of the basin is estimated to have almost the same age as that of the lower stratified layer at the margin. Then, the author estimates that the age

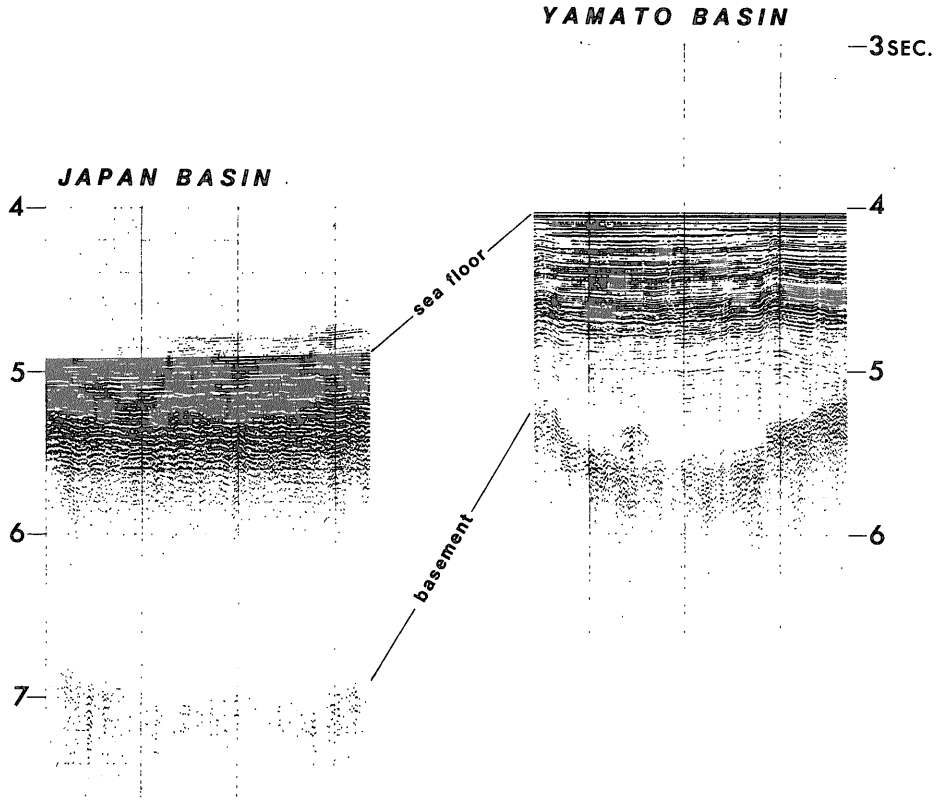

Figure 26 Typical profiles of the Japan Sea and the Yamato Basin. Both profiles represent the area of the thickest sediments of each basin.

of the acoustic basement or the age of the bottom of the sedimentary sequence of the Yamato Basin is around 10 Ma (Middle-Late Miocene).

Age estimation based on basement depth

Figure 26 shows a comparison between seismic profiles of the Japan Basin and the Yamato Basin. The figure shows the prominent difference on both basins. The Japan Basin is deeper in depth and greater in sediment thickness, and lies in deeper water. The basement depth of the Japan basin is 7.0 seconds while that of the Yamato Basin is 5.5 seconds or less. The sediment thickness of the Japan Basin is 2.1 seconds while that of the Yamato Basin is 1.5 seconds or less. The water depth is about 3650 m in the Japan Basin and about 3000 m in the Yamato Basin.

The greater basement depth of the oceanic crust is associated with the older age of the crust (PARSONS and SCLATER, 1977). The Japan Basin and the Yamato Basin are underlain by oceanic crusts (BERSENEV *et al.*, 1970 ; MURAUCHI, 1972 ; LUDWIG *et al.*, 1975). Then if the acoustic basement of the both basins represents an oceanic basaltic layer, the deeper basement of the Japan Basin indicates

Table 4 Theoretical depth of the basement ("Depth 1" and "Depth 2"), thickness of the lithosphere ("Thickness"), and heat flow value ("Heatflow 1" and "Heatflow 2") according to age variation.

Age (Ma)	Depth 1 (m)	Depth 2 (m)	Thickness (km)	Heatflow 1 (HFU)	Heatflow 2 (HFU)
5	3504	3283	16.75	5.05	5.37
6	3561	3357	18.35	4.61	4.90
7	3614	3426	19.82	4.27	4.54
8	3664	3490	21.18	4.00	4.24
9	3710	3550	22.47	3.77	4.00
10	3754	3607	23.69	3.57	3.79
11	3795	3661	24.84	3.41	3.62
12	3835	3712	25.95	3.26	3.46
13	3873	3762	27.01	3.13	3.33
14	3910	3810	28.03	3.02	3.21
15	3946	3856	29.01	2.92	3.10
16	3980	3900	29.96	2.83	3.00
17	4013	3943	30.88	2.74	2.91
18	4046	3985	31.78	2.66	2.83
19	4077	4026	32.65	2.59	2.75
20	4107	4065	33.50	2.53	2.68
21	4137	4104	34.32	2.47	2.62
22	4166	4142	35.13	2.41	2.56
23	4195	4179	35.92	2.36	2.50
24	4223	4215	36.69	2.31	2.45
25	4250	4250	37.45	2.26	2.40
26	4277	4285	38.19	2.22	2.35
27	4303	4319	38.92	2.17	2.31
28	4329	4352	39.63	2.14	2.27
29	4354	4385	40.33	2.10	2.23
30	4379	4417	41.02	2.06	2.19
31	4403	4449	41.70	2.03	2.16
32	4427	4480	42.37	2.00	2.12
33	4451	4511	43.03	1.97	2.09
34	4474	4541	43.67	1.94	2.06
35	4497	4571	44.31	1.91	2.03
36	4520	4600	44.94	1.88	2.00
37	4542	4629	45.56	1.86	1.97
38	4564	4658	46.17	1.83	1.95
39	4586	4686	46.78	1.81	1.92
40	4608	4714	47.37	1.79	1.90
41	4629	4741	47.96	1.76	1.87
42	4650	4768	48.54	1.74	1.85
43	4671	4795	49.12	1.72	1.83
44	4691	4822	49.68	1.70	1.81
45	4711	4848	50.24	1.68	1.79

Calculation formula is as follows. "Age" is in Ma.
Depth 1=2900+270*SQRT(Age)···HAYES (1983), Depth 2=2500+350*SQRT(Age)···PARSON & SCLATER (1977), Thickness=7.49*SQRT(Age)···YOSHII *et al.* (1976), Heatflow 1=11.3/SQRT(Age)···PARSON & SCLATER (1977), Heatflow 2=12/SQRT(Age)···DAVIS & LISTER (1977)

an older age than that of the Yamato Basin. The thicker sediments of the Japan Basin also supports this comparative age estimation. The thicker sediments in the Japan Basin correspond to an older age of the basin, although there is a problem with sedimentation rate. Both basins have a similar acoustic sedimentary sequence, which may suggest that the sedimentation rate in the both basins is similar. Thus, it is probable that the Japan Basin is older than the Yamato Basin, if the acoustic basements of the both basins are oceanic. Seismic refraction data, however, suggest that the acoustic basement of the Yamato Basin is different from that of the oceanic crust. The problem will be discussed in later in this section.

Table 4 shows the relation among the age of the oceanic crust, the theoretical water depths, lithospheric thickness, and heat flow values. Theoretical depths and heat flow values are shown for two cases. It should be noted that the theoretical water depth is the water depth without sediments. So, a sediment loading correction is needed in the case of the basins which have a thick sedimentary cover such as the basins in the Japan Sea. If the sedimentary cover is removed from the basin, the basement of the basin will rebound isostatically. The basement depth of isostatic compensation after removal of the sediments should be that estimated by the theoretical age.

CROUGH (1983) presented a simple formula for the sediment loading correction of an oceanic basin. The correction formula is as follows.

Basement depth after sediment loading correction (m)
= (water depth (m)) + 600
× (two-way sediment thickness (sec))

In the case of the Japan Basin on Figure 26, the water depth is 3630 m and the two-way sediment thickness is 2.1 seconds. Then the basement depth after the sediment loading correction is obtained as 4890 m as follows.

$$3630 + 6000 \times 2.1 = 4890 \text{ m}$$

For example, the basement depth of 4890 m corresponds to an age older than 45 Ma according to Table 4. Depth 1 and Depth 2 on the table, however, show the theoretical depths of an open ocean such as the Pacific and Atlantic Ocean.

The basement depth of back-arc basins is definitely greater than the theoretical depth, where the age determination is well established (SCLATER, 1972). The Shikoku Basin, which is documented to have been active during 30 Ma to 15 Ma based on the deep sea drilling results and the identification of magnetic anomaly lineations (KLEIN and KOBAYASHI, 1980), has a basement depth of 4500 to 5000 m. The range of age and basement depth of the Shikoku Basin shows a discrepancy with the theoretical age of Depth 1 and Depth 2 in the table. The basement depths of back-arc basins appear to be 1000 m greater than those of normal oceanic basins (KOBAYASHI, 1984). But no definite theoretical age-depth relation has been established in back-arc basins. Therefore, the author tried to compare the basement depths of the Japan and Yamato Basins with other back-arc basins where the age of the basins are well documented. The results are shown in Figure 27.

Figure 27 shows that the age range of the Japan Basin is comparable with those of the Shikoku Basin and South China Sea Basin. The Shikoku Basin has an age range of 30 to 15 Ma and the South China Sea Basin has an age range of 32 to 15 Ma. Then, it is probable that the Japan Basin has an age range of about 30 to 15 Ma. The depth range

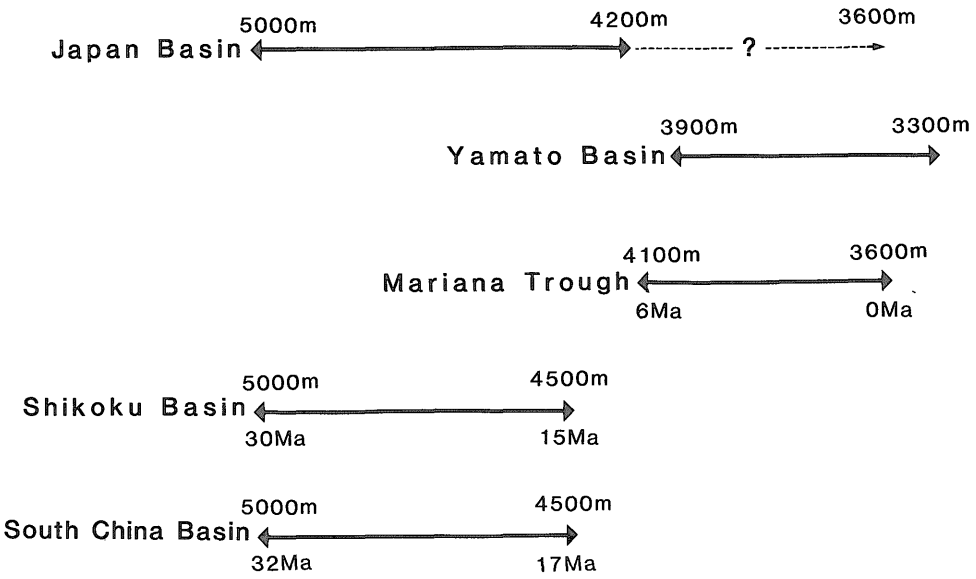

Figure 27 Basement depths after sediment loading correction of the Japan and Yamato Basins with those of other several back-arc basin whose ages are well established by DSDP holes and/or identification of magnetic anomaly lineations.

of the Kuril Basin is also comparable with that of the Japan Basin although the age is not established. The comparison between the both basins is discussed in Chapter 3.5.

Figure 27 also shows that the age range of the Yamato Basin is very young less than 6 Ma. This estimation shows a large discrepancy with the former stratigraphic age estimation of around 10 Ma. The problem will be discussed later in this section.

Age estimation based on heat flow value

The theoretical age-heat flow relation is applicable to back-arc basins, although the theoretical age-depth relation does not match in the back-arc basins. TAYLOR and HAYES (1983) confirmed that the theoretical age-heat flow relation in the open ocean is valid in the South China Sea Basin. The author examined the heat flow data in the Japan Sea based on the digital heat flow data file of YOSHII and YAMANO (1983).

The heat flow data of the basin area are selected from about 100 sites of the heat flow measurements in the Japan Sea. The sites were selected from the areas where the sediment thickness is greater than 300 m and where there are no seamounts in a range of 10 km. The other sites were rejected. The results are shown in Table 5 and Figure 28.

The average heat flow value of the Japan Basin is 2.26 HFU. The value of 2.26 HFU corresponds to an age of 25 to 28 Ma. The average heat flow value of the Yamato Basin is 2.34 HFU. The value of 2.34 HFU corresponds to an age of 23 to 26 Ma. It should be noted that the average heat flow value of the Japan and Yamato Basin are very close and that the age estimation based on the average heat flow value of the Yamato Basin show a large discrepancy with the age estimation based on other techniques such as stratigraphy and basement

Table 5 Heat flow values with the average of the basins in the Japan Sea and Okhotsk Sea. The heat flow values are selected from YOSHII and YAMANO's (1983) heat flow digital data file according to the manner that the sites of the sediment thickness less than 300 meters are rejected and that the sites near to topographic highs with the range of 10 km are also rejected.

JAPAN BASIN	2.88	2.69	2.66	2.65	2.64	average hf of
	2.64	2.62	2.62	2.60	2.60	Japan Basin=2.26
	2.58	2.57	2.53	2.51	2.50	
	2.50	2.48	2.48	2.44	2.44	
	2.42	2.39	2.38	2.37	2.32	
	2.28	2.28	2.25	2.24	2.22	
	2.20	2.20	2.19	2.18	2.15	
	2.14	2.14	2.13	2.13	2.13	
	2.12	2.12	2.11	2.08	2.07	
	2.07	2.07	2.05	2.05	2.03	
	2.02	2.02	2.01	2.00	1.99	
	1.98	1.95	1.91	1.89	1.87	
	1.70	1.40				
YAMATO BASIN	3.46	2.77	2.66	2.58	2.56	average hf of
	2.45	2.44	2.43	2.43	2.39	Yamato Basin=2.34
	2.36	2.35	2.34	2.33	2.32	
	2.32	2.31	2.21	2.16	2.16	
	2.15	2.13	2.12	2.12	2.07	
	2.05	2.02	1.95			
TSUSHIMA BASIN	2.46	2.40	2.36	2.25	2.16	average hf of
	2.12					Tsushima Basin=2.29
TARTARY TROUGH	3.28	2.40	2.32	2.29	2.18	average hf of
	1.99					Tartary Trough=2.41
MOGAMI TROUGH	1.28	1.39	1.40	1.61		average hf of
						Mogami Trough=1.42
OKI TROUGH	1.99	1.89	2.08	1.73		average hf of
						Oki Trough=1.92
KITAYAMATO T.	1.80	1.80				average hf of
						Kitayamato Trough=1.80
KURIL BASIN	2.82	2.58	2.57	2.53	2.41	average hf of
	2.33	2.28	2.27	2.22	2.21	Kuril Basin=2.33
	2.20	2.11	2.11	1.91		

depth. The average heat flow values of the Tsushima Basin (2.29 HFU) and the Tartary Trough (2.41 HFU) are also close to those of the Japan and Yamato Basins.

The heat flow data tend to appear less than the true heat flow value bacause of the mass heat transfer by water circulation in the sediments and the basement rocks, while they rarely appear larger than the true heat flow value. Thus, the discussion of the highest heat flow value is valid.

The highest heat flow value in the Japan Basin is 2.88 HFU which corresponds to an age of 15 to 18 Ma. The

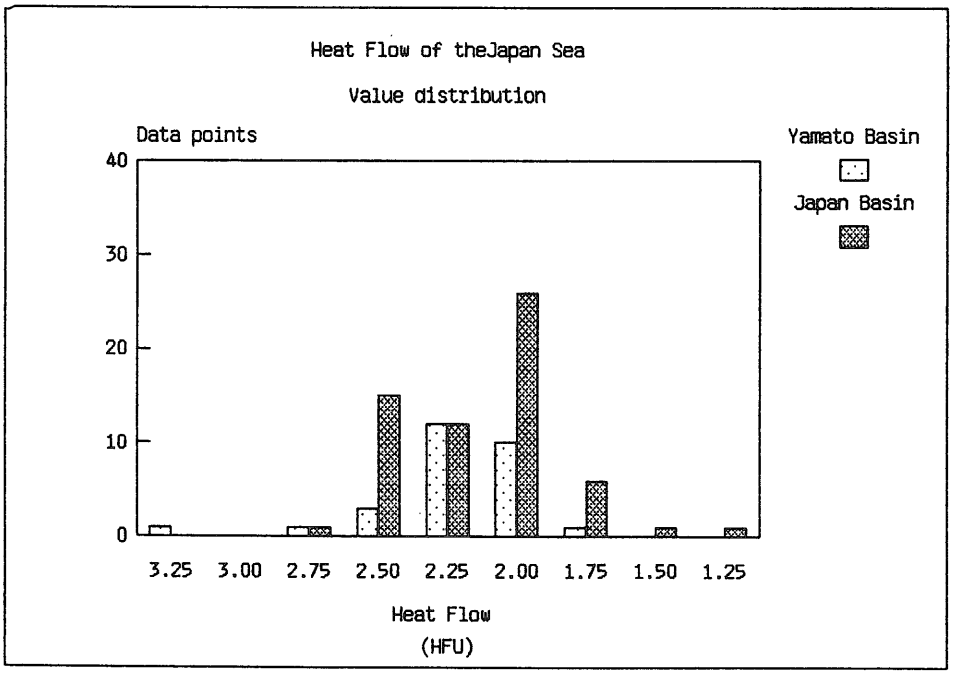

Figure 28 Distribution of heat flow values in the Japan Basin and the Yamato Basin. The heat flow data are after YOSHII and YAMANO's (1983) digital heat flow data file.

highest heat flow value in the Yamato Basin is 3.46 HFU which corresponds to an age of 10 to 12 Ma. An age of 10 to 12 Ma for the Yamato Basin is comparable to the stratigraphic age estimation. The comparison of the highest heat flow value in the Japan and Yamato Basins shows the younger age of the Yamato Basin. The sites of the highest heat flow of each basin are located at the central part of the Japan Basin and at the marginal part of the Yamato Basin. The highest value in the Yamato Basin is isolated on the distribution graph of Figure 28. The heat flow data present a valuable information for the age estimation of the Japan Sea but they appear to be insufficient for a detailed discussion.

Summary of the age of the basins

Figure 29 summarizes the above discussion about the age of the Japan and Yamato Basins. The results of the age estimation based on basement depth and heat flow of the Japan Basin show the range of 30 to 15 Ma. The true age determination will be made by further deep sea drilling and magnetic anomaly surveys.

On the contrary, the results on the Yamato Basin show a large discrepancy among the three age estimations of stratigraphy, basement depth, and heat flow. Heat flow values show the age range from 30 or more to 10 Ma. The stratigraphy shows the age to be around 10 Ma. The basement depth shows the age to be less than 6 Ma. The Yamato Basin is overlain by a thick accumulation of sediments which are not strongly deformed. The structural features do not show any active spreading in the basin. Therefore, the age estimation by

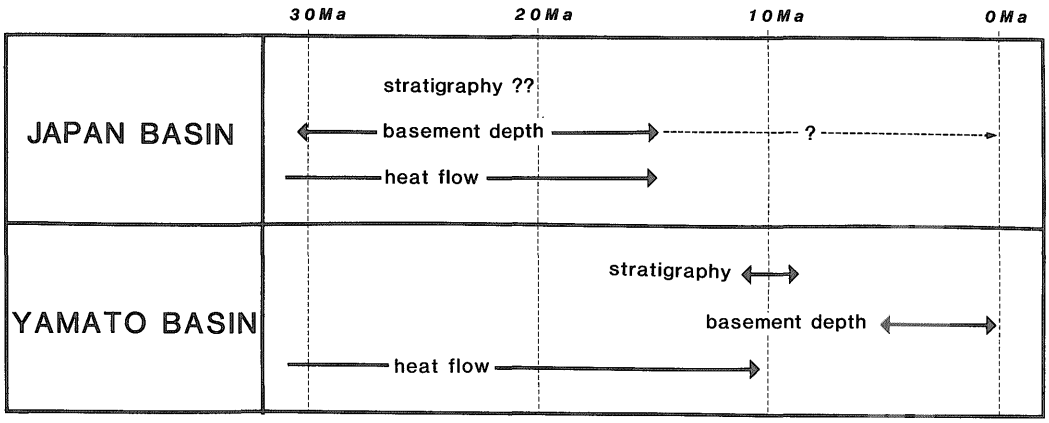

Figure 29 Summary sheet of the age of the Japan Basin and the Yamato Basin based on several estimation methods.

basement depth of 6 to 0 Ma is unrealistic.

A possible explanation for this discrepancy is that the acoustic basement of the Yamato Basin does not represent the oceanic crust and that the true oceanic crust underlies the acoustic basement. According to the seismic refraction study of the Japan Sea by LUDWIG *et al.* (1975), the acoustic basement of the Yamato Basin has slower sonic velocity of 3.5 km/sec than the normal oceanic basalt layer of 4.5 km/sec. If a deeper true basement is under the Yamato Basin, the heat flow value of the basin is probably comparable with that of the true basement. The stratigraphic estimation of the age of the Yamato Basin is based only on the thickness of sedimentary layer. The rather young age from the stratigraphic estimation is reasonable if the 3.5 km/sec layer intervenes between the sedimentary layer and the true basement.

LUDWIG *et al.* (1975) pointed out the possibility that the 3.5 km/sec layer is correlated to Green Tuff. Some profiles of the Yamato Basin such as Line N 8 of Figure 10 show more shallow acoustic basement in the marginal part and deeper basement in the central part of the basin. The back-arc basins commonly have a more shallow basement in the central part, because the back-arc basin was formed symmetrically by a spreading center as the younger crusts represent more shallow basement depth. The structure of the Yamato Basin with deeper basement in the central part is incompatible with back-arc spreading. Such structure, however, is not unreasonable on the assumption that the acoustic basement of the Yamato Basin represents volcaniclastics such as Green Tuff and that the marginal more shallow acoustic basement in due to thicker accumulation of the volcaniclastics. The thicker accumulation of the volcanoclastics in the margin of the basin will be discussed in Chapter 3.3.

The more shallow acoustic basement in the marginal part of the basin is also the case in the Japan Basin. A broken line arrow in Figure 29 shows this feature. Figure 30 shows a continuous profile through the Japan Basin and the Yamato Basin. The decreasing basement depth toward the Yamato Basin is observed on the profile. The profile may indicate thicker volcaniclastic accumula-

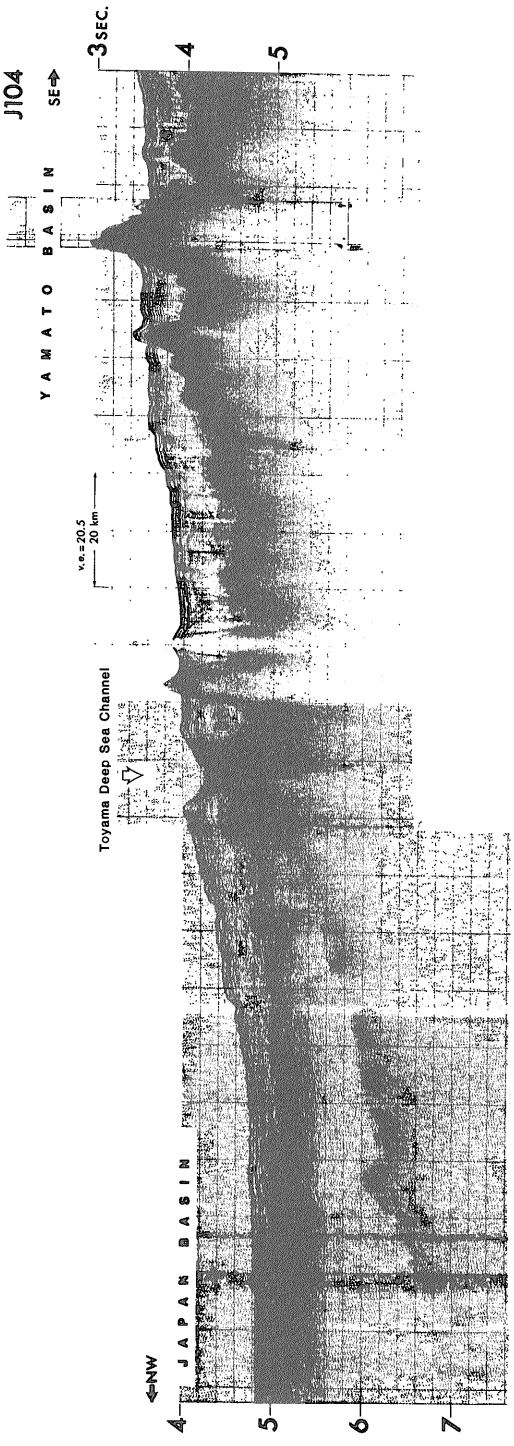

Figure 30 Continuous seismic profile from the Japan Basin to the Yamato Basin on Line J 104.

tions toward the margin of the Japan Basin and the Yamato Basin.

In conclusion, the Japan Basin has an age range of about 30 to 15 Ma and the Yamato Basin has that of 30 to 10 Ma. The Tartary and the Tsushima Basins are estimated to have similar age range of the Japan and the Yamato Basins.

3.2 Origin of the topographic highs of the Japan Sea

There are many topographic highs in the Japan Sea (Fig. 2). The Japan Sea has and extraordinary many topographic highs in comparison to other back-arc basins. The South China Sea Basin also has abundant of topographic highs, but the outstanding feature of the Yamato Rise in the center of the Japan Sea should be noted. The southern part of the Japan Sea is occupied by an especially large number of topographic highs (Fig. 31). The origin of the topographic highs should be closely related to the tectonics of the Japan Sea.

The author divided the topographic highs into four groups based on the geological structure. They are continental fragments, rifted continental fragments, tectonic ridges, and volcanic seamounts. Their distribution is summarized in Figure 32 excluding the tectonic ridges. The detail of each group is as follows.

(1) Continental fragments

The topographic highs composed of continental crust are assigned to this group. Many granitic rocks are recovered from the topographic highs in the Japan Sea. The Yamato Rise, the Korea Plateau, the Ullung Plateau, the Kita-Oki Bank, the Oki Bank, and the Musashi Bank are the typical example of continental fragments. The Bogorov Seamount is also included in this group according to the Russian scientists (e.g.,

Figure 31 3-D topographic view of the southern part of the Japan Sea. The data used for processing are GEBCO digital bathymetric data of JODC and GSJ digital bathymetric data. Processing system is SIGMA of Geological Survey of Japan.

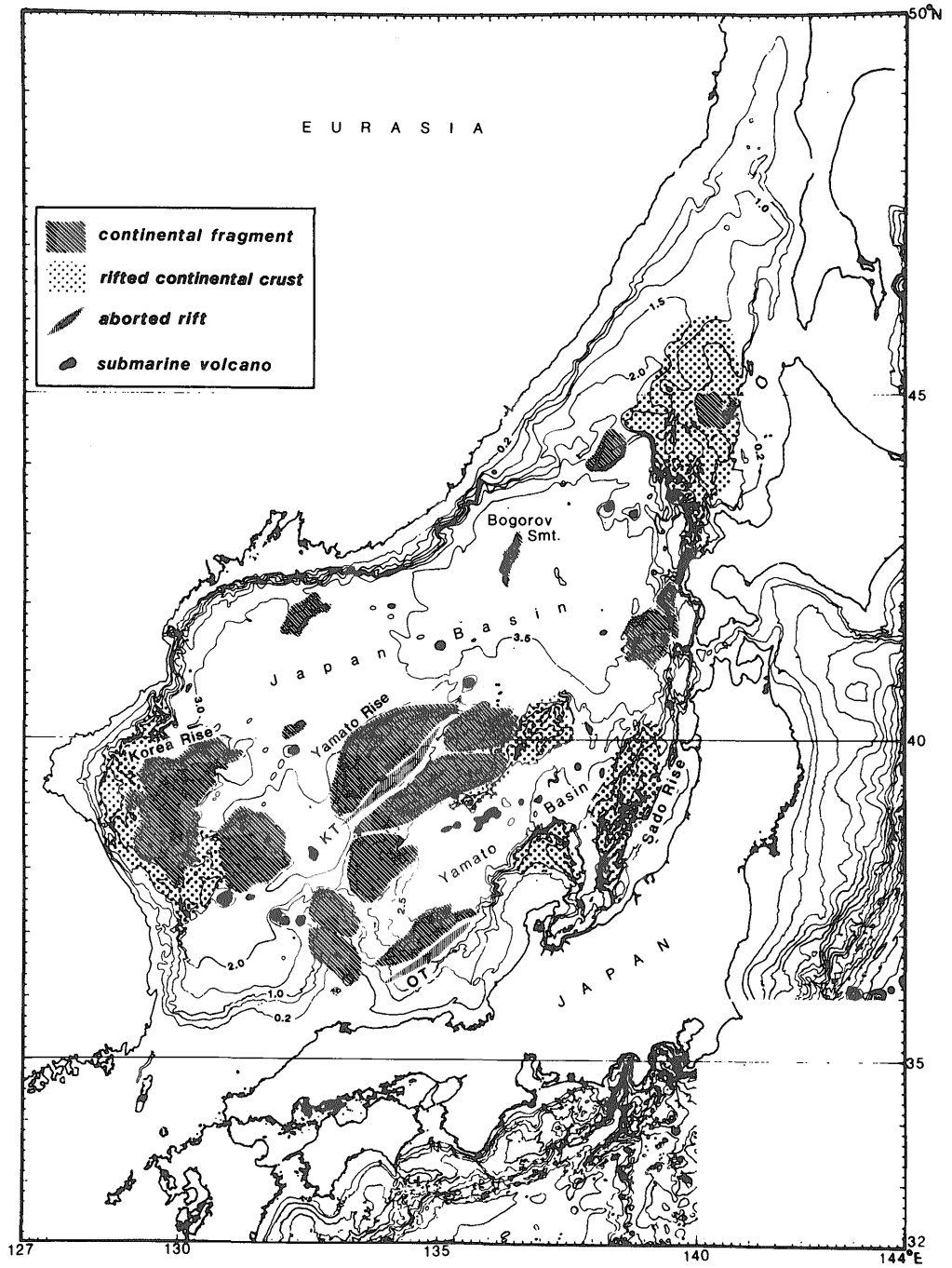

Figure 32 Classification of the topographic highs of the Japan Sea.

MELANKHOLINA and KOVYLIN, 1977; GNIBIDENKO, 1979). Older granitic rocks from Precambrian to Cretaceous are distributed on the topographic highs as described in Chapter 2.4. Most of the large topographic highs in the Japan Sea are included in this group. The scattered distribution of continental fragments makes an effective constraint for discussing the spreading system of the Japan Sea. The mechanisms that caused such a scattered distribution of the numerous continental fragments is a principal problem for discussion. This discussion is in Chapter 3.3.

(2) Rifted continental fragments

A rifted continental fragment is a continental fragment which was thinned and stretched by the rifting activity. This group was identified as deeply submerged basement highs with very rugged morphology. One typical example is the northern extension of the Musashi Bank which is shown in Figure 15. Horst and graben structures are prominent there. This structure is analogous to that of the lower continental slope of the Atlantic continental margin (DINGLE and SCHURUTTON, 1977). Such features are inferred to be foundered continental crust which was rifted by the initial generation of oceanic crust within the continental crust (MONTADERT *et al.*, 1977). The Takuyo Bank and the Sado Rise are inferred to be the other examples of rifted continental fragments. The Sado Rise is the foundation rise of the Sado Ridge which is shown in Figure 10. The Sado Rise is also included in the rifted continental fragments. The Sado Ridge itself is classified as a tectonic ridge. The small rises around the Yamato Rise, especially the northeastern end of the rise, are also included in this group. The Hakusanse Bank off the Note Peninsula may also belong to this group. A rifted continental fragment is inferred to be stretched from its original configuration. The identification of the distribution of the rifted continental fragments is important for the reconstruction of the spreading history of the Japan Sea.

(3) Tectonic ridges

The Okushiri Ridge and the Sado Ridge belong to this group. Recent EW convergent tectonics is evident along these ridges accompanying the active thrust faults and compressional type earthquakes. The ridges are bounded by thrust faults on either side or both sides. The thrust faults have been active since latest Pliocene. Several compressional type earthquakes with magnitudes of M 6.9 to M 7.7 occurred along these thrust faults. The topographic highs of this group are formed by the thrust movements associated with the uplift of the hanging side over the footwall. A detailed discussion about the Okushiri and the Sado Ridges is made in Chapter 3.4.

(4) Volcanic seamounts

Many seamounts and knolls are distributed throughout the Japan Sea besides the large topographic highs such as rises, plateaus, and banks. They are almost all volcanic in origin. There are two groups of volcanic seamounts. The one group was formed by the recent day island arc activity. The Northeast Japan Arc and the Southwest Japan Arc have a broad volcanic zone which extends into the offshore area of the Japan Sea. Takeshima Island, Ullung Island, and possibly the Shiribeshi Seamount west of Hokkaido are included in this group. Takeshima and Ullung Islands are covered by alkali basalt which is related to the recent volcanism of the Southwest Japan Arc. The other group consists of older seamounts and knolls whose

activities were presumably synchronous with the spreading activity of the basin area. Such seamounts and knolls are commonly observed in the Japan Basin and the Yamato Basin. The Yamato Seamount Chain and the Central Yamato Seamount chain are the typical examples of this group. Both seamount chains appear to be composed of andesites. Andesites from the Matsu Seamount of the Yamato Seamount Chain are dated to be 4.16 ± 0.16 Ma (UENO *et al.*, 1971). Unknown rocks from Meiyo No. 2 Seamount are dated to be about 13 Ma (OZIMA *et al.*, 1972). The age of these seamounts is possibly synchronous with the basin formation and presents information for the formation age of the basin area.

Aborted rifts are annotated in Figure 32. Some possible major aborted rifts are common on and in between the continental fragments in the Japan Sea. Figure 33 shows a profile of the Kita-Yamato Trough in the Yamato Rise which is the largest possible aborted rift in the Japan Sea.

The tectonic origins of topographic highs mentioned above are discussed in Chapters 3.3 and 3.4.

3.3 Tectonics of back-arc spreading

The tectonics of back-arc spreading have been controversial since KARIG (1981) originally proposed the concept of back-arc spreading. There are several ideas about the origin of the back-arc spreading. They are classified into three groups as follows.

1) Excess mass upwelling, which is generated in association with subduction of the oceanic plate beneath the island arc, causes the back-arc spreading (KARIG, 1971).

2) Secondary induced mantle convection beneath the island arc causes the back-arc spreading. The convection is generated by the drag force of the subducting oceanic plate (e.g., SLEEP and TOKSOZ, 1971).

3) Divergent movement between the plates causes the generation of new oceanic crust in the gap. In this case, back-arc spreading occurs passively. There are two ideas on the divergent vectors over island arcs. MOLNAR and ATWATER (1978) considered that oceanward retreat of trench is significant for back-arc spreading. They considered that the old and cold lithosphere sinks into the asthenosphere and causes the oceanward retreat of trench. On the contrary, UYEDA and KANAMORI (1979) considered that the retreat of the back-arc plate is significant for the generation of the back-arc basin.

There is a significant difference between the former two models and the last one mentioned above. The former two models are based on the active extension or spreading force in the back-arc basin which is caused by mass upwelling or secondary induced mantle convection. In these two cases, the spreading center in the back-arc basin will cause compressional stresses in the surrounding area including the arc region and also the spreading center should be fixed in the reference frame of the trench axis. The study of the Mariana Arc, which is associated with a typical active back-arc basin, however, shows that the Mariana Arc is entirely under tensional stresses including the forearc area (HUSSONG and UYEDA, 1982; FRYER and HUSSONG and FRYER, 1982). Almost all the back-arc basins are generated symmetrically from a spreading center which migrates landward from the trench axis. These observations indicate that there is no active force from the spreading ridge.

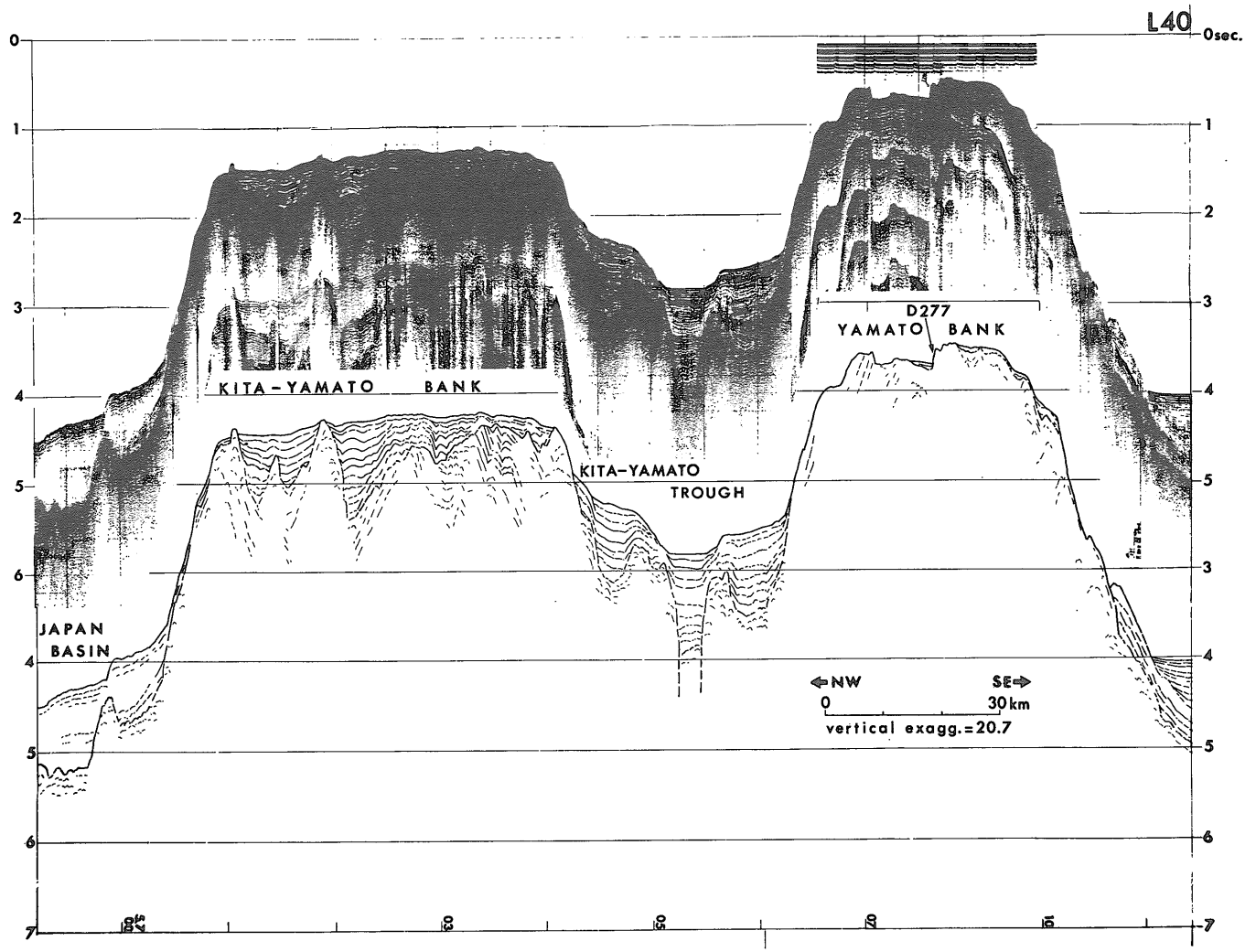

Figure 33 Seismic profile and its interpretation of the Kita-Yamato Trough. Graben structure is remarkable in the trough.

DEWEY (1980) summarized the tectonics of island arcs in the reference frame of three significant plates ; the back-arc plate, the forearc sliver (forearc plate), and the oceanic plate. DEWEY explained the tectonic origin of back-arc spreading very reasonably. His model is a refined version of the third model, the passive spreading model. The tectonics of island arcs are well described by three plates, the subducting oceanic plate, the back-arc plate, and the forearc plate (Fig. 34). The arc volcanic zone marks a boundary between the back-arc plate and the fore-arc plate, because the lithosphere of the island arc is hot, thin, weak, and then ductile along the volcanic zone. In other words, the arc is decoupled along the volcanic zone and forms two plates, the forearc plate and the back-arc plate. The subducting oceanic plate, the forearc plate, and the back-arc plate have their own moving vectors. The significant vectors for back-arc spreading are the moving vectors of the back-arc and the forearc plates. If the back-arc plate and the forearc plate are diverging to each other, the volcanic zone is placed under tensional stress and the tensional stress produces a rift system along the volcanic zone. Such a rift system is observed in the present day Bonin Arc (TAMAKI *et al.*, 1981 b ; TAMAKI and MIYAZAKI, 1984).

The Bonin Arc is presently undergoing incipient back-arc spreading. Rifting of the arc is in progress just along the volcanic front. The volcanism of the Bonin Arc is concentrated in the volcanic front, forming an active volcanic ridge (the Shichito Ridge), due to the high dip angle (60° to 75°) of the subducting slab. The rifts are not continuous but segmented (Fig. 35). Figure 36 shows one of the typical profiles of the rift near Sumisu Island in the Bonin Arc. The rifts are now extending and will join together to make a single rift system parallel with the trench. If the extensional stress is sustained, the rift system will cause a spreading center of a new back-arc basin. The rifting feature of the Bonin Arc shows that, when the arc is extensional, the break-up of the arc occurs along the volcanic front where the arc is weakest.

It should be noted that the moving vector of the subducting oceanic plate scarcely affects the movement of the forearc plate and that the vector is not significant for back-arc spreading. The significant factor for constraining the movement of the forearc plate is the migration of the trench. DEWEY (1980)

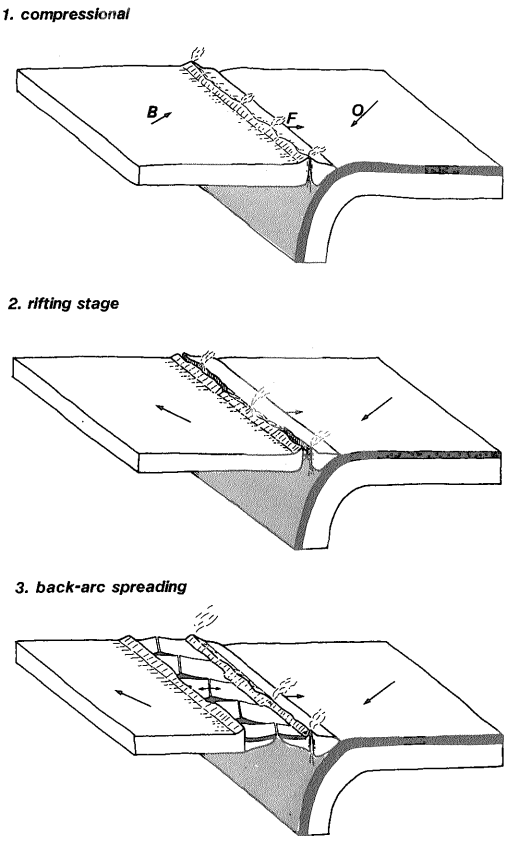

Figure 34 Rifting and back-arc spreading of the arc with single volcanic chain.

proposed that the trench should substantially retreat oceanwards or roll back. This roll back of trench is according to the idea of MOLNAR and ATWATER (1978). The greater is the age of the oceanic plate, the larger is the roll back vector of the trench will be. Thus, the roll back vector of the trench is significant for constraining the movement of the forearc plate. The migration of trench, however, is not restricted to roll back movement. CARLSON and MELIA (1984) pointed out the possibility of landward migration or roll forward of the trench in the case of the Bonin Trench. The moving vector of the forearc plate is also constrained by drag forces which are caused by the oblique subduction of the oceanic plate when the arc is under compressional stresses (KIMURA and TAMAKI, 1985). The drag force vector parallels to the trench. The magnitude of the drag force vector is less than the trench-parallel component of the moving vector of the subducting oceanic plate which is parallel to the trench. The moving vector of the forearc plate is calculated by the summation of the trench roll back vector and the drag force vector. The trench roll back vector is more significant for back-arc spreading than the drag force vector.

Thus, the two vectors, the trench roll back vector and the moving vector of back-arc plate, are significant for back-arc spreading. If there is some divergent component between the two vectors, rifting of the arc is initiated and it will be developed into back-arc spreading (Fig. 34). Then, when we discuss the tectonics of the back-arc spreading of the Japan Sea, we have to estimate the trend and the magnitude of both vectors.

The spreading of the Mariana and Bonin Arcs causes simple single rift system, as the volcanic chain along the island arc is arranged on a line. The single volcanic chain is due to the concentration of volcanic activity along the volcanic front which is further due to the steep dip angle of the subduction slab. A spreading system developed from the single rift system usually causes a single lineated remanent arc such as the Kyushu-Palau Ridge and the west Mariana Ridge in the Philippine Sea. The spreading of a single rift system like this would not cause scattered continental fragments in the oceanic basins as shown in the Japan Sea. Spreading with a single rift system is not the case for the Japan Sea. The plausible spreading causing the scattered continental fragments is as follows. Figure 37 summarizes this concept in 3-D cartoons.

In the case of the Japan Sea, many parallel rifts appear to have been formed in a wide volcanic zone. The wide volcanic zone of the island arc corresponds to the low dip angle of the subducting slab. Large tensional forces over the wide volcanic zone caused many rifts accompanying the volcanoes as multi rift system (Fig. 37, 2). Some of the rifts were failed and left as remnant rifts such as the Kita-Yamato Trough and the Oki Trough. Other rifts were joined together and developed into spreading centers of the back-arc basin. In the course of the development, many continental fragments were formed and trapped in the Japan Sea as remnant arcs such as the Yamato Rise, the Korea Rise, the Bogorov Seamount, and so on. Stretching of the continental lithosphere may also have occurred at some places due to the activity of multi rift system and caused the rifted continental fragment such as the Sado Rise.

The low dip angle subduction causes a wide volcanic zone of island arc. Arc volcanism should still be active during

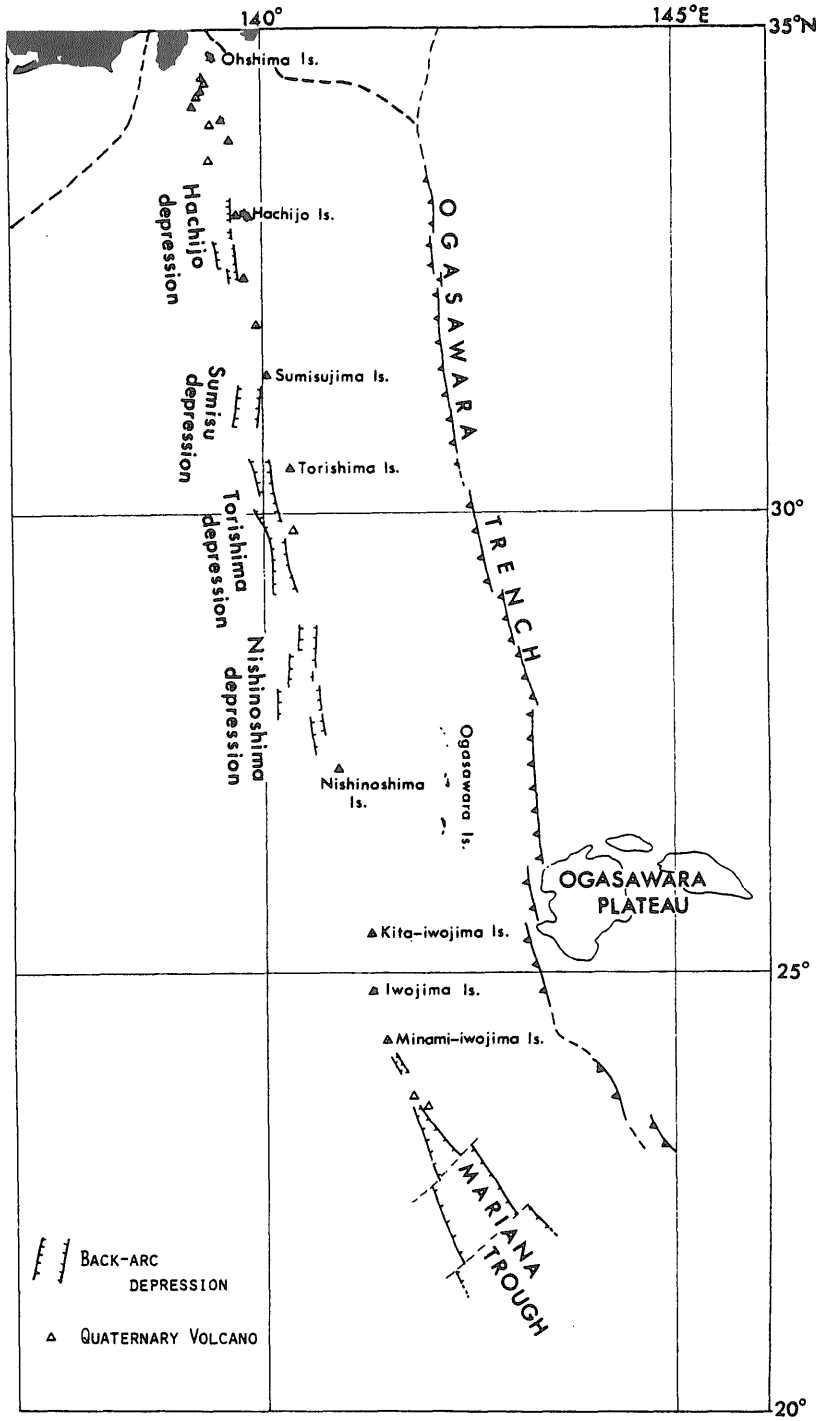

Figure 35 Rift system of the Bonin Arc (TAMAKI *et al.*, 1981).

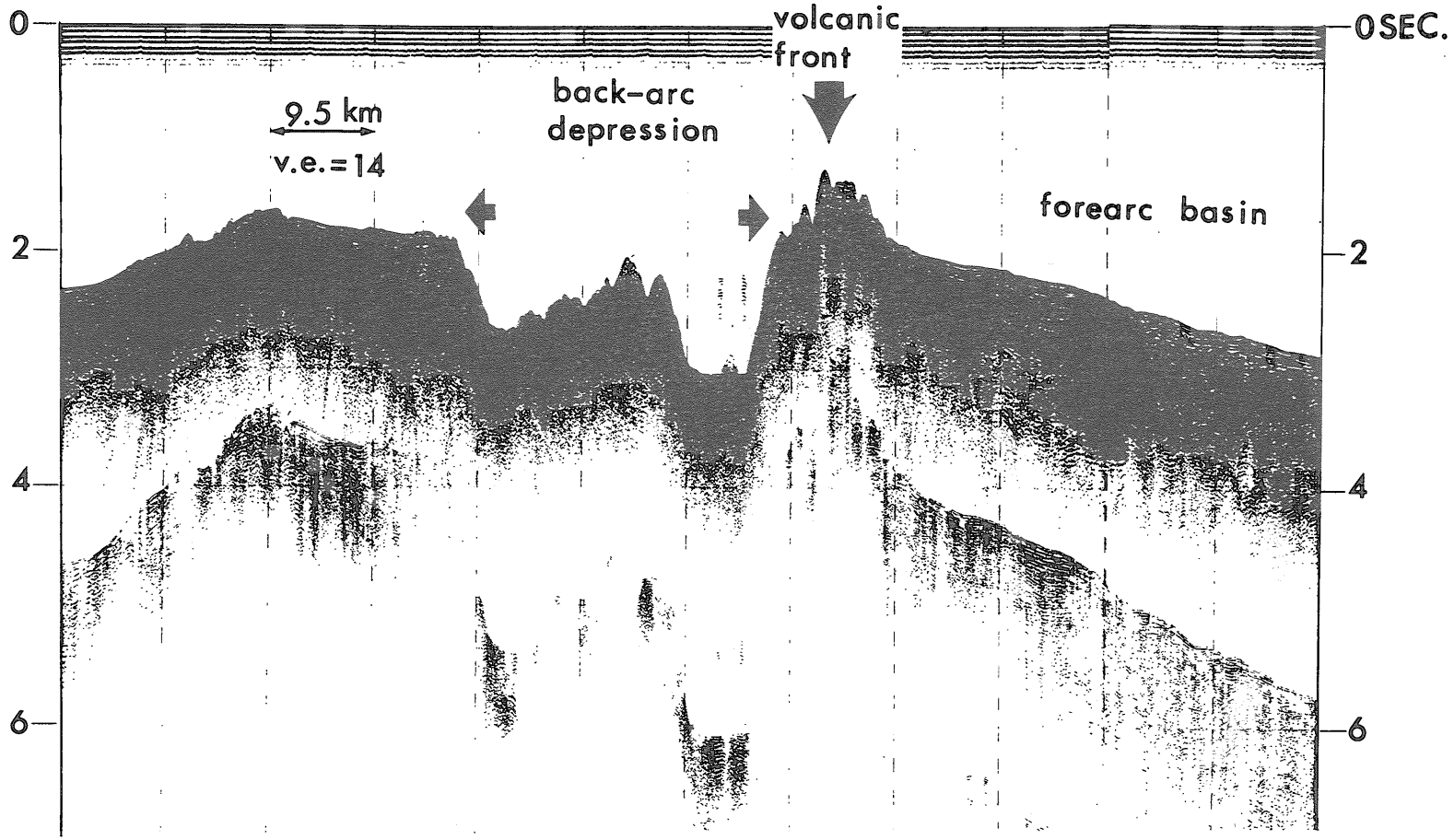

Figure 36 Seismic profile of the Sumisu Depression, one of the rift of the Bonin Arc.

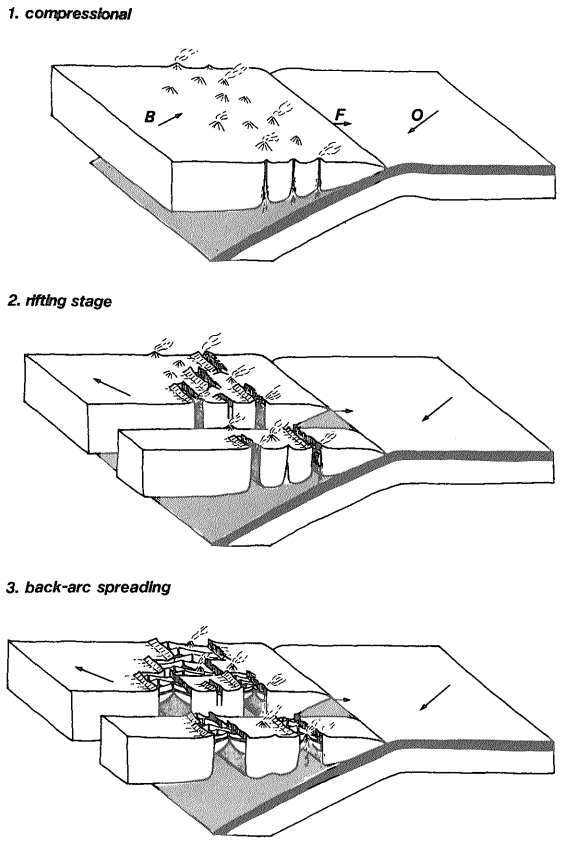

Figure 37 Rifting and back-arc spreading of the arc with broad volcanic zone.

the development of rifts and spreading systems. Large tensional stress in the back arc area improves the arc volcanism resulting in an accumulation of thick volcanic materials on the basaltic layer of the basement along with the occurrence of many seamounts and knolls. The accumulated volcanic materials are correlated to Green Tuff. The overprinting of arc volcanism and back-arc spreading activity is the case of the Yamato Basin, where thick accumulations of volcanic materials on the oceanic basaltic layer are presumed and abundant andesitic seamounts and knolls are observed. The overprint of arc volcanism over the back-arc spreading activity occurs in the arc volcanic zone. Thus, the distribution of such overprinting features is prominent in the marginal area of the back-arc basin and back-arc side of the Japanese Islands.

Thus the back-arc spreading of the Japan Sea is different from that of the Mariana-Bonin Arc. The author calls the case of the Mariana-Bonin Arc as a single rift type back-arc spreading and the case of the Japan Sea a multi rift type back-arc spreading (Fig. 38). The back-arc spreading systems and their resultant geological and geophysical features are quite different each other (Table 6). Remnant arcs are single and continuous in the single rift type but segmented in the multi rift type. Seamounts are rare in the single rift type but abundant in the multi rift type. The crust is pure oceanic in the single rift type but overprinted by island arc volcanism in the multi rift type. Aborted rifts are rare in the single rift type but common in the multi rift type. As a result, the spreading system is simple in the single rift type and complicated in the multi rift type. The multi type causes a complicated geological and geomorphological feature of the back-arc basin.

The two types are end members and there are probably many gradual variations between the two types. Typical multi rift type back-arc spreading like the Japan Sea, however, is very scarce. The South China Sea may be rare another case of the multi rift type.

In conclusion, back-arc spreading is initiated with the rifting along a volcanic zone of the arc when the arc is under extensional tectonics, because the arc is hottest, thinnest, and weakest along the volcanic zone (DEWEY, 1980). Then, the width of volcanic zone of the arc, which is closely related to the dip angle of subducting slab, should cause a variation

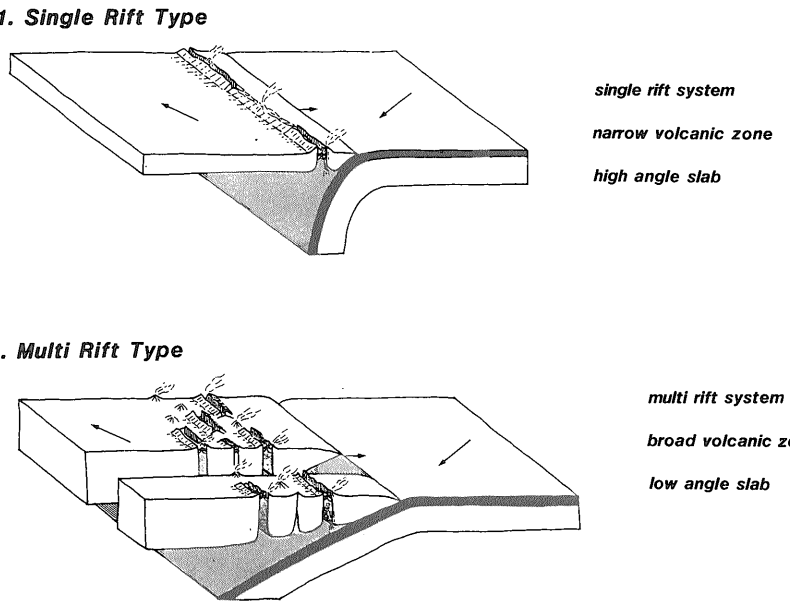

Figure 38 Two modes of arc rifting and back-arc spreading : multi rift type and single rift type.

Table 6 Summary of characteristics of the single rift type and the multi rift type.

	Single Rift Type	Multi Rift Type
remnant arc	single/continuous	segmented
seamount	rare	abundant
crust	oceanic	overprinted by island arc volcanism
aborted rift	rare	common
spreading system	simple	complicated

in the initial rifting and succeeding back-arc spreading ; the multi rift type and single rift type. The multi rift type back-arc spreading is the case of the Japan Sea with the resultant complicated geological and geomorphological feature. The origin of the large tensional stress over the broad volcanic zone may be possible when the continent behind the Japan Sea retreats.

3.4 Recent crustal movement along the eastern margin of the Japan Sea

Submarine topography of the Japan Sea shows an outstanding contrast between the western side (continental side) and the eastern side (Japan side) as is well shown in Figure 2. The continental slope of the western side of the Japan Sea shows a simple slope, while the continental slope of the eastern side shows a complicated feature with many ridges and troughs parallel to the coast line (Fig. 39). This topographic contrast indicates that the continental side and the Japanese side of the Japan Sea have a different geological history.

The complicated topography of the

eastern side of the Japan Sea is shown from the north of the Toyama Bay to the west of the Soya Strait. The complicated topography consists of the Okushiri Ridge and the Sado Ridge. There are several basins and troughs developed between the Okushiri/Sado Ridges and the Japanese Islands, such as the Mogami Trough, the Nishitsugaru Basin, the Okushiri Basin, the Shiribeshi Trough, and the Futago Basins. The Okushiri Ridge is developed north of the Oga Peninsula and is nearly NS trending. The Sado Ridge is developed south of the Oga Peninsula and trends NNE.

Origin of the ridges and basins along the eastern margin of the Japan Sea

It is rather easy to identify the faults on the seismic profiles. The identification of their nature in terms of normal or reverse (thrust), however, is difficult on the single channel seismic profiles. This is because the vertical exaggeration on the record is high, such as 10 to 20, usually. For example, a fault with a dip angle of 30 degrees shows an apparent dip angle of 85 degrees on a record with a vertical exaggeration of 20. Thus, almost all faults show a nearly vertical dip angle on the single channel seismic records. So, it is important to identify the nature of the faults according to basement morphology and sedimentary structure across the faults. In the case of thrust faults, the hanging side should make an uplifted peak along the fault. Such feature should not be observed, in the case of normal faults. The uplifted peak along the fault is considered to be an indication of a thrust fault. Figure 40 shows the case of thrust faulting. Two eastward dipping thrust faults are identified on the foot of the Oshima Plateau, which are evidenced by the observation of the typical uplifted ridge on the hanging sides of the faults.

The interpretation of the seismic profiles across the Okushiri and Sado Ridges, according to the above methods, shows that the ridges are formed by the activity of the thrust faults. It means that the ridges are formed by the thrusting of the hanging side crust over the footwall crust.

Three types of ridges are distinguished in terms of the mechanism of their formation (Fig. 41).

1) Type E : The ridges which are formed associated with eastward dipping thrust fault along their west sides.

2) Type W : The ridges which are formed associated with westward dipping thrust faults along their east sides.

3) Type EW : The ridges which are formed associated with eastward dipping thrust fault and westward dipping thrust faults along both sides of the ridges.

An example of Type E is shown in Figure 42 across the southern Okushiri Ridge. The sedimentary sequence on the eastern slope of the ridge is the lower sedimentary layer in the Okushiri Basin and is correlated to Pliocene age. Thick Quaternary deposits are trapped in the Okushiri Basin, which is caused by the uplift of the Okushiri Ridge after the deposition of the Pliocene sediments. A large eastward dipping thrust fault, which caused the uplift of the ridge, is assumed along the western side of the Okushiri Ridge on this profile.

Figure 43 shows a seismic profile crossing the Okushiri Ridge along 43°N. A typical case of Type W is shown on this profile. A westward dipping thrust fault is observed along the eastern margin of the ridge. It is suggested that the oceanic crust of the Japan Sea thrusted up to the east. The depth of the basement of the Shiribeshi Trough is evidently

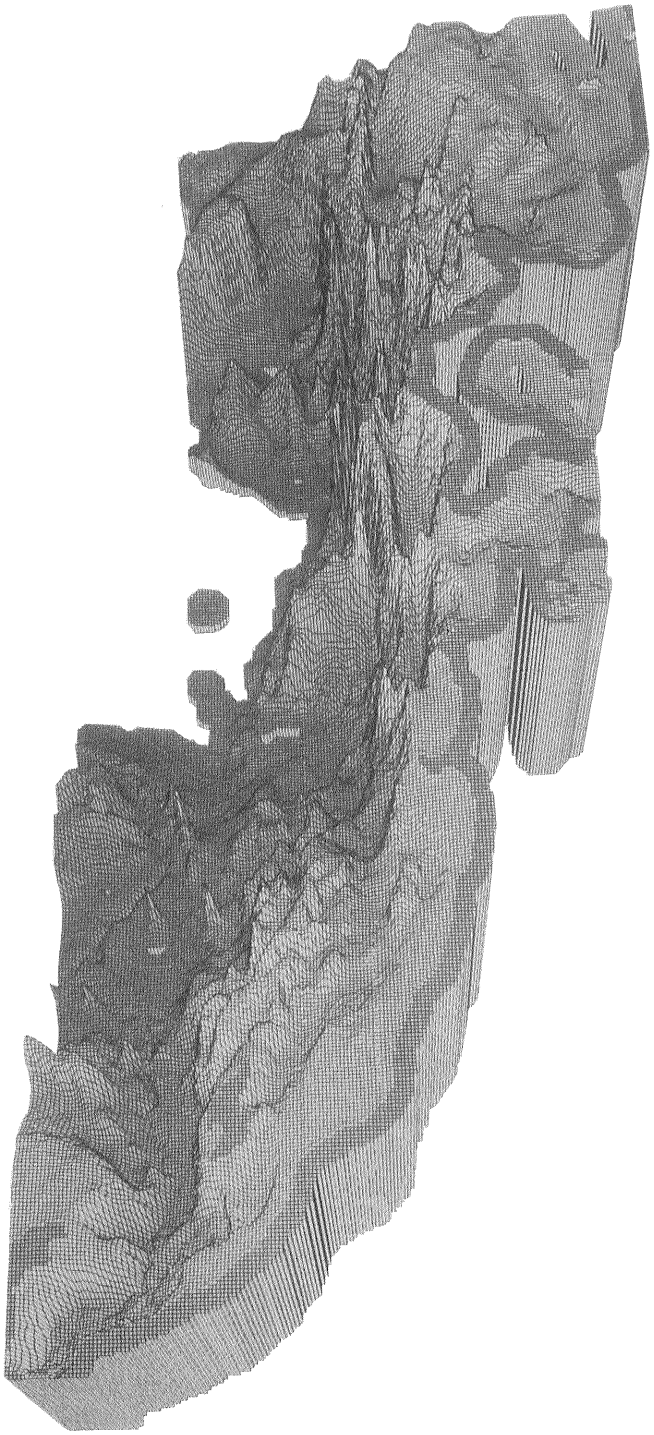

Figure 39 3-D topographic view of eastern margin of the Japan Sea. The data used for processing are GSJ digital bathymetric data after Bathymetric Maps 6311 and 6312 (Maritime Safety Agency of Japan, 1980 ab). Processing system is SIGMA of Geological Survey of Japan.

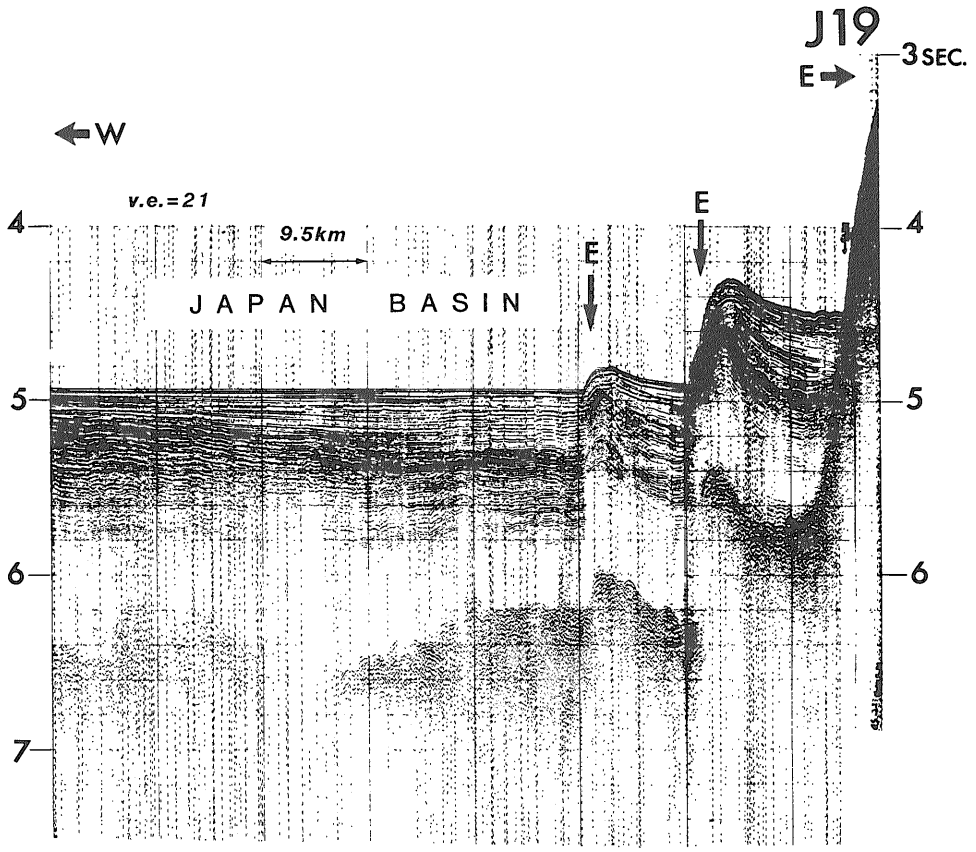

Figure 40 Typical example of thrust faults on the foot of the Oshima Plateau in the eastern margin of the Japan Sea on Line J 19. An arrow with annotation "E" shows a fault dipping eastward.

greater than that of the Japan Basin although the basement cannot be detected on this seismic profile. This feature suggests that the basement of the Shiribeshi Trough was forced down by the thrusted-up oceanic crust of the Japan Basin along the Okushiri Ridge. The ocean-continent boundary on this profile is considered to be located at the foot of the basement of the continental slope along the eastern margin of the Shiribeshi Trough. Then, from this profile, it is interpreted that a thrust fault was formed in the oceanic crust of the Japan Basin and that the western oceanic crust thrusted up over the eastern oceanic crust. This interpretation is supported by a geophysical observation that there is a large low gravity anomaly of −47 milligals in the Shiribeshi Trough. A low gravity anomaly is common along the ocean-continent boundary of the Japan Sea. The gravity anomaly along the ocean-continent boundary ranges from −20 to −30 milligals in the Japan Sea. The gravity low of −47 milligals is definitely anomalous. So, the gravity anomaly of −47 milligals at the Shiribeshi Trough should include the inequilibrium effect of isostasy. The gravity anomaly

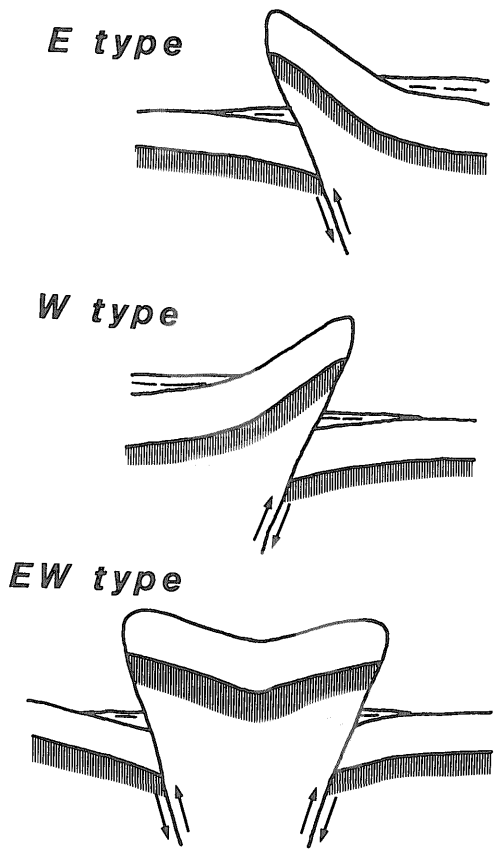

Figure 41 Three types of ridge formation mechanism observed in the eastern margin of the Japan Sea.

is concordant with the interpretation that the oceanic crust of the Shiribeshi Trough is forced down by the thrust up of the Okushiri Ridge. A gravity High of 37 milligals over the Okushiri Ridge is considerably higher than the gravity anomaly of 0 milligal over the continental slope at the same depth with the summit of the Okushiri Ridge on the profile. The gravity high over the Okushiri Ridge is inferred to be due to the uplift of the high density of the oceanic crust. This tectonic feature suggests the obduction tectonics of the oceanic crust of the Japan Basin along the Okushiri Ridge. Figure 44 also shows several ridges of Type W north of the Okushiri Island.

A Typical example of Type EW is observed in the northern Okushiri Ridge as shown in Figure 45. The sedimentary sequence on the Ridge is Miocene and Pliocene in age. The bottom sampling data of GH 77-3 and GH 78-2 cruises show that deposition of the Quaternary is thin on the ridge. This depositional feature on the ridge shows a marked contrast with the thick deposition of the Quaternary sediments in the Musashi Basin to the east. The contrast suggests that the Okushiri Ridge initiated its uplifting after or during the deposition of the Pliocene layer and that the Musashi Basin was formed by trapping the Quaternary deposits eastward behind of the Okushiri Ridge. Several basins along the eastern side of the Okushiri Ridge, such as the Futago Basins, the Shribeshi Trough, the Okushiri Basin, and the Nishitsugaru Basin, are formed by the same mechanism. Uplift of the Okushiri Ridge trapped the sediments which were derived from the Japanese Islands and formed the many sedimentary basins along the eastern side of the Okushiri-Sado Ridges.

Initiation of the thrust activity along the eastern margin of the Japan Sea

The profile in Figure 43 presents good information for identifying the age of the initiation of thrust up of the Okushiri Ridge, bacause the sedimentary sequence is well preserved on the Okushiri Ridge. It is possible to trace the sedimentary sequence from the Japan Basin to the Okushiri Ridge.

The sedimentation of the Japan Sea since Pliocene is mainly controlled by distal turbidity activity. The turbidity activity causes the present day configuration of abyssal plain of the Japan

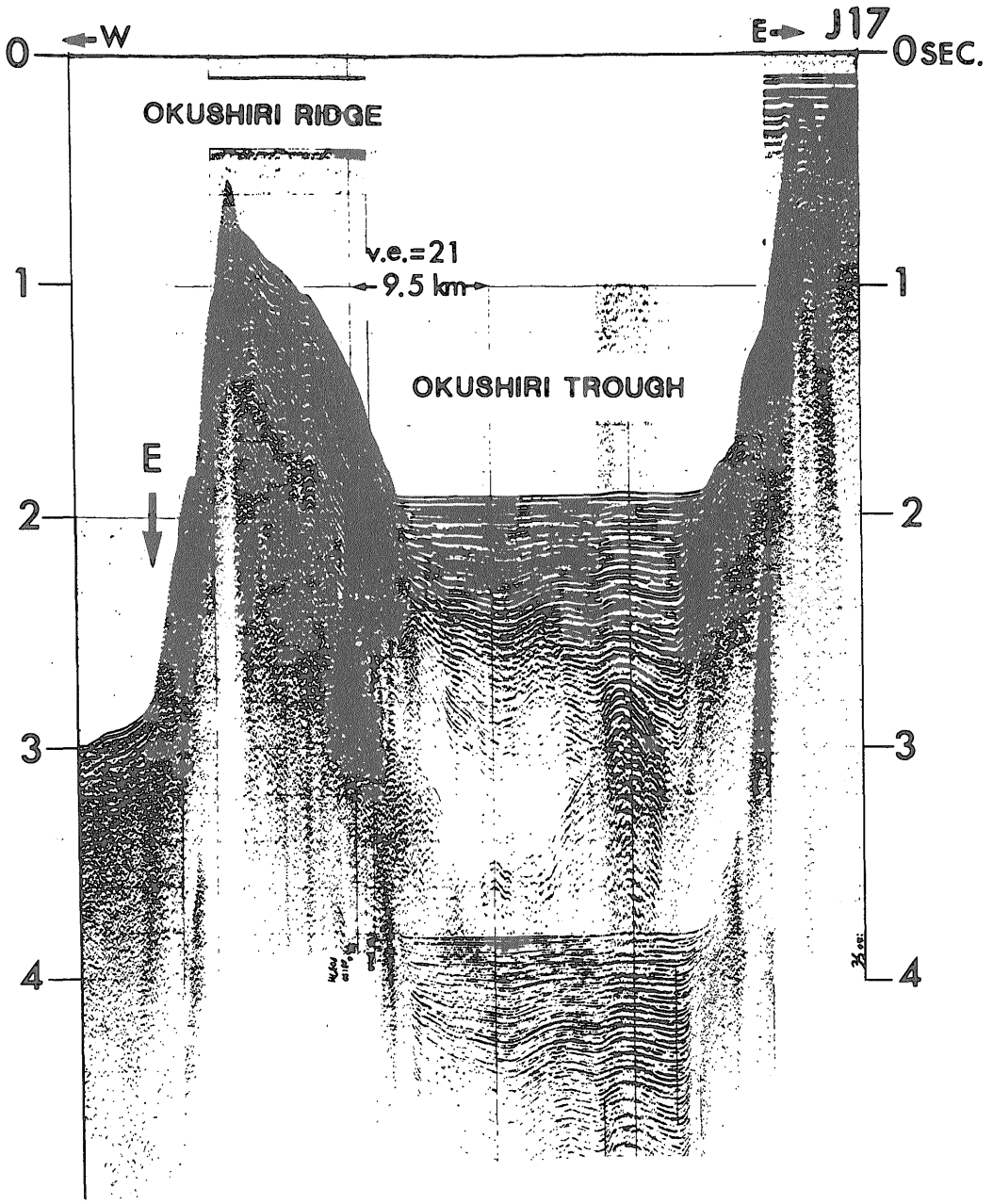

Figure 42 A seismic profile across the southern part of the Okushiri Ridge on Line J 17. Example of Type E is observed. An arrow with annotation "E" shows a fault dipping eastward.

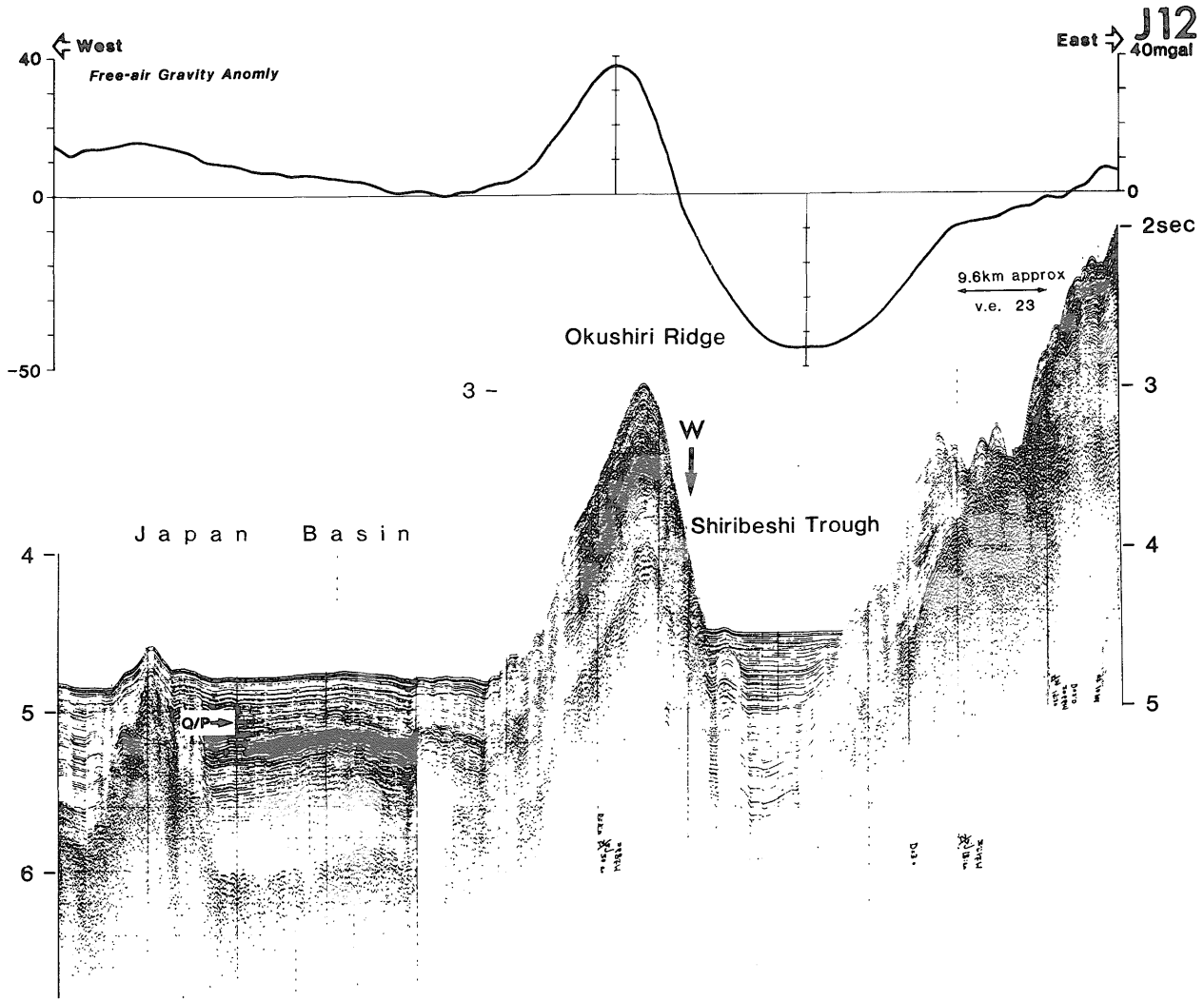

Figure 43 A seismic profile across the Okushiri Ridge on Line J 12 with free-air gravity anomaly profile. Example of Type W is observed. An arrow with annotation "W" shows a fault dipping westward. "Q/P" shows boundary of Quaternary and Pliocene deduced from DSDP Site 301.

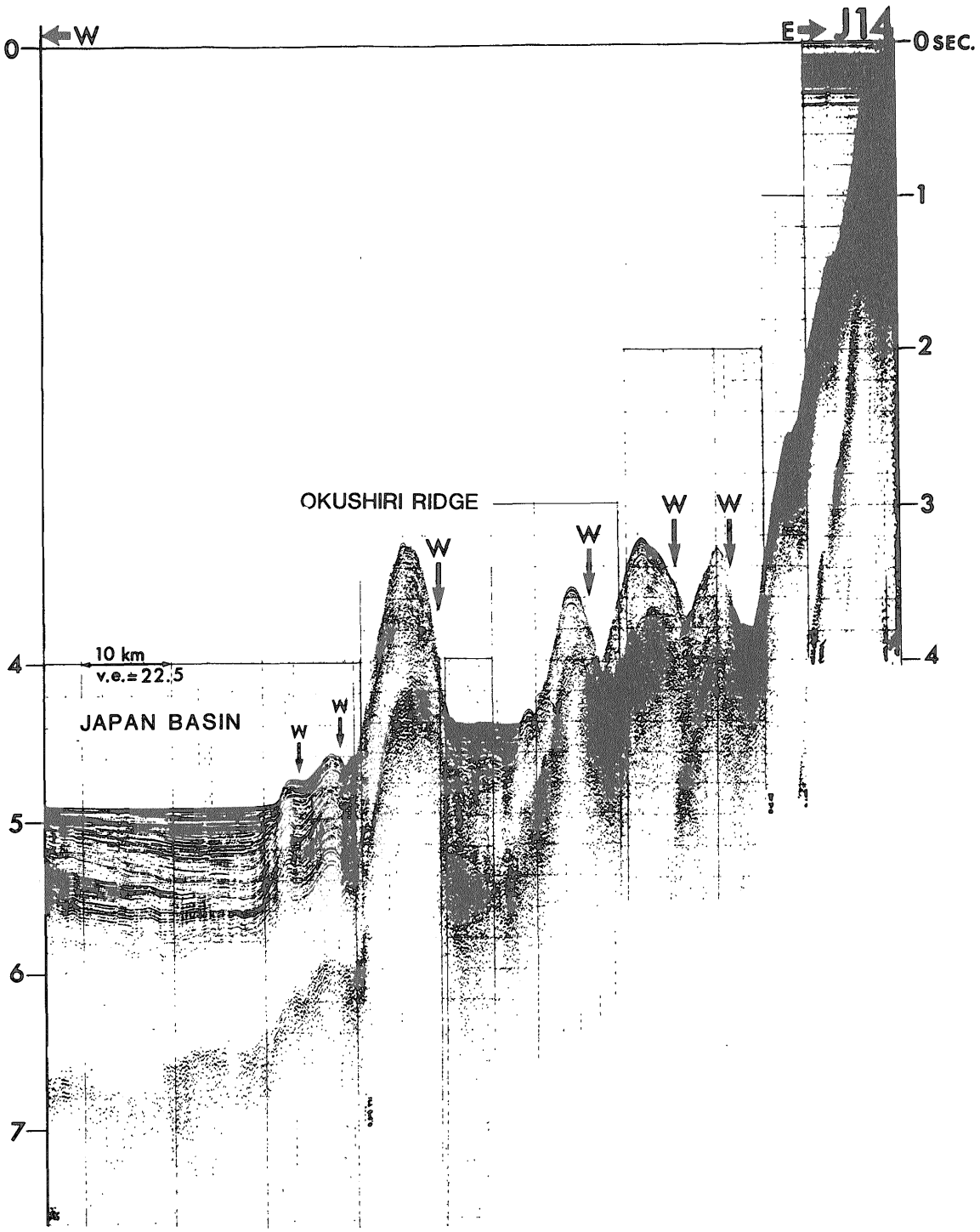

Figure 44 Seismic profile of the Okushiri Ridge north of Okushiri Island on Line J 14.

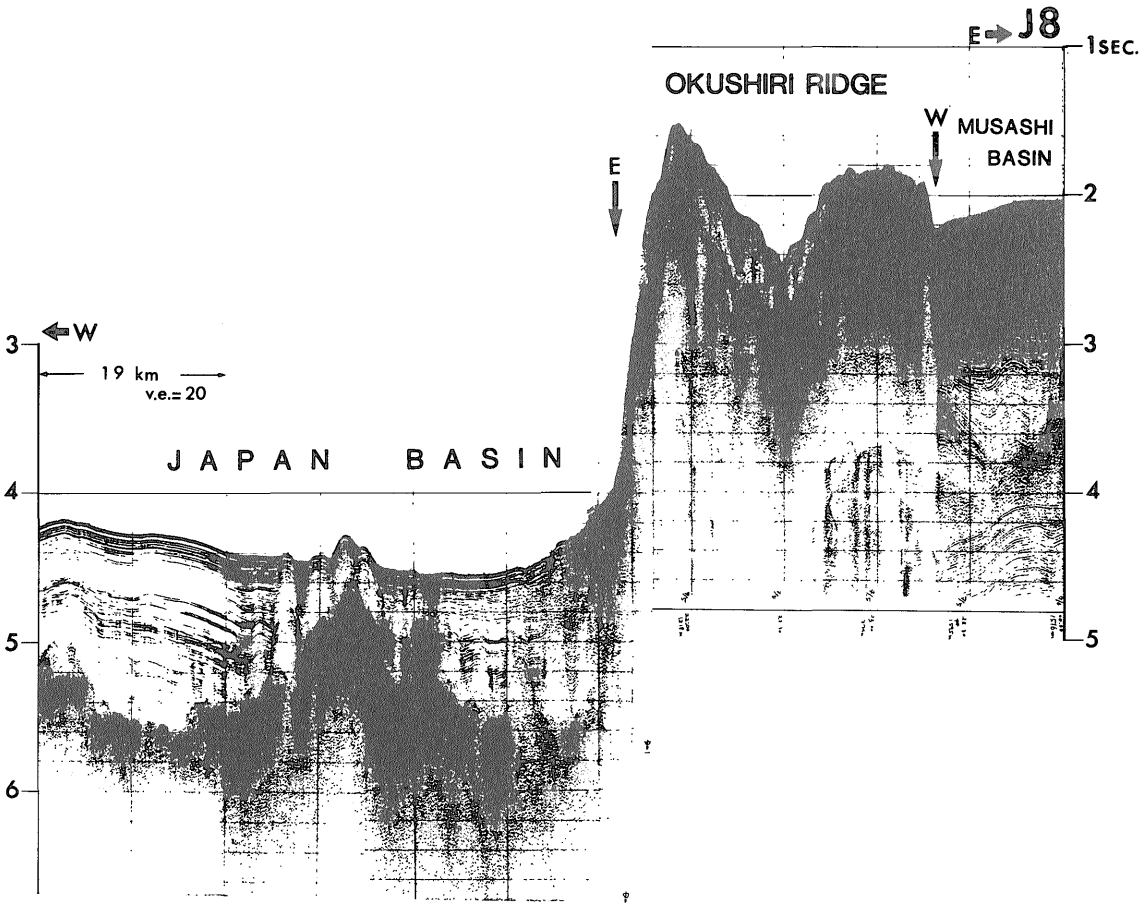

Figure 45 A seismic profile across northern part of the Okushiri Ridge on Line J 8. Example of Type EW is observed.

Basin. The turbidites are not deposited on the topographic highs. So, after the Okushiri Ridge were uplifted by the thrust fault activity, there should be little sedimentation on the ridge. This results in the reduction of the sedimentation rate or thinning of the sedimentary layer after the initiation of activity of the thrust faults.

The thickness of the upper stratified layer in the Japan Basin of 0.8 sec decreases to 0.6 sec on the Okushiri Ridge on the seismic profile of Figure 43. As the bottom of the upper stratified layer is nearly correlated to the Pliocene/Miocene boundary according to the results of DSDP Site 301 in the Japan Basin, the change in the sedimentation rate on the Ridge is inferred to have occurred some time after Pliocene. Reflector Q/P on the profile of Figure 43 is an assumed boundary between the Quaternary and the Pliocene which is interpolated from deep sea drilling results at Site 301. The tracing of the reflector onto the Okushiri Ridge gives an important information for the initial timing age of the uplift of the ridge. The reflector Q/P is situated at 0.25 sec below the sea floor in the Japan Basin.

Although it is difficult to trace the reflector onto the Okushiri Ridge due to the limit of the resolution of record and the structural disturbance at the western foot of the ridge, the reflector appears to be at most less than 0.1 sec below the sea floor on the Okushiri Ridge. So, a difference in the sediment thickness between the Japan Basin and the Okushiri Ridge of 0.2 sec appears to be mainly due to the reduction of the sedimentation rate in the Quaternary. According to the above discussion, it is assumed that the uplift of the Okushiri Ridge, or the activity of the thrust faults, was initiated around latest Pliocene.

Characteristics of the distribution of the active thrust faults in the eastern margin of the Japan Sea

The distribution of thrust faults is summarized in Figure 46 based on the seismic reflection data and recently published submarine topographic maps (Maritime Safety Agency of Japan, 1980 ab). Active synclines are also summarized in the figure according to the identification of a thick accumulation of the Quaternary deposits.

There are two types of thrusts faults observed ; eastward (landward) dipping thrust faults and westward (oceanward) dipping thrust faults. Eastward dipping thrust faults are predominant north of the Musashi Bank at the northernmost part of the eastern margin of the Japan Sea. The northern end of the Okushiri Ridge is bounded by eastward dipping thrust faults on its west side and by westward dipping thrust faults on its east side as is well shown in Figure 45. The middle part of the Okushiri Ridge, between 42°N and 43°N, is characterized by well developed westward dipping thrust faults as typically shown in Figure 43 and Figure 47. Eastward

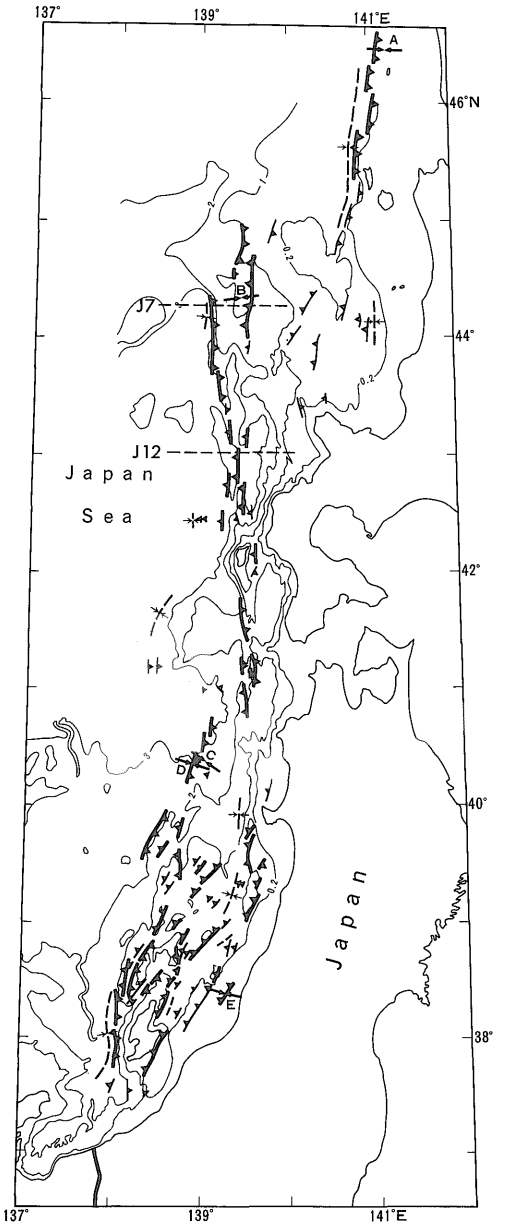

Figure 46 Distribution of active thrusts faults and active synclines. Several previous large earthquakes are shown with paired arrows. The direction of arrows shows compressional axes based on focal mechanism solution. The earthquakes are A : Off Sakhalin (1971, M 7.1), B : Off Shakotan (1940, M 7.0), C : Off Oga (1964, M 6.9), D : Central Japan Sea (1983, M 7.7), and E : Niigata (1964, M 7.5).

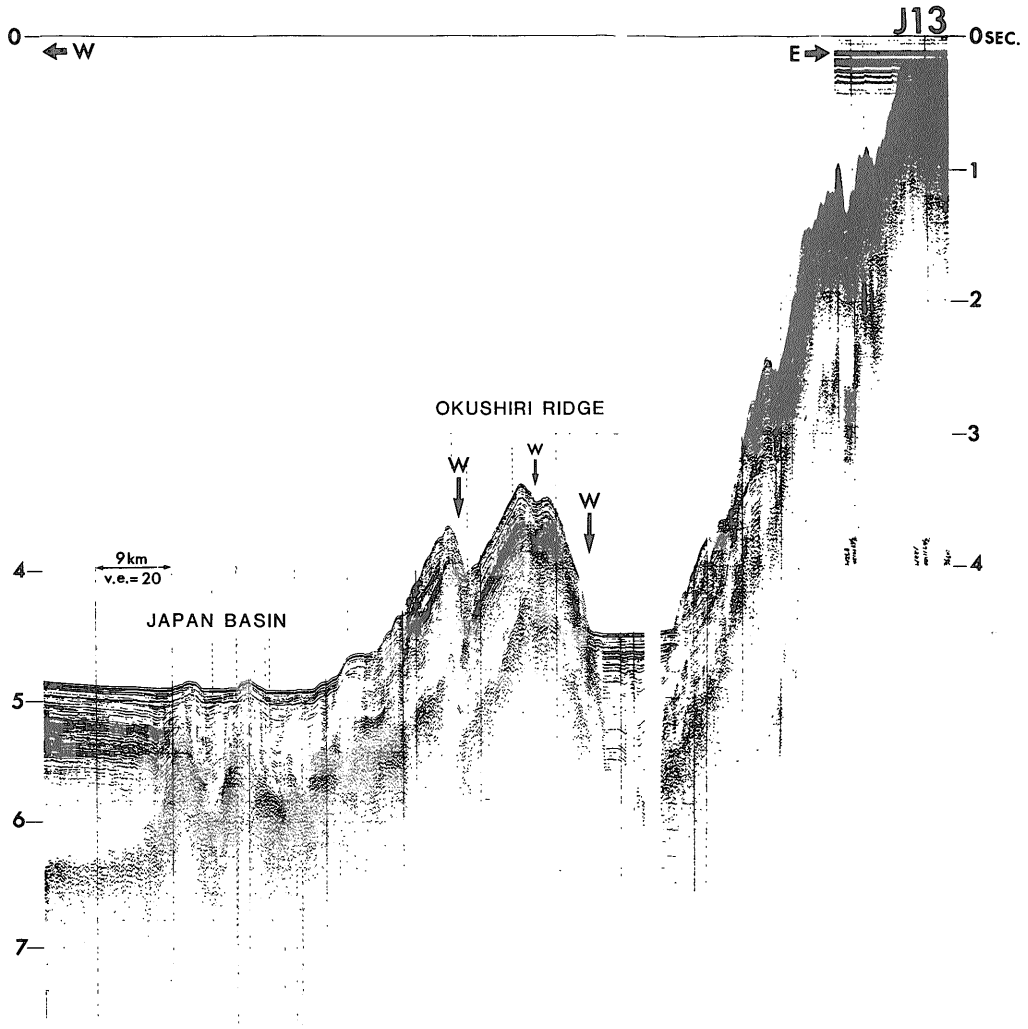

Figure 47 Westward dipping thrust faults along the Okushiri Ridge on Line J 13.

dipping thrust faults are predominant in the southern part of the Okushiri Ridge as shown in figure 42. Thus, the distribution of the thrust fault types is variable along the Okushiri Ridge, but it should be noted that the general trend of the thrust faults associated with the ridge is quite linear with strike of N 12° W showing an en-echelon arrangement.

One of the other characteristics of the Okushiri Ridge is the variation in the basement geology. The basement of the northernmost part of the Okushiri Ridge is composed of the rifted basin margin which includes both of continental and oceanic crust, as discussed in Chapter 3.2. The basement of the middle part of the Okushiri Ridge has the oceanic crust, while that of the southern part has the continental crust and is exposed as Mesozoic granitic rocks on Okushiri Island. Thus, the Okushiri Ridge is developed with quite a liner trend through the rifted continental fragments, the oceanic crusts, and the continental crusts.

The Sado Ridge shows a different fea-

ture from that of the Okushiri Ridge. While the Okushiri Ridge shows a linear distribution, the Sado Ridge shows a distribution within a broad zone 100 km in width, trending N 30° E. Many ridges lie within the wide zone, showing the same trend of N 30° E. Each ridge shows mostly Type W as well shown in Figure 48. The basement of the Sado Ridge is composed of rifted continental crust as discussed in Chapter 3.2.

Eastward dipping thrust faults are again developed at the Toyama Trough of the southern end of the eastern margin of the Japan Sea. Large eastward dipping thrust faults are observed west of the Sado Island.

Thrust faults and focal mechanism solutions of earthquakes

There is a concordant relationship between the distribution of the thrust faults and focal mechanism solution of the earthquakes which occurred in this century. There are five earthquakes of which focal mechanism solutions are published. They are all thrust-type earthquakes. The distribution of the thrust faults is shown in Figure 46 and the parameters for the thrust faults and earthquakes are summarized in Table 7. The relationship between the thrust faults and the earthquakes is discussed below for each earthquake.

(1) Earthquake off Sakhalin

A large thrust fault is developed along the eastern margin of the Rishiri Trough from west of Rebun Island and to west of southern Sakhalin as shown in Figure 46. The thrust fault is eastward dipping with a strike of N 5° E. The Earthquake off Sakhalin occurred at the depth of 22 km and 10 km east of the thrust fault. If the earthquake occurred on the thrust fault, the dip angle of the thrust fault is calculated to be 65° with an eastward dip. According to the focal mechanism solution by FUKAO and FURUMOTO (1975), the fault is a thrust type and has dip angle of 38° with a strike of N 16° E if the eastward dipping nodal plane is adopted as a fault plane. There is some discrepancy of the dips and strikes between the thrust fault and mechanism solution of earthquake. However, as there is no other corresponding active thrust fault near the earthquake epicenter, the thrust fault along the Rishiri Trough is possibly related to this earthquake.

(2) Earthquake off Shakotan

The epicenter of this earthquake is located at the northernmost part of the Okushiri Ridge. The focal depth is 33 km. The eastward dipping nodal plane of FUKAO and FURUMOTO's (1975) mechanism solution, dip of 45° and strike of NS, shows quite a good coincidence with a large thrust fault with the strike of N 5° E along the western margin of the northern Okushiri Ridge. If the large thrust fault is assumed to have dip angle of 45°, the earthquake is located just on the fault plane. Active thrust faults which correlate to the westward dipping nodal plane of the solution are not observed. As the thickness of the lithosphere of the Japan Sea is 30 km (ABE and KANAMORI, 1970), the focal depth of 33 km suggests that the thrust fault at the northern Okushiri Ridge cuts the entire lithosphere (FUKAO and FURUMOTO, 1975). Vertical displacement of the thrust fault is 3 km. The displacement of 3 km may be the accumulated displacements since latest Pliocene. Some extent of the initial displacement before latest Pliocene, however, is plausible because the northern Okushiri Ridge is Originally composed of rifted continental crust and is supposed to have originally been a rise. A displacement of 3 km for

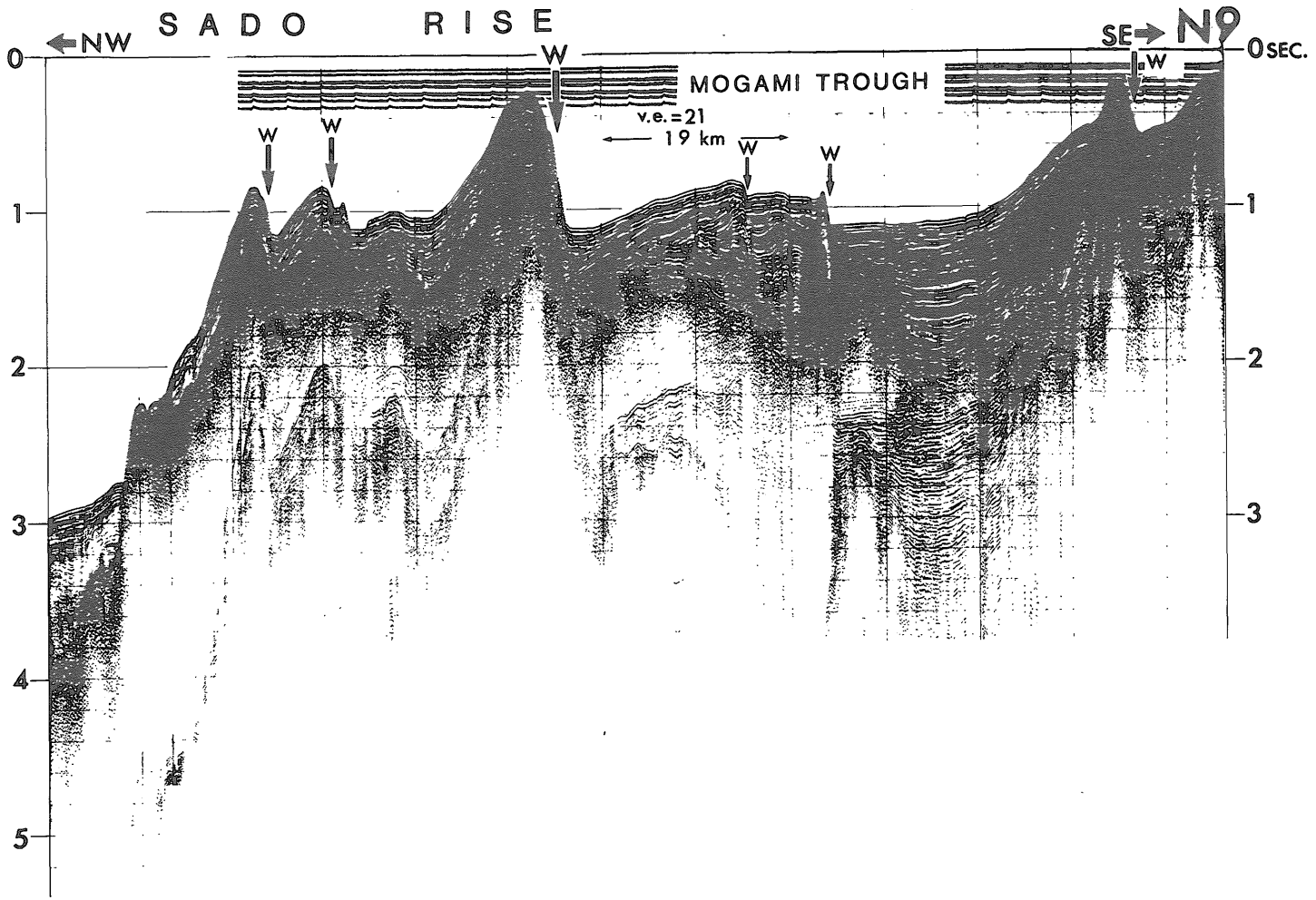

Figure 48 A seismic profile crossing the Sado Ridge on Line N 9. Ridges of Type W associated with west dipping thrust faults are outstanding.

Table 7 Dips and strikes of the submarine thrusts faults and their correlative earthquake faults. "Dip angle" and "Strike" show the dip angles and strikes of the nodal plane of mechanism solution after FUKAO and FURUMOTO (1975). "Fault dip" show the dip angle of the fault on assumption that the submarine fault and hypocenter are located on a same fault plane. "Fault strike" shows the strike of the submarine fault.

Earthquake	Date	Magnitude	Dip angle	Strike	Fault dip	Fault strike
Central JS	May 26, 1983	M 7.7	36	N 20 E	40	N 18 E
Niigata	Jun. 16, 1964	M 7.5	56	N 9 E		NS
Off Oga	May 7, 1964	M 6.9	50	N 31 E	57	N 18 E
Off Sakhalin	Sep. 5, 1971	M 7.1	38	N 16 E	65	N 5 E
Off Shakotan	Aug. 1, 1940	M 7.0	45	NS	45	NS

this thrust fault may be over-estimated. It should be emphasized that the focal mechanism of the Earthquake off Shakotan and the active thrust fault on the sea floor show an excellent coincidence and that the thrust fault is the largest in the eastern Japan Sea, cutting entire lithosphere.

(3) Earthquake off Oga

This earthquake occurred at a focal depth of 19 km just 10 km east of a large fault. The dip angle of this fault is 57° on the assumption that this earthquake occurred on the plane of this fault. The mechanism solution by ICHIKAWA (1971) shows dip angle of 50° with a strike of N 31°E if the eastward dipping nodal plane is adopted as the fault plane, The strike of the corresponding fault is N 18°E. There is discrepancy of strikes between the submarine topographic fault and the earthquake fault. The difference may be due to the ambiguous mechanism solution of ICHIKAWA. The slight discrepancy between both dip angels is explained by the steep dip angle in the shallow part of the fault plane.

(4) Central Japan Sea Earthquake

The epicenter of this earthquake (40° 21.4′ N, 139°04.6′ E) is located 13 km east of the corresponding fault (Fig. 23) with a focal depth of 14 km. The corresponding fault of this earthquake is identical to the fault of the Earthquake of Oga. The dip angle of this fault is calculated to be about 40° on the assumption that this earthquake occurred on the plane of this fault. The eastward dipping nodal plane by the mechanism solution of the pre-event of the main shock by ISHIKAWA *et al.* (1984) shows a strike of N 20°E and dip angle of 36° which are in good coincidence with the strike of N 18°E and the dip angle of 40° of the corresponding fault on the sea floor. There appears to be some problem about main event of the main shock (ISHIKAWA *et al.*, 1984). The maximum displacement of the basement by the fault activity is 1400 m (HONZA, 1983). The displacement of 1400 m should be the summation of the displacements since latest Pliocene.

(5) Earthquake off Niigata

There are several westward dipping thrust faults around the epicenter of this earthquake (HONZA *et al.*, 1977; HONZA, 1983). ABE (1975) reported the mechanism solution of this thrust-type earthquake as dip angle of 56° and a strike of N 90°E with westward dipping feature. It is difficult to identify a single corresponding thrust fault on the sea floor from the available data because there are several westward dipping thrust faults around the epicenter. SATAKE and ABE (1983) discussed a revised mechanism solution of an eastward dipping fault type. The geological structure,

however, does not show a corresponding eastward dipping thrust fault. There are an abundant distribution of westward dipping thrust faults in the southern part of the eastern margin of the Japan Sea (Fig. 46). This earthquake is inferred to have occurred on one of the westward dipping thrust faults.

The distribution of active thrust faults along the eastern margin of the Japan Sea, including several large thrust-type earthquakes with EW compressional axes, shows an evident EW compressional stress field in the area as described above. The tectonic significance of the EW compressional stress will be discussed in Chapter 3.5.

3.5 Tectonic evolution of the Japan Sea

Two significant phases of the tectonic evolution of the Japan Sea are introduced through the above discussions. One is the back-arc spreading tectonics of the Japan Sea. The other is the neotectonics of the Japan Sea along its eastern margin. In this section, the author discusses and summarizes the two phases of the tectonic evolution of the Japan Sea respectively. The back-arc spreading of the Japan Sea is summarized on the basis of the discussion in Chapters 3.1, 3.2, and 3.3. The neotectonics of the Japan Sea is summarized on the basis of the discussion in Chapter 3.4.

Back-arc spreading of the Japan Sea

Through the discussion in Chapter 3.3, the author presented a model of back-arc spreading for the case of the Japan Sea. The model is a multi rift type back-arc spreading system (Fig. 37). The model reasonably explains the present geological structure of the Japan Sea with numerous continental fragments scattered in the basins, the occurrence of rifted continental fragments, the several prominent aborted rifts, the abundant occurrence of seamounts and knolls, and the thick accumulation of volcanic clastics on the oceanic basalt layer. In this section, the author discusses the tectonics of back-arc spreading by applying this model to the history of the Japan Sea.

Large tensional stress is necessary for the initiation of the back-arc spreading. According to the DEWEY's (1980) concept, there are two possible causes for the tensional stress. One is trench roll back and the other is retreat of the back-arc plate. A combination of both causes is also possible.

SENO and MARUYAMA (1984) proposed the trench roll back origin of the Japan Sea with the simultaneous spreading of the Kuril Basin in the Okhotsk Sea and the Shikoku Basin. Trench roll back occurs according to the age of the subducting oceanic plate (MOLNAR and ATWATER, 1978; SENO, 1983). An older plate has the tendency of roll back. The time range of the back-arc spreading of the Japan Sea is suggested to be 30 to 10 Ma in Chapter 3.1. The Shikoku Basin had been active simultaneously during 30 to 15 Ma just south of the Southwest Japan Arc. The young lithosphere south of the southwestern Japanese Islands rejects the possibility of trench roll back at that time. Trench roll back along the Japan Trench may be possible because of the subduction of the older Pacific Plate. Geographic reconstruction during the back-arc spreading of the Japan Sea, however, is difficult to be accommodated only by the roll back of the Japan Trench.

The other possibility is the retreat of the back-arc plate from the trench line. The back-arc plate of the Japan Sea is

the Eurasia Plate. The back-arc spreading of the Japan Sea is possible by the retreat of the Eurasia Plate during 30 to 10 Ma. The movement of the Eurasia Plate at that time is calculated by the model of ENGEBRETSON (1982). The moving vector of the Eurasia Plate is calculated to be 1.25 cm/yr with a direction of S 78°E at the central part of the present Japan Sea. This calculation does not support the retreating sense of the Eurasian Plate as a back-arc plate of the Japan Sea during 30 to 10 Ma. It appears to be difficult to deduce the retreat of the back-arc plate in the reference frame of the major plates.

KIMURA and TAMAKI (1986) presented an alternative origin of the back-arc spreading of the Japan Sea with the simultaneous spreading of the Kuril Basin in the Okhotsk Sea. They have presented the concept that the retreat of the back-arc plates of the Japan Sea and the Kuril Basin is explained by the deformation of the Asian Continent due to the India-Eurasia collision. MOLNAR and TAPPONNIER (1975) documented the intra-plate deformation of the Eurasia Plate in East Asia due to the India-Eurasia collision. ZONENSHAIN and SAVOSTIN (1981) also interpreted the deformation as relative movements of microplates in East Asia due to the India-Eurasia collision. The collision began prior to 40 Ma. (TAPPONNIER *et al.*, 1982). MOLNAR and QIDONG (1984) calculated the movement velocity of the Southeast China block and concluded that the block has moved with velocity of 2.3 cm/yr to the east-southeast with respect to the Eurasia Plate for the last 80 years. As the rate of movement of the Eurasia Plate in East Asia is 0.3 to 0.4 cm/yr, the rate of 2.3 cm/yr is quite large and fairly comparable to the movement of the major plates such as the North America Plate and the South America Plate. The deformation or the movement of microplates in East Asia may be large enough to influence the tectonics of its marginal area including the Japanese Islands.

ZONENSHAIN and SAVOSTIN (1981) postulated that the India-Eurasia collision fragmented East Asia into several microplates and that compressional tectonics and extensional tectonics have occurred along the boundaries of the microplates. The compressional tectonics caused mountain ranges such as the Tien Shan Range and the Altai Range. The extensional tectonics caused the rift or graben system such as the Baikal Rift and Shansi Grabens. KIMURA and TAMAKI (1986) suggested that relative movements of the microplates could be the cause of the back-arc spreading and that a microplate behind the Japan Sea may retreat from the trench in spite of the immobility of the Eurasia Plate. KIMURA and TAMAKI further considered that the microplates in East Asia are correlated to each of the allochthonous terranes which were accreted to the Eurasia Continent prior to the India-Eurasia collision. The movement of microplates occurred in a manner of rearrangement of accreted allochthonous terranes due to a new large accretion of the India terrane to Eurasia. They also stressed on simultaneous spreading of the Japan Sea and the Kuril Basin.

The Kuril Basin is the back-arc basin of the Kuril Arc. The basin shows prominent a fan-shaped geographic configuration which opens southwestward (Fig. 49). The basin narrows to the northeast and disappears just south of the Kamchatka Peninsula. The Kuril Basin has similar characteristics with the Japan Basin. Basement depth after the sediment loading correction and the acoustic stratigraphy are similar to those of the

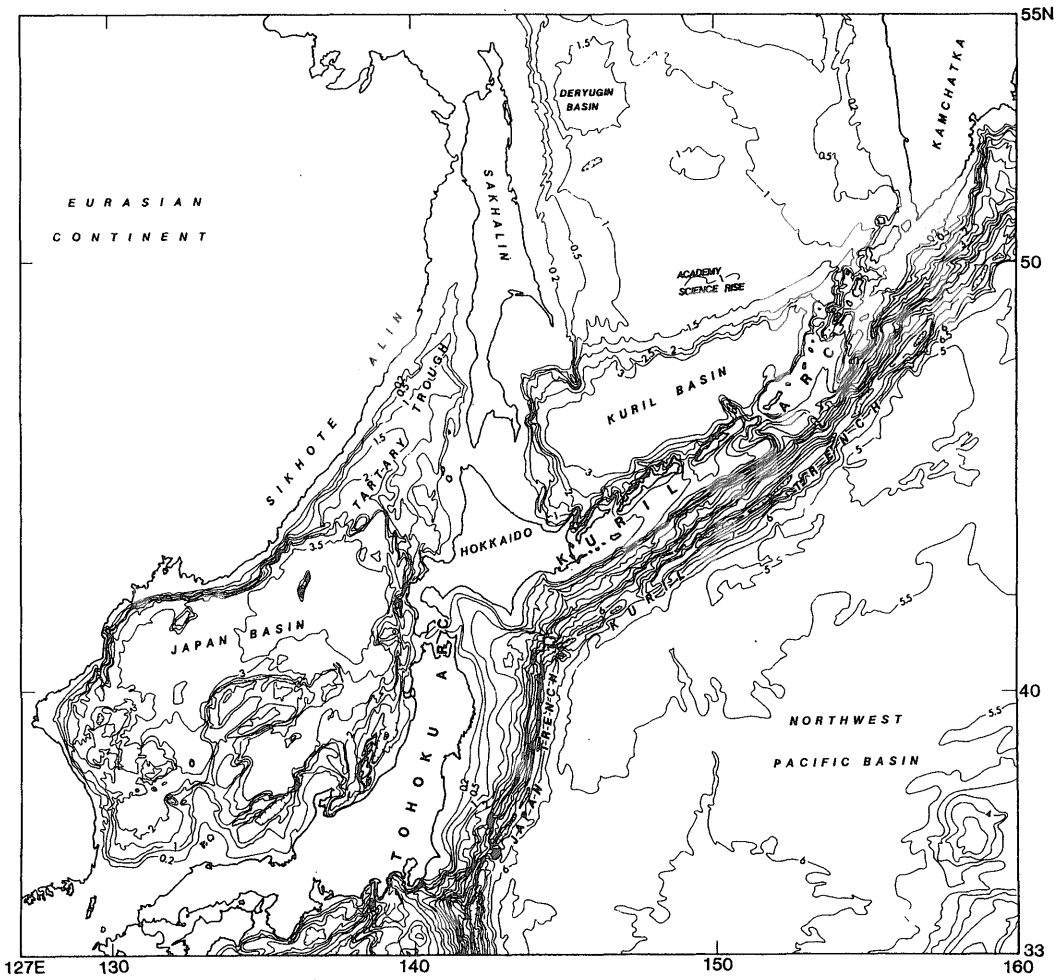

Figure 49 Physiography of the Japan Sea and the Kuril Basin.

Japan Basin (Fig. 50). The upper part of the sedimentary sequence of the Kuril Basin is also stratified while the lower part is transparent. The maximum sediment thickness of the Kuril Basin is 2.8 seconds which is much greater than that of the Japan Basin. The basement depth of 7.2 seconds is also deeper than of the Japan Basin. The basement depth after the sediment loading correction, however, is 5000 m which is almost comparable to that of the Japan Basin. The range of the corrected basement depth of the Kuril Basin, 5000 to 4000 m, is also comparable with that of the Japan Basin (Fig. 27). The average heat flow value of the Kuril Basin is 2.33 HFU. The value is slightly higher than average heat flow value of the Japan Basin of 2.26 HFU and almost comparable to that of the Yamato Basin of 2.34 HFU (Table 5). A rough estimate of the age range of back-arc spreading of the Kuril Basin, on the basis of basement depth and heat flow value, is 30 to 15 Ma or little more younger.

The age range of the back-arc spreading of the Kuril Basin is almost the

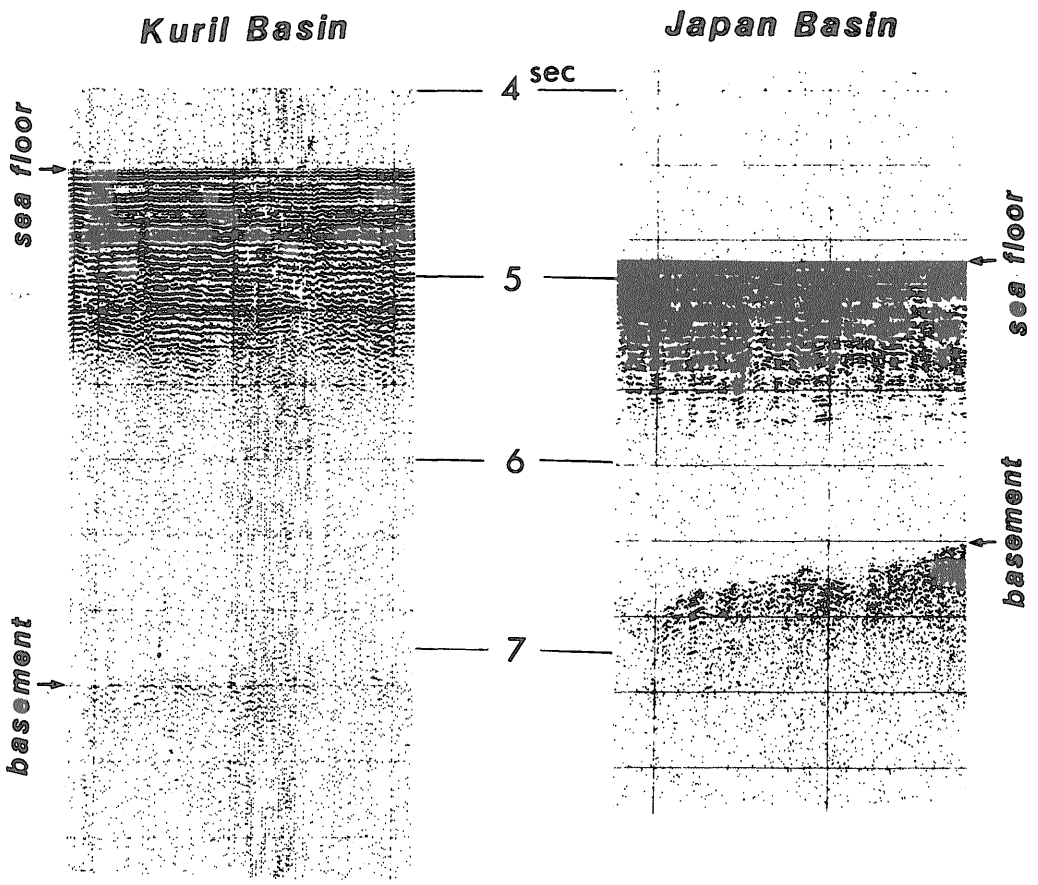

Figure 50 Typical Seismic profiles of the Japan Basin and the Kuril Basin. The sediment stratigraphy and the basement depth after sediment loading correction are comparable to each other.

same as that of the Japan Sea. The simultaneous formation of the Kuril Basin and the Japan Sea is implied by their physiographic similarities as shown in Figure 49. If it is assumed that both of the back-arc basins are generated by the retreat of their back-arc plates, the separated feature of both basins implies that the back-arc plates are not the same, but just tectonically related each other. The back-arc plate of the Japan Sea is the Amurian Block, one of the microplates of Easta Asia, which is bounded by the Baikal Rift on its western side and by the Japan Sea on its eastern side. The back-arc plate of the Kuril Basin is the Okhotsk Block which occupies most part of the Okhotsk Sea. The simultaneous spreading of the both basins also suggests that the both blocks moved simultaneously.

KIMURA and TAMAKI (1986) stressed on another event which occurred simultaneously with the back-arc spreadings of the Japan and Kuril Basins. The event is the dextral collision between the Okhotsk Block and the Amurian Block. The dextral collision is evident in the en-echelon arrangement of the folding of the Paleogene formations on the

Sakhalin–Hokkaido islands (KIMURA *et al.*, 1983). KIMURA *et al.*, (1983) have indicated that the dextral collision may be an expression of the collision between the Eurasia and the North America Plates. The relative motion of the two plates at that time, however, dose not show a dextral sense. According to ENGEBRETSON's (1982) reconstruction, the collision between the Eurasia and North America Plates should show a perpendicular sense along the Hokkaido–Sakhalin islands.

KIMURA and TAMAKI presented an idea which reasonably explains the simultaneous events of back-arc spreadings in the Japan and Okhotsk Seas and the dextral collision along the Hokkaido–Sakhalin islands. The concept is summarized in Figure 51 and its details are as follows.

The retreat of the Amurian and Okhotsk Blocks occurred simultaneously and their movement caused the back-arc spreading of the Japan Sea and the Kuril Basin. The motion of both retreat-

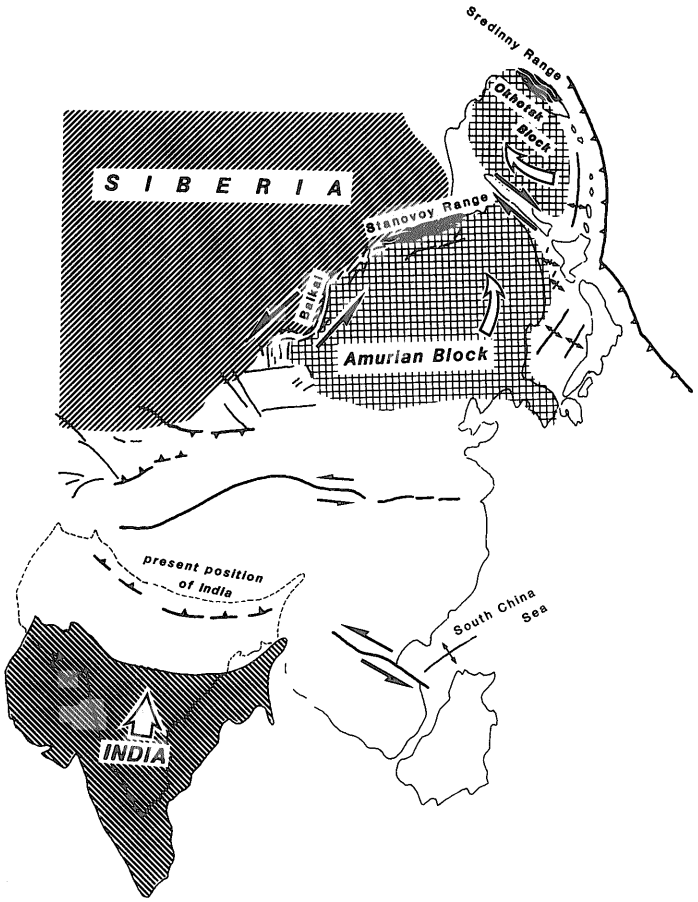

Figure 51 Movement of microplates in relation to Indo-Eurasia collision and spreading of the Japan Sea and Kuril Basin. This figure is modified from TAPPONNIER *et al.* (1982).

ing back-arc plates was different to each other. The movement of the Amurian Block was to the northeast direction causing the pull-apart opening of the Baikal Rift along the transform-like boundary between the Siberia and the Amurian Block. A sinistral collision is expected along the Stanovoy Range at the northern end of the Amurian Block. The northeastward movement of the Amurian Block simultaneously caused the clockwise rotation of the Okhotsk Block. The movement of the Okhotsk Block was caused by the drag force of the dextral collision between the Amurian Block and the Okhotsk Block along the Sakhalin-Hokkaido line. The clockwise rotation of the Okhotsk Block is suggested by the fan-shape configuration of the Kuril Basin which opens southwestward. The Kuril Basin closes toward the northeast and diminishes at the south of the Kamchatka Peninsula, where the relative rotation pole of the Okhotsk Block is inferred to be located. They proposed that the Kamchatka Peninsula was the zone of collision between the Okhotsk Block and the forearc plate of the Kuril Arc during the spreading of the Kuril Basin. The Sredinny Range in the Kamchatka Peninsula is a possible result of the collision. The Sredinny Range was active during Late Oligocene (FUJITA and WATSON, 1983), and the duration of activity is consistent with the above idea.

The above idea is rough and hypothetical. There are many problems to be resolved for the documentation of this hypothesis. HONZA (1979) presented a fan shape spreading model of the Japan Sea associated with the clockwise rotation of Southwest Japan based on geological and geophysical considerations. OTOFUJI and MATSUDA (1983) proposed almost the same model for the generation of the Japan Sea on the basis of their paleomagnetic data in Southwest Japan. They suggested that the formation of the Japan Sea occurred rapidly over a period of only a few million years around 15 Ma. Their model is inconsistent with that of KIMURA and TAMAKI. The spreading tectonics of the Japan Sea is still controversial.

Neotectonics of the Japan Sea

NAKAMURA (1983) and KOBAYASHI (1983) have proposed a hypothesis of ongoing eastward subduction along the eastern margin of the Japan Sea, on the basis of the general tectonic view around the Japanese Islands. If their hypothesis is the case, it will have a significant influence on the discussion of neotectonics in the Japanese Islands. The author discusses the possibility of subduction in the Japan Sea, on the basis of the interpretation of seismic reflection data, for verifying the hypothesis.

To identify an ongoing subduction process, it should be confirmed that the basement of the oceanic crust is downgoing beneath the landward trench wall. This feature is commonly observed on seismic profiles of the subduction zone. There is no such feature observed in the eastern margin of the Japan Sea. There are thick accumulations of sediments, reaching 2.0 seconds, in the Japan Basin. If the oceanic basement overlain by such a thick accumulation of sediments is subducted, then, dynamic sediment accretion will occur along the landward slope and it will make an accretionary prism, as is well observed in the Nankai Trough in the Philippine Sea. An accretionary prism is characterized by many imbricated thrust faults dipping landward and by a rough topography with many ridges and troughs. Such features are also not observed in the eastern

margin of the Japan Sea. Thus, it is difficult to identify ongoing subduction in the eastern Japan Sea. However, there is a possibility of incipient subduction as discussed below.

Many active thrust faults are distributed along the eastern margin of the Japan Sea. They indicate the present compressional stress in the eastern margin of the Japan Sea. Some of them cut the entire oceanic lithosphere of the Japan Sea as discussed in Chapter 3.4. The existence of large thrust faults which cut the entire lithosphere indicate that convergent tectonics between the lithospheres or plates is occurring in the eastern margin of the Japan Sea.

The largest displacement along the thrust faults reaches 3 km at the northern end of the Okushiri Ridge. As the thickness of the lithosphere of the Japan Sea is 30 km, the displacement of 3 km correlates to 10% of the entire lithosphere. This displacement of 3 km is a cumulative displacement for the past 2 or 3 Ma. If the compressional stress is maintained in the future, will the displacement increase further? It is impossible for the displacement to reach the entire thickness of the lithosphere, because there are no such large displacements of 30 km observed on the earth. It is reasonable to consider that there is a maximum values of displacement along thrust faults which cut the entire lithosphere. After the displacement of the thrust fault reaches some maximum value, what will happen with continuing convergence between the hanging side and footwall lithospheres?

There may be two possibilities in such a case. One is the formation of another thrust fault in the different place on the same transect. The convergence between the two lithospheres is compensated by the displacement of the new thrust fault. The other possibility is the conversion of the fault into a subduction zone after the fault reaches the maximum displacement. After subduction is initiated, further lithospheric convergence will not result to increase the displacement over the critical displacement.

It should be noted that subduction is different from thrust fault activity and that it means the overlapping of the two lithospheres. Subduction is defined as a process where the upper surface of one lithosphere subducts beneath the other lithosphere. When the subduction is ongoing, the convergence between the two lithospheres does not cause a compressional stress proportional to the convergence rate, because the convergence is consumed by the subduction of the footwall lithosphere. On the contrary, when the converging lithospheres are bounded by thrust faults, the compressional stress should be proportional to the convergence rate and the displacement of the thrust fault increases according to the convergence.

If there is a critical displacement for the conversion from trust fault to the initiation of subduction, how large is the critical displacement? An assumption should be introduced to discuss this problem. The assumption is that the Okushiri Ridge is correlated to the initial stage of the basement high at the trench slope break and that the Musashi Basin on Figure 52 is also correlated to the initial stage of the forearc basin. The forearc basin and basement high at the trench slope are commonly observed in the present island arcs. So, the present day height of the trench slope break basement high above the subducting ocean floor may be an expression of the critical displacement. There are a variety of the origins of the basement high at the trench slope break. For example,

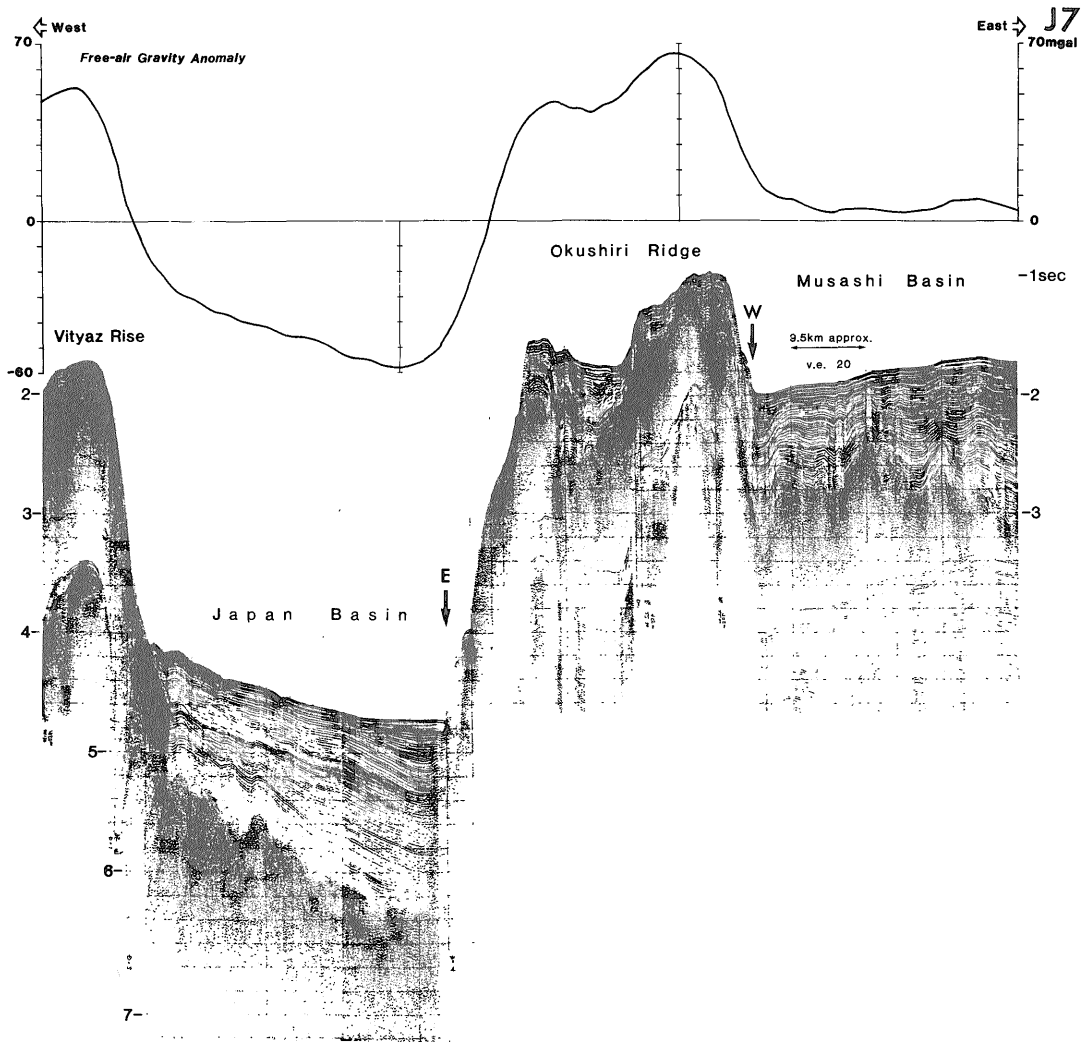

Figure 52 Seismic reflection profile with free-air gravity anomaly profile on Line J 7. The free-air gravity low of −57 mgals is the lowest one in the Japan Sea.

the basement high at the trench slope break of the Sunda Trench is composed of an ancient accretionary wedge (KARIG and SHERMAN III, 1975), and that of the Japan Trench is composed of the oceanward edge of the continental crust (von HUENE *et al.*, 1980). Since the original configuration of the trench slope break basement high may be changed by the active subduction process, and analogy with a young trench is better for the present discussion, because young trenches are considered to represent a more original configuration of the basement high at the trench slope break.

The South China Sea is a marginal basin whose water depth, sediment thickness, crustal structure, and age (32–17 Ma) are quite similar to those of the Japan Sea. The Manila Trench, which was formed during Miocene, represents an active eastward subduction zone along

the eastern margin of the South China Sea (TAYLOR and HAYES, 1983). A basement high at the trench slope break is well developed and makes a ridge along the Manila Trench. The west Luzon Trough is trapped just east of the ridge. The relative height of the basement high of the Manila Trench above the basement of the basin area of the South China Sea is 2.2 to 2.8 km according to the seismic profiles of LUDWIG *et al.* (1967). If the value, 2.2 to 2.8 km, is considered to be the critical displacement for the initiation of subduction, the northern Okushiri Ridge with the displacement of 3 km may be the site of incipient subduction. The Manila Trench, however, is not very young subduction zone. The Trench was formed before 10 Ma. It should be noted that there is a possibility that the basement high at the trench slope break uplifted or subsided after the initiation of subduction.

The Mussau trench along the Caroline and Pacific Plate boundaries in the western Pacific is one of the youngest trenches on the earth (HEGARTY *et al.*, 1982). The Mussau Trench initiated eastward subduction at 1 Ma and the Caroline Plate has been subducted to an extent of 10 km beneath the Pacific Plate. The Mussau Ridge is a linear feature on the western edge of the Pacific Plate along the Mussau Trough. The elevation range of the Mussau Ridge above the basement of the East Caroline Basin is 1.8 to 3.8 km. The analogy of the Okushiri Ridge with the Mussau Ridge, also, does not reject the possibility of the incipient subduction at the northern Okushiri Ridge. The thrust fault at eastern margin of the Rishiri Trough (Fig. 15), which has the displacement of 2.5 km, also has the possibility of being an incipient subduction zone.

The above discussion on the initiation of subduction is only based on some analogies. The thickness of the lithosphere may also have to be taken into consideration for such discussion, and the bending effect of the subduction lithosphere is also significant problem. A detailed geophysical and geological model for the initiation of subduction from a thrust fault is significant for future study.

The possibility of incipient subduction is also supported by the free-air gravity anomaly data. One of the largest free-air gravity anomalies in the Japan Sea, −57 milligals, is observed along the western margin of the northern Okushiri Ridge (Fig. 52). The normal free-air gravity anomaly along an ocean-continent boundary is −20 to −30 milligals, then, anomaly of −57 milligals may indicate that the crust of the Japan Basin along the northern Okushiri Ridge is being forced down. Such a feature may be explained by a simple thrust fault model. The inequilibrium of isostasy, however, is evident along the northern Okushiri Ridge.

The seismic profile on Figure 52 shows the eastward thickening of the upper part of the sedimentary sequence of the Japan Basin. This feature suggests ongoing subsidence of the crust of the Japan Basin. Ponded sediments are observed along the foot of the Okushiri Ridge. The presence of the ponded sediments also suggests the recent subsidence of the Japan Basin along the Okushiri Ridge. The subsidence is also evident in the eastward declining sea floor surface of the ponded sediments. The distribution of the ponded sediments, however, is not common along the northern Okushiri Ridge (Fig. 46).

There is possibility of incipient subduction in the eastern margin of the Japan Sea as discussed above. The subduction

sense, however, does not prevail over the entire eastern Japan Sea. Figure 53 shows a composite distribution of the eastward dipping thrust faults and westward dipping thrust faults in the eastern margin of the Japan Sea. Zone of eastward dipping thrust faults are observed to the west of southern Sakhalin and northern Hokkaido, at the northern end of the Okushiri Ridge, to the west of the Oga Peninsula, and to the west of Sado Island. These zones have the possibility of incipient subduction. Zones of westward dipping thrust faults are observed north of Okushiri Island and along the Sado Ridge as discussed in Chapter 3.4. The westward dipping thrust faults indicate an opposite sense against the subduction sense.

Thus, the subduction sense (zone of eastward dipping thrust faults) and the obduction sense (zone of westward dipping thrust faults) show a composite distribution throughout the eastern margin of the Japan Sea. The change of polarity of the thrust faults occurs in a short distance. The cause of such a polarity change is ambiguous. HEGARTY *et al.* (1982) also observed a polarity change of subduction sense to obduction sense at the Mussau Trench. The Mussau Trench shows a prominent eastward subduction structure in its southern part but, in the northern part, it changes to an eastward obduction sense with a swarm of thrust faults. They presented an explanation that the polarity change may be due to the change in convergence rate. The convergence rate in the southern part of the Mussau Trench is more than 1.5 cm/yr while that of the northern part is less than 1.5 cm/yr. Such explanation is difficult for the composite distribution of subduction and obduction sense in the eastern Japan Sea. One possible inference is that a density contrast between the two convergent lithospheres may control the polarity of the thrust faults in the manner that the heavier side makes footwall and the

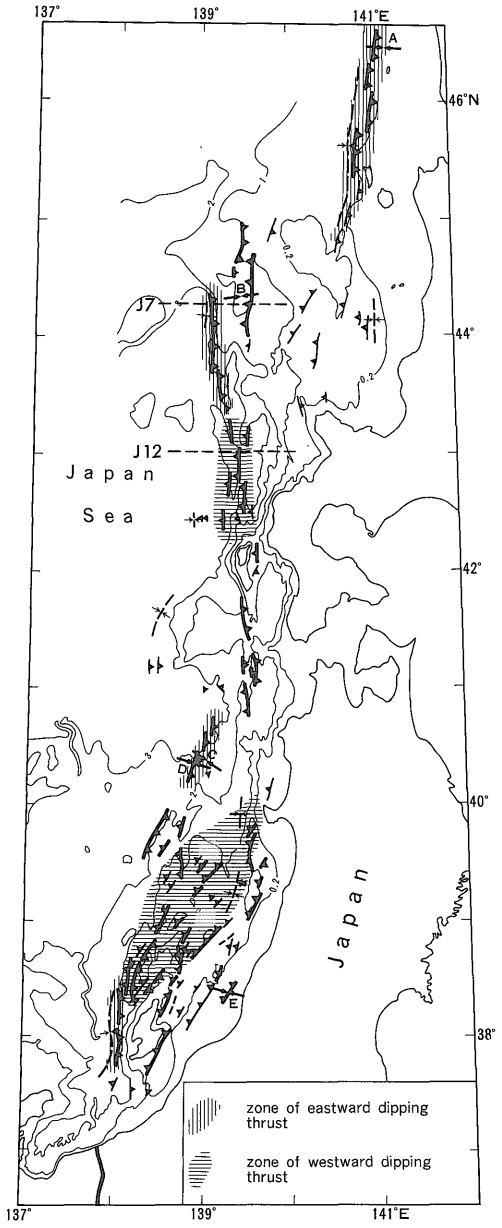

Figure 53 Composite distribution of eastward dipping thrust faults and the westward dipping thrust faults in the eastern margin of the Japan Sea.

lighter side makes the hanging wall of the faults.

NAKAMURA (1983) and KOBAYASHI (1983) have presented a hypothesis that the eastern margin of the Japan Sea is a new Eurasia–North America plate boundary. According to their idea, the plate boundary in the eastern margin of the Japan Sea extends to the Itoikawa–Shizuoka Tectonic Line in the central Japan and reaches to the Nankai Trough in the Philippine Sea. The new plate boundary is considered to have jumped from the former plate boundary along the central axis of Sakhalin–Hokkaido in early Quaternary. This attractive hypothesis, however, has some problems.

KELLER (1980) and von HUENE *et al.* (1980) documented that the vertical movement of the basement in the forearc basin of the Northeast Japan Arc has changed from subsidence to an uplift sense since early Quaternary, on the basis of deep sea drilling results. The change in vertical movement suggests the prevalence of compressional stress since early Quaternary in the forearc area. The compressional stress field in the forearc area of the Northeast Japan Arc in the Quaternary is comparable with the compressional tectonics in the eastern Japan Sea since latest Pliocene. The compressional stress field in the forearc area, however, is inconsistent with the new plate boundary hypothesis. According to the hypothesis, the Northeast Japan Arc is included in the North America Plate which moves westward with a rate of greater than 1.0 cm/yr at the Japan Trench (MINSTER and JORDAN, 1978). Such movement should produce a tensional stress field over the forearc area if the trench axis is fixed. The compressional stress over the forearc area of the Northeast Japan Arc in the Quaternary does not support that the Northeast Japan Arc is on the North America Plate.

FUKAO and YAMAOKA (1983) presented the trends of the axes of maximum compression along the Itoikawa–Shizuoka Tectonic Line on the basis of focal mechanism solutions of several small earthquakes. The P axes show NW–SE to WNW–ESE. The trend of convergence should be N 50°E if the tectonic line is the boundary between the Eurasia and North America Plates (MINSTER and JORDAN, 1978). This discrepancy also does not support the new plate boundary hypothesis.

Thus, the new plate boundary hypothesis is ambiguous. The author presents another possible explanation, that the convergent stress in the Japan Sea is also due to the India–Eurasia collision and its associated intra-plate or inter microplate movement in East Asia. The Baikal Rift has reactivated its extension at some time in the Pliocene (ZONENSHAIN and SAVOSTIN, 1981). The reactivated Baikal extension at some time in the Pliocene is roughly comparable with the initiation of convergence along the eastern Japan Sea at about 2 Ma. The Baikal Rift and the eastern margin of the Japan Sea bound the Amurian Plate on its western and eastern sides respectively. The recent tectonics of the eastern margin of the Japan Sea is well understood in the reference frame of the eastward movement of the Amurian Plate. The eastward movement of the Amurian Plate causes the Baikal extension along its western margin and Japan Sea convergence along its eastern margin (Fig. 54). If this is the case, the condition should be identical with the initiation of the Manila Trench along the eastern margin of the South China Sea in Miocene which is possibly due to the eastward movement of the South China Block in relation

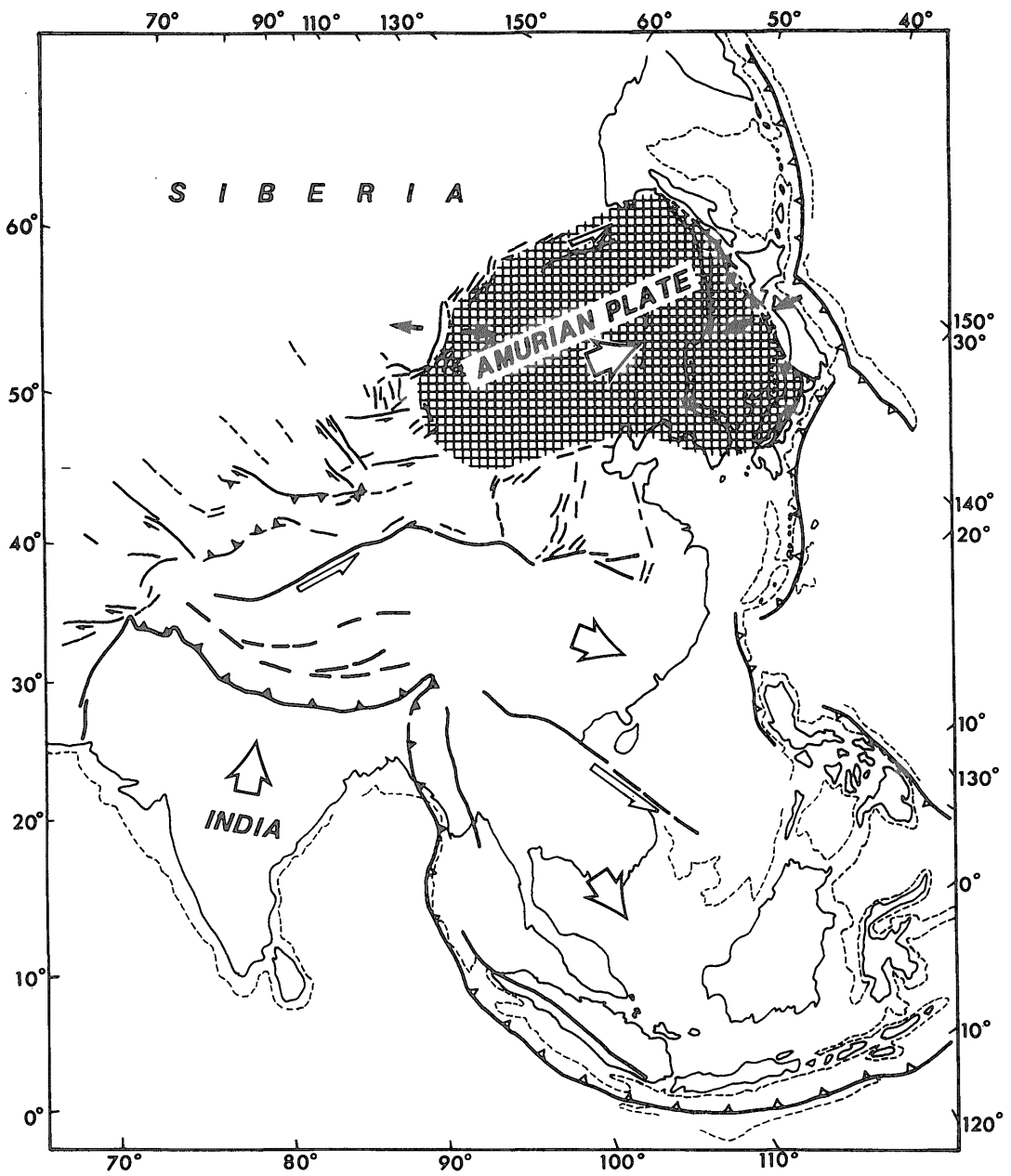

Figure 54 Movement of microplate, the Amurian Plate, in relation to Indo-Eurasia collision and convergence along the eastern margin of the Japan Sea. This figure is modified from TAPPONNIER *et al.* (1982).

to the India-Eurasia collision. This explanation, however, also has problems. ZONENSHAIN and SAVOSTIN (1981) calculated the relative movement of the Amurian Plate against the Eurasia Plate (Siberia Block). The rotation pole of the Amurian Block is located just north of the Baikal Rift. This results do not support the eastward movement of the Amurian Plate.

The origin of compressional stress in the eastern margin of the Japan Sea is still uncertain. The incipient subduction and obduction in the eastern Japan Sea, however, are rather evident. Further detailed studies and discussion about the tectonics of the Japan Sea will produce general models for tectonics of lithospheric convergence, especially on its initial stage.

4. Summary and Conclusions

The tectonic evolution of the Japan Sea for a long time has been a controversial subject and models for its development have often been ambiguous. its evolution has a close relation with the tectonics of the Japanese Islands, but the lack of a well constrained model has been an obstacle for studying the tectonic evolution of the Japanese Islands and the adjacent area. This study provides new constraints on the age and nature of the tectonic evolution of the Japan Sea through new and detailed discussion of its geological structure, based in large part on marine geological and geophysical data obtained during the research cruises GH 77-2, GH 77-3, GH 78-2, and GH 78-3 conducted by the Geological Survey of Japan. Marine geological maps were compiled on the basis of the stratigraphic correlation of seismic profiles and the bottom sampling results. The distribution of geologic features on these maps, their structural characteristics, and the age-depth-heat flow relationships of the basins have been combined to interpret the tectonic evolution of the Japan Sea.

The age of the basins were examined by a comparative study of sediment stratigraphy, basement depth, and heat flow data. Presented age estimation is about 30 to 15 Ma for the Japan Basin, 30 to 10 Ma for the Yamato Basin, and comparable age ranges for the Tartary Trough and the Tsushima Basin. The acoustic basement of the Japan Basin is mostly correlated to a oceanic basalt layer, excluding its marginal area. The acoustic basement of the Yamato Basin is inferred to be volcaniclastics which are correlated to the Green Tuff formation in Japan. The volcaniclastics overlie a deeper oceanic basement. When these deposits are considered, the greater oceanic basement depth of the Yamato Basin is consistent with its estimated age range of 30 to 10 Ma.

The topographic highs of the Japan Sea are classified into four groups ; continental fragments, rifted continental fragments, tectonic ridges, and volcanic seamounts. Continental fragments are composed of older rocks including rocks of Precambrian age. These fragments are clearly of a pre-rift age. They consist of large and elevated topographic highs such as the Yamato Ridge and the Korea Plateau. Rifted continental fragments represent a low topographic rise because of its transitional nature from continental to oceanic. The Takuyo Bank and the Sado Rise are examples of this group. The tectonic ridges are observed along the eastern margin of the Japan Sea. They were elevated by the convergent tectonics since about latest Pliocene. The Okushiri and Sado Ridges are the typical cases of this group. Vol-

canic seamounts which were caused by arc volcanism since the initiation of the spreading of the Japan Sea are abundantly observed. The distribution of these topographic highs are closely related to the tectonic evolution of the Japan Sea.

Two types of back-arc spreading were proposed ; a single rift type and a multi rift type. The multi rift type is the case for the Japan Sea. Large tensional stresses over the former island arc caused a multi rift system in its broad volcanic zone along which the lithosphere of the Island arc is weakest. Some of the rifts developed into multi back-arc spreading ridge system and others were left as aborted rifts such as the Kita-Yamato Trough. The broad volcanic zone of the former Japanese island arc overprinted the volcanism of back-arc spreading due to a shallow subduction angle. Arc volcanism under the tensional tectonics caused a thick accumulation of volcaniclastics and the abundant occurrence of seamounts and knolls in the basins. The multi back-arc spreading system resulted in the fragmentation of the continental crust which generated topographic highs classified as continental fragments.

The large tensional stress in the overriding plate is significant for initiating the above tectonics. It is inferred to be possible only by retreat of the continental block from the trench line. The Eurasia Plate itself did not retreat as a whole from the western Pacific trench systems at the corresponding time. The back-arc continental block of the Japan Sea, the Amurian Block, however, is postulated to have retreated northward due to the India-Eurasia collision and associated lithospheric deformation in East Asia which initiated at about 40 Ma. The northward movement of the Amurian Block generated the Stanovoy Range along its northern margin by the collision with Siberia, and the pull-apart basin of Baikal Rift along its western transform boundary with Siberia. The movement also caused clockwise rotation of the Okhotsk Block by drag forces along Sakhalin-Hokkaido line. The clockwise rotation of the Okhotsk Block is evidenced by opening of the fan-shaped Kuril Basin and the Sredinny collision on the Kamuchatka Peninsula.

The Okushiri and Sado Ridges along the eastern margin of the Japan Sea are bounded by thrust faults. The thrust faults have been active since latest Pliocene. The ridges are formed by the thrust movements associated with the uplift of the edge of hanging side over the footwall. The zone of eastward dipping thrust faults and the zone of westward dipping thrust faults are discriminated. They are distributed compositely. Incipient subduction may be the case in some parts of the zone of eastward dipping thrust faults. Incipient obduction of the oceanic crust of the Japan Sea also is taking place in the zone of westward dipping thrust faults. Lithospheric convergence is evident along these thrust zones on the basis of the synthetic study of the thrust faults and their corresponding earthquakes. The origin of the convergent stress is inferred also to be due to the India-Eurasia collision and its associated intra-plate or inter microplate movements in East Asia. The recent tectonics of the area are well understood in the reference frame of the eastward movement of the Amurian Block relative to the Japanese Islands. The eastward movement of the Amurian Block caused the Baikal extension along its western margin and the eastern Japan Sea convergence along its eastern margin.

In conclusion, the two major stages of tectonic evolution are deduced for the Japan Sea

1) Divergent tectonics over the Japanese island arcs caused back-arc spreading of the Japan Sea from 30 to 10 Ma. The spreading system was initiated from a multi rift system over a broad arc volcanic zone. Through the development of the spreading system, many continental fragments were left in the basins. Overprinting of the arc volcanism on the back-arc spreading activity resulted in the occurrence of abundant volcanic seamounts and knolls and a thick accumulation of volcaniclastics in the basins. The tensional stress for generating such tectonics is considered to be due to the India-Eurasia collision and associated lithospheric deformation in East Asia.

2) Lithospheric convergence has been concentrated along the eastern margin of the Japan Sea since latest Pliocene. The Okushiri and Sado Ridges, bounded by many active thrust faults, are consequences of the convergence along this new lithospheric boundary. This tectonic stage is also due to the India-Eurasia collision. The eastward movement of the Amurian Block has caused extension along the Baikal Rift at its western margin and convergence in the Japan Sea along its eastern margin.

Aknowledgements: This research was done when the author was a research scientist of the Geological Survey of Japan from 1974 to 1986. The original version of this paper was submitted to Kyushu University as a doctoral thesis in 1985. The author would like to express his sincere thanks to Prof. Ryohei TAKAHASHI, Prof. Tsugio SHUTO, Prof. Kametoshi KANMERA, and Assoc. Professor Yujiro OGAWA of Kyushu University for their expert guidance and discussion. The author would like to acknowledge the critical reading of the manuscript and encouragement by Dr. Eiji INOUE and Dr. Eiichi HONZA of the Geological Survey of Japan and Prof. Atsuyuki MIZUNO of Yamaguchi University. The author also would like to express his thanks to Dr. Hideki IMAI for his constant guidance and encouragement. The author should extend his thanks to the captains and crews of the research vessel Hakurei-maru for the cruises of GH 77-2, 77-3, 78-2, and 78-3, aboard which he had the opportunity to collect data for this study. The author appreciate the help of all the scientific staff and assistant staff of the cruises and his previous colleagues of the Geological Survey of Japan for their constant discussion. Discussion with the late Prof. Kazuaki NAKAMURA improved this research extensively. Discussions with Profs. Seiya UYEDA and Kazuo KOBAYASHI and Drs. Tetsuzo SENO and Gaku KIMURA are gratefully acknowledged. The author thanks Profs. Thomas W.C. HILDE and Roger L. LARSON for their partial critical reading of the manuscript. The author must acknowledge the English correction by Mr. David B. SHEPARD and proof reading of final manuscript by Mr. Manabu TANAHASHI. Last of all the author would like to thank Dr. Yasumoto SUZUKI of the Geological Survey of Japan for critical review of the manuscript and Dr. Teruo SHIRAHASE of the Geological Survey of Japan for editing the manuscript. Without their patient efforts, this paper would not have been published.

References

ABE, K. (1975) Re-examination of the fault model for the Niigata earthquake of 1964. *J. Phys. Earth,* vol. 23, p. 349-

366.

ABE, K. and KANAMORI, H. (1970 a) Mantle structure beneath the Japan Sea as revealed by surface wave. *Bull. Earthq. Res. Inst. Univ. Tokyo,* vol. 48, p. 1011–1021.

BERSENEV, A.F., GAINANOV, A.G., KOVYLIN, V.M. and STROEV, P.A. (1970) Structure of the earth's crust and upper mantle of the Japanese Sea and the zone of the Pacific Ocean adjoining Japan. In *Problems of Structure of the Earth's Crust and Upper Mantle,* Nauk, Moscow, p. 50–61 (translated from Russian to Japanese, Nihonkai (Japan Sea), no. 6, p. 53–61).

——— and LELIKOV, E.P. (1979) Geological map of the Japan Sea. *Priroda,* vol., p. 74–79 (in Russian, translated by KASENO, Y. and KUWANO, Y., 1980, Bull. Japan Sea Res. Inst., Kanazawa Univ., no. 12, p. 97–103.).

BIKKENIA, S.K., ZHILTSOV, E.G., LIVSHITZ, M. KH., NIKONOVA, N.A., SUVOROV, A,A. and TRESKOVA, YU.A. (1968) Deep seismic soundings in the vicinity of Sakhalin. *The Crust and Upper Mantle of the Pacific Area. Geophys. Monogr. Ser.,* vol. 12, p. 349–366.

CARLSON, R.L. and MELIA, P.J. (1984) Subduction hinge migration. *Tectonophys.,* vol. 102, p. 399–411.

CHAPMAN, M.E. and SOLOMON, S.C. (1976) North–American–Eurasian plate boundary in northeast Asia. *J. Geophys. Res.,* vol. 81, p. 921–930.

CROUGH, S.T. (1983) The correction for sediment loading on the seafloor. *J. Geophys. Res.,* vol. 88, p. 6449–6454.

DAVIS, E.E. and LISTER, C.R.B. (1977) Heat flow measured over the Juan de Fuca Ridge : Evidence for widespread hydrothermal circulation in a highly heat transportive crust. *J. Geophys. Res.,* vol. 82, p. 4845–4860.

DEWEY, J.F. (1980) Episodicity, sequence and style at convergent plate boundaries. *Geol. Soc. Canada Special Paper,* vol. 20, p. 553–573.

DINGLE, R.V. and SCHURUTTON, R.A. (1977) Continental margin fault pattern mapped southwest of Ireland. *Nature,* vol. 268, p. 720–722.

ENGEBRETSON, D.C. and COX, A. (1984) Relative motions between oceanic plates of the Pacific Basin. *J. Geophys. Res.,* vol. 89, p. 10291–10310.

FUJITA, K. and WATSON, B.F. (1983) Tectonic evolution of Kamchatka and adjacent regions. *EOS Trans. AGU,* vol. 64, p. 871.

FUKAO, Y. and FURUMOTO, M. (1975) Mechanism of large earthquakes along the eastern margin of the Japan Sea. *Tectonophys.,* vol. 25, p. 247–266.

——— and YAMAOKA, K. (1983) Stress estimate for the highest mountain system in Japan. *Tectonics,* vol. 2, p. 453–471.

GNIBIDENKO, H. (1979) The tectonics of the Japan Sea. *Marine Geol.,* vol. 32, p. 71–87.

HAYES, D.E. (1983) Global studies of ocean crustal depth–age relationships. *EOS Trans. AGU,* vol. 64, p. 760.

HEGARTY, K.A., WEISSEL, J.K. and HAYES, D.E. (1982) Convergence at the Caroline–Pacific plate boundary : collision and subduction. In *The Tectonic and Geologic Evolution of Southeast Asian Seas and Islands Part 2. AGU Geophys Monogr Ser.,* edited by D.E. HAYES, AGU, Washington, D.C.,vol. 27, p. 326–348.

HILDE, T.W.C. and WAGEMAN, J.M. (1973) Structure and origin of the Japan Sea. In *The Western Pacific,* edited by P.J. COLEMAN, Univ. Western Australia Press, p. 415–434.

HONZA, E. ed. (1978 a) Geological Investigation in the Northern Margin of the Okinawa Trough and the Western Margin of the Japan Sea. *Geol. Surv. Japan*

Cruise Rept., vol. 10, p. 79.

HONZA, E. ed. (1978 b) Geological Investigation of the Okhotsk and Japan Seas off Hokkaido. *Geol. Surv. Japan Cruise Rept.*, no. 11, p. 72.

——— ed. (1979) Geological Investigation of the Japan Sea. *Geol. Surv. Japan Cruise Rept.*, no. 13, p. 99.

——— (1979) Sediments, structure and origin of Japan Sea -concluding remarks-. In *Geological Investigation of the Japan Sea,* edited by E. HONZA, Geol. Surv. Japan Cruise Rept., no. 13, p. 89–93.

——— (1983) Central Japan Sea earthquake and submarine faults. *Kagaku (Science)*, vol. 53, p. 510–514 (in Japanese).

———, KAGAMI, H. and NASU, N. (1977) Neogene geological history of the Tohoku arc system. *J. Oceanographical Soc. Japan,* vol. 33, p. 297–310.

———, TAMAKI, K. and NISHIMURA, K. (1978) Sono-buoy refraction measurement. In *Geological Investigation of the Okhotsk and Japan Seas off Hokkaido,* edited by E. HONZA, Geol. Surv. Japan Cruise Rept., no. 11, p. 46–49.

———, ———, YUASA, M. and MURAKAMI, F. (1979) Geological map of the southern Japan Sea and Tsushima Straits. *Marine Geol. Map Ser.*, no. 13, Geol. Surv. Japan.

HOSHINO, M. and HONMA, H. (1966) Geology of submarine banks in the Japan Sea. *Chikyu Kagaku,* vol. 82, p. 10–16 (in Japanese with English abstract).

HOTTA, H. (1967) The structure of sedimentary layer in the Japan Sea. *Geophys. Bull. Hokkaido Univ.*, vol. 18, p. 111–131.

——— (1971) Sediment distribution in the continental borderland off Japanese Islands. In *Island Arc and Marginal Seas,* edited by S. ASANO and G.B. UDINTSEV, Tokai University Press, p. 147–153 (in Japanese with English abstract).

HUSSONG, D.M. and FRYER, D. (1982) Structure and Tectonics of the Mariana arc and fore-arc: drilling selection surveys. In *Initial Reports of the Deep Sea Drilling Project,* edited by D.M. HUSSONG and S. UYEDA, *et al.*, U.S. Govt. Printing Office, Washington, D.C., vol. 60, p. 33–44.

——— and UYEDA, S. (1982) Tectonic process and the history of the Mariana Arc: a synthesis of the results of Deep Sea Drilling Project Leg 60. In *Initial Reports of the Deep Sea Drilling Project,* edited by D.M. HUSSONG, and S. UYEDA, *et al.*, U.S. Government Printing Office, Washington D.C., vol. 60, p. 909–929.

ICHIKAWA, M. (1971) Reanalysis of mechanism of earthquakes which occurred in and near Japan, and statistical studies on the nodal plane solutions obtained, 1929–1968. *Geophys. Mag.*, vol. 35, p. 207–273.

INOUE, E. (1982) Geological problems on Cretaceous and Tertiary rocks in and around Tsushima-Korea straits. *CCOP Technical Bull.*, vol. 15, p. 85–121.

——— and HONZA, E. (1982) Marine Geological Map around Japanese Islands. Marine Geol. Map. Ser., no. 23, Geol. Surv. Japan.

ISEZAKI, N. (1975) Possible spreading centers in the Japan Sea. *Marine Geophys. Res.*, vol. 2, p. 265–277.

——— (1979) On the age of opening of the Japan Basin inferred from the magnetic lineations. *Nihonkai (Japan Sea),* vol. 19, p. 111–119 (in Japanese).

——— and UYEDA, S, (1973) Geomagnetic anomaly pattern of the Japan Sea. *Marine Geophys. Res.*, vol. 2, p. 51–59.

ISHIHARA, T. (1983) Gravity field around Japan-sea gravimetry by the geological survey of Japan. *Marine Geodesy.*, vol. 7, p. 227–256.

ISHIKAWA, Y,, TAKEO, M., HAMADA, N., KATSUMATA, M., SATAKE, K., ABE, K., KIKUCHI, M,, SUDŌ, K., TAKAHASHI, M., KASHIWABARA, S. and MIKAMI, N. (1984) Mechanism of the Central Japan Sea Earthquake, 1983. *Chikyu (The Earth Monthly)*, vol. 6, p. 11–17 (in Japanese).

ISHIWADA, Y. and OGAWA, K. (1976) Petroleum geology of offshore areas around the Japanese Islands. *CCOP Technical Bulletin,* vol. 10, p. 23–34.

———, HONZA, E. and TAMAKI, K. (1984) Sedimentary Basins of the Japan Sea. *Proc. 27th Intern. Geol. Congr.,* vol. 23, p. 43–65.

IVANOV, V.V., PUCHAROVSKIY, YU.M. and TIL'MAN, S.M. (1981) Tectonic position and structure of sedimentary basins on the northwestern margin of the Pacific Ocean. *Geotectonics,* vol. 15, p. 291–298 (translated in English from Russian).

IWABUCHI, Y. (1968) Submarine geology of the southeastern part of the Japan Sea. *Tohoku Univ. Inst. Geology and Paleontology Contr.,* vol. 66, p. 1–76 (in Japanese).

KARIG, D.E. (1971) Origin and development of marginal basins in the western Pacific. *J. Geophys. Res.,* vol. 84, p. 6796–6802.

——— and SHARMAN III, G.F. (1975) Subduction and accretion in trenches. *Geol. Soc. America Bull.,* vol. 86, p. 377–389.

——— and INGLE Jr., J.C.M. eds. (1975) *Initial Reports of the Deep Sea Drilling Project,* U.S. Govt. Printing Office, Washington, D.C., vol. 31, p. 927.

KATSURA, T. and KITAHARA, S. (1977) Geological structure of the marginal plateau off Tottori, south-west of Honshu, Japan. *J. Oceanograph. Soc. Japan,* vol. 33, p. 259–266.

KELLER, G. (1980) Benthic foraminifers and paleobathymetry of the Japan Trench area, Leg. 57, Deep Sea Drilling Project. In *Initial Reports of the Deep Sea Drilling Project,* edited by Scientific Party, U.S. Govt. Printing Office, Washington, D.C., vol. 56, p. 835–865.

KIMURA, G., MIYASHITA, S. and MIYASAKA, S. (1983) Collision tectonics in Hokkaido and Sakhalin. In *Accretion Tectonics in the Circum-Pacific Regions,* edited by M. HASHIMOTO and S. UYEDA, Terra Pub., Tokyo, p. 69–88.

——— and TAMAKI, K. (1985) Tectonic framework of the Kuril Arc since its initiation. In *Formation of Active Ocean Margins,* edited by N. NASU *et al.*, Terra Pub., Tokyo, p. 641–676.

——— and ———(1986) Collision, rotation, and back-arc spreading: the case of the Okhotsk and Japan Seas. *Tectonics,* vol. 5, p. 389–401.

KLEIN, G. deV. and KOBAYASHI, K. (1980) Geological summary of the north Philippine Sea, based on Deep Sea Drilling Project Leg 58 results. In *Initial Reports of the Deep Sea Drilling Project,* edited by G. deV. KLEIN, K. KOBAYASHI, *et al.*, U.S. Government Printing Office, Washington, D.C., vol. 58, p. 951–961.

KOBAYASHI, K. (1983) Spreading of the Sea of Japan and drift of Japanese Island Arc: A synthesis and speculation. In *Island Arcs, Marginal Seas, and Kuroko Deposits, Mining Geology Special Issue,* edited by E. HORIKOSHI, The Society of Mining Geologists of Japan, Tokyo, vol. 11, p. 23–36 (in Japanese with English abstract).

——— (1984) Subsidence of the Shikoku back-arc basin. *Tectonophys.,* vol. 102, p. 105–117.

——— (1985) Sea of Japan and Okinawa Trough. In *The Ocean Basins and Margins,* edited by A.E.M. NAIRN, F.S. STEHLI, and S. UYEDA, vol. 7 A, p. 419–458.

——— and NOMURA, M. (1972) Iron sulfide in

the sediments cores from the Sea of Japan and their geophysical implications. *Earth Planet. Sci. Lett.*, vol. 16, p. 200–206.

KOBAYASHI, Y. (1983) Initiation of "subduction" of plates. *Chikyu (The Earth Monthly)*, vol. 3, p. 510–518 (in Japanese).

KOIZUMI, I. (1979) The geological history of the Sea of Japan –based upon sediments and microfossils–. *Nihonkai (Japan Sea)*, vol. 10, p. 69–90 (in Japanese).

KONO, Y. and AMANO, M. (1977) Thickening plate model with sedimentation. *J. Seismol. Soc. Japan*, vol. 30, p. 163–178 (in Japanese with English Abstract).

LELIKOV, Ye.P. and BERSENEV, I.I. (1973) Early Proterozoic gneiss–magmatite complex in the southwestern part of the Sea of Japan. *Doklady Akad. Nauk SSSR*, vol. 223, p. 74–76. (translated in English from Russian).

LUDWIG, W.J., HAYES, D.E. and EWING, J.I. (1967) The Manila Trench and West Luzon Trough, 1, bathymetry and sediment distribution. *Deep Sea Res.*, vol. 14, p. 533–544.

———, MURAUCHI, S. and HOUTZ, R.E. (1975) Sediments and structure of the Japan Sea. *Geol. Soc. Am. Bull.*, vol. 86, p. 651–664.

Maritime Safety Agency of Japan (1980 a) Bathymetric map of Hokkaido, 1 : 1,000,000, no. 6311.

Maritime Safety Agency of Japan (1980 b) Bathymetric map of north–east Japan, 1 : 1,000,000, no. 6312.

MARKOV, M.S., PUSHCHAROVSKIY, Yu.M., TIL'MAN, S.M., FEDOROVSKIY, V.S. and SHILO, N.A. (1979) Tectonics of East Asia and Far Eastern Seas. *Geotectonics*, vol. 13, p. 1–11 (translated in English from Russian).

MELANKOLINA, YE.N. and KOVYLIN, V.M. (1977) Tectonics of the Japan Sea. *Geotectonics*, vol. 10, p. 273–281 (translated in English from Russian).

MINAMI, A. (1979) Distribution and characteristics of the sedimentary basin offshore San–in to Tsushima strait. *J. Japanese Assoc. Petrol. Technologists*, vol. 44, p. 407–414 (in Japanese with English abstract).

MINSTER, J.B. and JORDAN, T.H. (1978) Present–day plate motions. *J. Geophys. Res.*, vol. 83, p. 5331–5354.

MOLNAR, P. and ATWATER, T. (1978) Interarc spreading and Cordilleran tectonics as alternates as related to the age of subducted oceanic lithosphere. *Earth Planet. Sci. Lett.*, vol. 41, p. 330–340.

——— and QUIDONG, D. (1984) Faulting associated with large earthquakes and the average rate of deformation in Central and Eastern Asia. *J. Geophys. Res.*, vol. 89, p. 6203–6228.

——— and TAPPONNIER, P. (1975) Cenozoic tectonics of Asia : effects of a continental collision. *Science*, vol. 189, p. 419–426.

MONTADERT, L., ROBERTS, D.G., AUFFRET, G.A., BOCK, W., DUPEUBLE, P.A., HAILWOOD, E.A., HARRISON, W., KAGAMI, H., LUMSDEN, D.N., MULLER, C., SCHNITKER, D,, THOMPSON, R.W., THOMPSON, T.L. and TIMOFEEV, P.P. (1977) Rifting and subsidence on passive continental margins in the North East Atlantic. *Nature*, vol. 268, p. 305–309.

MOROZOWSKI, C.L. and HAYES, E.H. (1978) Sediment isopachs. In *A Geophysical Atlas of the East and Southeast Asian Seas*, edited by HAYES, E., Geol. Soc. Amer., vol. MC–25.

MURAUCHI, S. (1972) Crustal structure of the Japan Sea. *Kagaku (Science)*, vol. 38, p. 367–375 (in Japanese).

———, ASANUMA, T. and HAGIWARA, K. (1970) Geological studies on the area, off San'in district in the Japan Sea by means of seismic profiler. *Bull. Nat.*

Sci. Museum. vol. 13, p. 83–93 (in Japanese with English abstract).

NAKAMURA, K. (1983) Possible nascent trench along the eastern Japan Sea as the convergent boundary between Eurasian and North American Plates. *Bull. Earthq. Res. Inst. Univ. Tokyo,* vol. 58, p. 711–722 (in Japanese with English abstract).

NIINO, H. (1933) On the bottom materials of the Yamato Bank in the Japan Sea. *J. Geol. Soc. Japan,* vol. 40, p. 86–100 (in Japanese).

——— (1935) On the newly discovered bottom materials of the "Kita-Yamato Bank". *J. Geol. Soc. Japan,* vol. 42, p. 676–684 (in Japanese).

——— (1942) Bottom materials of the Oki Bank in the Japan Sea. *J. Geol. Soc. Japan,* vol. 49, p. 232–233 (in Japanese).

OTOFUJI, Y. and MATSUDA, T. (1983) Paleomagnetic evidence for the clockwise rotation of Southwest Japan. *Earth Planet. Sci. Lett.,* vol. 62, p. 349–359.

OZIMA, M., KANEOKA, I. and UENO, N. (1972) Spreading Japan Sea ?. *Kagaku (Science),* vol. 42, p. 350–352 (in Japanese).

PARSONS, B. and SCLATER, J.G. (1977) An analysis of the variation of ocean floor bathymetry and heat flow with age. *J. Geophys. Res.,* vol. 82, p. 803–827.

RODNIKOV, A.G. and KHAIN, V.B. (1971) On the trend in evolution of the earth's crust in the north-western part of the Pacific mobile belt. In *Island Arc and Marginal Sea,* edited by S. ASANO and G.B. UDINTSEV, Tokai University Press, p. 65–76 (translated in Japanese with English abstract).

SAHNO, B.G. and VASILIEV, B.I. (1974) Basaltoids of the Japan Sea bottom. In *Problems of Geology and Geophysics of the Marginal Seas of the NW Pacific,* edited by N.P. BASILKOVSKY and B.Ya. KARP, Far East Sci., p. 52–55 (in Russian).

SAKURAI, M. and SATO, T. (1971) Submarine geological structures and history of the Mogami Trough. *J. Geol. Soc. Japan,* vol. 77, p. 489–496 (in Japanese with English abstract).

———, ———, TAGUCHI, H,, NAGANO, M. and UCHIDA, M. (1971) Submarine topography and geological structure of the continental shelf west of the Noto peninsula. *J. Geol. Soc. Japan,* vol. 77, p. 645–654 (in Japanese with English abstract).

———, ———, ———, ———, ——— and HAMAMOTO, F. (1972) Submarine geological structures and submarine canyons in the area north of Toyama Bay. *J. Geol. Soc. Japan,* vol. 78, p. 475–484 (in Japanese with English abstract).

SATAKE, T. and ABE, K. (1983) A fault model for the Niigata, Japan, earthquake of June 16, 1964. *J. Phys. Earth,* vol. 31, p. 217–223.

SATO, T. (1971) Sea bottom survey in westward of the Northeast Japan. *Chigaku Zasshi,* vol. 80, p. 285–301 (in Japanese with English abstract).

——— and ONO, K.(1964) The submarine geology off San'in district, southern Japan Sea. *J. Geol. Soc. Japan,* vol. 70, p. 434–445.

———, SAKURAI, M., TAGUCHI, H., NAGANO, M., UCHIDA, M. and OMORI, T. (1973) Submarine geology of the continental borderland west of Hokkaido. *Rept. Hydrograph. Res.,* no. 8, p. 1–49 (in Japanese with English abstract).

SAWAMURA, M. (1978 MS) Diatom analysis of the bottom sample data of GH 77-3 cruise.

SCLATER, J.G. (1972) Heat flow and elevation of the marginal basins of the western Pacific. *J. Geophys. Res.,* vol. 77, p. 5705–5719.

SENO, T. (1983) Age of subducting lithosphere

and back-arc tectonics : evolution of the western Pacific since the early Tertiary. *Abstracts. OJI international Seminar on the Formation of Ocean Margins,* p. 50.

SENO, T. and MARUYAMA, S. (1984) Paleogeographic reconstruction and origin of the Philippine Sea. *Tectonophys.,* vol. 102, p. 53–84.

SHIMAZU, M. (1968) Absolute age determination of granite in Yamato Bank. *Nihonkai (Japan Sea)*, p. 55–56.

——— (1979) "Green tuff" in the core from DSDP Leg 31 Site 302 : Kita-Yamato tai. *J. Geol. Soc. Japan,* vol. 85, p. 655–656.

SLEEP, N.H. and TOKSOZ, M.N. (1971) Evolution of marginal basins. *Nature,* vol. 33, p. 548–550.

STROYEV, P.A. (1971) Gravity anomalies in the Sea of Japan. *Doklady Akad. Nauk SSSR,* vol. 198, p. 18–21 (translated in Japanese with English abstract).

SUZUKI, U. (1979) Petroleum geology of the Sea of Japan, northern Honshu. *J. Japanese Assoc. Petrol. Technologists,* vol. 44, p. 291–307.

TAMAKI, K., HONZA, E., YUASA, M., NISHIMURA, K. and MURAKAMI, F. (1981 a) Geological map of the central Japan Sea. *Marine Geol. Map Ser.,* no. 15, Geol. Surv. Japan.

———, INOUCHI, Y., MURAKAMI, F. and HONZA, E. (1977) Continuous seismic reflection profiling survey. In *Geological Investigation of Japan and Southern Kurile Trench and Slope Areas,* edited by E. HONZA, Geol. Surv. Japan Cruise Rept., no. 7, p. 50–71.

———, INOUE, E., YUASA, M., TANAHASHI, M. and HONZA, E. (1981 b) Possible active back-arc spreading of the Bonin Arc. *Abstract of Symposium on "Geotectonics of Sagami Trough-Suruga Trough Junction Area" (First French-Japanese Symposium on Japanese Subduction Program). Jun. 04–05. 1981. Tokyo.*

TAMAKI, K. and MIYAZAKI, T. (1984) Rifting of the Bonin Arc. *Abstracts. for the International Symposium on Recent Crustal Movements of the Pacific Region. Feb. 1984,* p. 57.

———, MURAKAMI, F., NISHIMURA, K. and HONZA, E. (1979 b) Continuous seismic reflection profiling survey. In *Geological Investigation of the Japan Sea,* edited by E. HONZA, Geol. Surv. Japan Cruise Rept., no. 13, p. 48–51.

———, YUASA, M., NISHIMURA, K. and HONZA, E. (1979 a) Geological map of the Japan and Okhotsk Seas around Hokkaido. *Marine Geol. Map Ser.,* no. 14, Geol. Surv. Japan.

TANAKA, T. (1979) Distribution and nature of the sedimentary basins off Hokuriku and San-in, Japan. *J. Japanese Assoc. Petrol. Technologists,* vol. 44, p. 308–320 (in Japanese with English abstract).

——— and OGUSA, K. (1981) Structural movement since middle Miocene in the Offshore San-in sedimentary basin, the Sea of Japan. *J. Geol. Soc. Japan,* vol. 87, p. 725–736 (in Japanese with English abstract).

TAPPONNIER, P., PELTZER, G., LEDAIN, A.Y., ARMIJO, R. and COBBOLD, P. (1982) Propagating extrusion tectonics in Asia : new insights from simple experiments with plasticine. *Geology,* vol. 10, p. 611–616.

TAYLOR, B. and HAYES, D.E. (1980) The tectonic evolution of the South China Basin. In *The Tectonics and Geologic Evolution of Asian Seas and Islands. Geophys. Monogr. Ser.,* edited by D.E. HAYES, AGU, Washington, D.C., vol. 23, p. 89–104.

——— and ———(1983) Origin and history of the South China Sea Basin. In *The Tectonics and Geologic Evolution of Southeast Asian Seas and Islands Part 2. Geophys. Monogr. Ser.,* edited by

D.E. HAYES, AGU, Washington, D.C., vol. 27, p. 23–56.

TOMODA, Y. (1873) Maps of free air and Bouguer gravity anomalies in and around Japan. Tokyo Univ. Press.

——— and FUJIMOTO, H. (1981) Maps of gravity anomalies and bottom topography in the western Pacific and reference book for gravity and bathymetric data. *Bull. Ocean. Res. Inst.*, p. 1–158.

TOZAKI, T., KATO, S. and KITAHARA, S. (1978) Submarine geology off San-in. *Rept. Hydrograph. Res.*, p. 1–36 (in Japanese with English abstract).

TSUYA, H. (1932) On some pebbles collected from the floor of the Japan Sea. *Bull. Earthq. Res. Inst. Tokyo Imp. Univ.*, vol. 40, p. 864–875.

TUEZOV, I.K. (1969) Geophysical study of far eastern part of the circum Pacific. *Bull. Sakhalin Complex Science Institute,* vol. 20, p. 5–26.

——— (1971) Crustal structure of the Okhotsk and Japanese area from regional seismic prospecting data. In *Island Arc and Marginal Sea,* edited by S. ASANO and G.B. UDINTSEV, Tokai Univ. Press, p. 121–135.

UENO, N., KANEOKA, J., OZIMA, M., ZASHU, S., SATO, T. and IWABUCHI, Y. (1971) K-Ar age, Sr isotopic ratio and K/Rb ratio of the volcanic rocks dredged from the Japan Sea. In *Island arc and marginal sea,* edited by S. ASANO and G.B. UDINTSEV, Tokai Univ. Press, p. 305–309 (in Japanese).

UYEDA, S. and KANAMORI, H. (1979) Back-arc opening and the mode of subduction. *J. Geophys. Res.*, vol. 84, p. 1049–1062.

——— and VAQUIER, V. (1968) Geothermal and geomagnetic data in and around the island of Japan, in the crust and upper mantle of the Pacific area. In *The crust and upper mantle of the Pacific area. Geophys. Monogr. Ser.*, edited by L. KNOPOFF *et al.*, AGU, Washington, D.C., vol. 12, p. 349–366.

VASILIEV, B.I. (1975) New data on age and mechanism of formation of marginal-sea basins and deep-sea trenches in the northwestern Pacific. *Doklady Akad. Nauk USSR,* vol. 225, p. 60–62.

von HUENE, R., LANGSETH, M., NASU, N. and OKADA, H. (1980) Summary, Japan Trench transect. In *Initial Reports of the Deep Sea Drilling Project,* edited by Scientific Party, U.S. Govt. Printing Office, Washington, D.C., vol. 56–57, p. 473–503.

YASUI, M., KISHII, T., WATANABE, T. and UYEDA, S. (1967) Studies of the thermal state of the earth, the 18th paper; terrestrial heat flow in the Japan Sea (2). *Bull. Earthq. Res. Inst.*, vol. 44, p. 1501–1518.

YOSHII, T. (1972) Terrestrial heat flow and features of the upper mantle beneath the Pacific and Sea of Japan. *J. Phys. Earth,* vol. 20, p. 271–285.

———, KONO, Y. and ITO, K. (1976) Thickening of the oceanic lithosphere. In *The Geophysics of the Pacific Ocean Basin and Its Margins. Geophys. Monogr. Ser.*, edited by G.H. SUTTON *et al.*, AGU, Washington, D.C., vol. 19, p. 423–430.

——— and YAMANO, M. (1983) Digital heat flow data file around Japanese Islands.

YUASA, M., KANAYA, H. and TERASHIMA, S. (1979) Rocks and sediments. In *Geological Investigation of the Japan Sea,* edited by E. HONZA, Geol. Surv. Japan Cruise Rept., no. 13, p. 54–60.

———, TAMAKI, K., NISHIMURA, K. and HONZA, E. (1978) Welded tuff dredged from Musashi Bank, northern Japan Sea and its K-Ar age. *J. Geol. Soc. Japan,* vol. 84, p. 375–377.

ZONENSHAIN, L.P. and SAVOSTIN, L.A. (1981) Geodynamics of the Baikal rift zone and plate tectonics of Asia. *Tectonophys.*, vol. 76, p. 1–45.

日本海の海底地質構造とテクトニクス

玉 木 賢 策

要 旨

西太平洋に発達する多くの縁海の一つである日本海のテクトニクスは日本列島のテクトニクスと密接な関係を有しており，日本海の正しい理解は日本列島のテクトニクスの研究にとって不可欠である．縁海のテクトニクスにおいて最も重要なその形成時期は，地磁気縞状異常の年代同定と，深海掘削による基盤岩層の年代決定により求められるが，残念ながら，日本海では地磁気縞状異常の発達は微弱かつ複雑で既存のデータでは年代同定は困難であり，また DSDP による深海掘削も基盤岩まで達していない．このため他の西太平洋の大部分の縁海の形成時期が確定しているにもかかわらず，日本海の形成時期については，新第三紀から白亜紀までの多くの意見に分かれ，まだ定説といえるものはなく，日本列島周辺のテクトニクス研究において大きな足かせとなっている．

本研究は，1977 年から 1978 年にかけて地質調査所によって行われた，日本海においては初めての広域的かつ系統的海洋地質・地球物理調査データと過去に数多くなされている日本海の調査研究結果を統合することにより，日本海の海底地質層序構造を検討し，その結果にもとづいて日本海の海盆部と海膨，海嶺，海山部の形成，および，現在のテクトニクスについて論じたものである．海底地質層序構造は音波探査記録の解析と海底サンプリング結果の対比により検討された．従来，日本海のテクトニクスは周辺陸域の地質との関連で論じられることが多かったが，本研究では全面的に海域のデータにもとづいて議論しているのが特徴である．

日本海には大陸側の日本海盆，タータリー舟状海盆と，日本列島側の大和海盆，対馬海盆の 4 つの大きな海盆が存在し，それぞれに特徴を有する．日本海盆では堆積層の厚さは 2500 m 程度，音響的基盤の深度は 6000 m 程度である．一方，大和海盆は堆積層の最大層厚 1500 m，音響的基盤深度 4000 m 程度で，日本海盆とは大きく異なる．基盤深度の差異は，日本海盆の音響的基盤が大洋性玄武岩層と一致するのに比べて，大和海盆の音響的基盤はグリーンタフ層に対比される火山性砕屑物に相当し，真の大洋性玄武岩層はさらに下位にあることにより生じるものと解釈される．日本海盆と大和海盆の地殻熱流量の平均値はそれぞれ 2.3 HFU 前後で，このことは両海盆がほぼ同等の生成年代を有することを意味する．日本海盆の基盤深度，地殻熱流量と，大和海盆の地殻熱流量をそれぞれ検討すると，日本海盆の生成年代は 30～15 Ma，大和海盆の生成年代は 30～10 Ma 程度と推定される．タータリー舟状海盆，対馬海盆も同様の検討をすると，その生成年代はやはり 30～10 Ma の間に入るものと考えられる．

日本海の海嶺，海山，堆などの地形的高まりはその成因からみて次の 4 つのグループに分けられる．

1. 大陸地殻の断片よりなるグループ

   海底拡大による日本海の形成の際，海洋地殻中に取り込まれてしまった大陸地殻の断片で，大和堆，隠岐堆，北隠岐堆，隠岐海嶺，朝鮮海台，武蔵堆が主な例である．このグループの基盤岩の地質は中生代以前のものより構成され，古いものではプレカンブリアンのものも含まれる．このグループは岩相によってさらに細分され，火山性のもの，深成岩性のもの，堆積岩性のものがある．これらの地形的高まりは，その形成以降沈降運動を行っており，これは周辺海洋地殻の年代経過にともない沈降したものと考えられる．

2. 断裂化した大陸地殻の断片

   日本海の形成初期に大陸地殻の間に起こった断裂運動が海洋底拡大活動に発達する前に中絶したため生じた，半陸・半海洋的な地殻よりなる高まりで，水深の深いのが特徴である．佐渡海膨，北海道西方の大陸斜面部がこの例と考えられる．

3. 構造性海嶺群

富山トラフより北海道西方まで南北に発達する佐渡海嶺，奥尻海嶺よりなる．これらの海嶺群は，鮮新世後期以降の日本海の東西性収縮テクトニクスによってスラストアップすることにより形成されたものである．

4. 火山性の海山，堆群

大和海盆の中の海山列などの，海底拡大活動と同時期の海底火山群，および，ウツリョウ島，竹島などの，島弧火成活動によるアルカリ玄武岩性の海山とからなる．

以上のような日本海の海底地質構造の特徴と，マリアナ弧のマリアナトラフ，小笠原弧の背弧凹地などの活動的背弧海盆の拡大テクトニクスとの比較検討を行うと，日本海は，単一リフト系によって生成されたマリアナ-小笠原弧の背弧海盆とは異なり，多重リフト系から生成されてきたものと考えることができる．多重リフト系は，そもそも緩傾斜でスラブがもぐり込みにより形成された巾の広い島弧火山帯が巨大な引張応力場のもとにおかれたため，島弧における弱線としての島弧火山帯上にリフトが並列して多数発生して生じたものと推定される．このような多重リフト系から多重の海底拡大系が生じ，これによって多くの大陸地殻の断片が海洋性地殻中にとりこまれたものであろう．さらに，リフト群の中で海底拡大系にまで発達するものはわずかで，多くのリフトは未発達のまま活動を停止し，断裂化した地殻の断片を形成するであろう．活動を停止したリフトの典型的な例が大和海嶺中の北大和トラフである．また，緩い傾斜のもぐり込みによって生じた巾の広い島弧火山帯は海底拡大活動と複合され，巨大な引張応力場のもとで活発な火山活動を行い，海洋性地殻上に多くの海山や，グリーンタフのような厚い火山性砕屑物を生ぜしめることになるものと考えられる．

上記のようなテクトニクスを発生させるには大きな引張応力場が必要であるが，このような引張応力は大陸の島弧からの後退によってのみ可能であろう．日本海の後背のユーラシアプレートの動きは新生代を通じてほぼ不動であるかわずかに東方へ移動している程度であり，日本海の形成時期に後退した様子はない．しかし，40 Ma 前に起こったインド亜大陸のユーラシアプレートへの衝突は，その後，東アジア内に大規模なプレート内変形あるいはマイクロプレート化をもたらしており，日本海後背大陸の後退はそのようなマイクロプレートの動きによって説明可能であるかも知れない．

日本海東縁部の海陸境界部の地形は複雑な様相を呈し，大陸側の単純な大陸斜面とは対照的である．この複雑な地形は一連の海嶺・海盆群により構成されており，富山湾より北方にのみ見られ，西南日本の日本海側には見られない．海嶺群は男鹿半島より北方の NS 系の走向を持つ奥尻海嶺と，南方の NNE-SSW 系の走向を有する佐渡海嶺からなる．この海嶺・海盆群が鮮新世後期以降（約 3 Ma～）に形成されており，その運動が現在も継続中であることが鮮新世堆積層の変形からわかる．すなわち，海嶺群は鮮新世堆積層堆積中あるいは堆積後に，その堆積層を持ち上げ上昇することによって形成され，その東方にそれ以降の新しい堆積層がトラップされて海盆群が発達している．これらの隆起構造は，プレート収れん域に見られるスラスト性隆起構造と同様のものであり，鮮新世後期以降日本海東縁部が東西性の圧縮応力場におかれていることを示す．日本海東縁部に発生するスラスト性地震と海底断層の関係を検討すると，このような圧縮応力は，日本海東縁部においてリソスフェア間の収束をもたらしていることがわかる．バイカルリフトにおける東西系の引張力が鮮新世以降活発化していることを考えると，このような収束運動もまた，インド亜大陸のユーラシアプレートへの衝突に起因する，アムリアンマイクロプレートの東方移動の結果として説明できる．

以上の考察にもとづき日本海の主なテクトニクスをまとめると，次の 2 つのイベントに分けることができる．

1. 30 Ma から 10 Ma にかけて多重リフトから発達した背弧拡大活動による日本海盆，大和海盆，対馬海盆，タータリー舟状海盆などの海盆群の形成．それにともなう大和海嶺，朝鮮海台，北隠岐堆，隠岐海嶺，ボゴロフ海山などの大陸地殻の断片よりなる堆・海嶺群の形成．さらに，拡大中の背弧海盆内における活発な島弧火成活動による厚い火山性砕屑物の堆積，および海山群の形成．
2. 3～2 Ma 以降現在までに至る日本海東縁部における東西性圧縮テクトニクス．それにともなう奥

尻海嶺，佐渡海嶺のスラストアップによる形成，および，その東方の後志海盆，奥尻海盆，西津軽海盆，最上海盆のトラップによる形成.

以上の日本海形成以降のテクトニクスには，40 Ma 以降現在まで続いているインド亜大陸のユーラシアプレートへの衝突によって引き起こされた，東アジア付加テレーン群の再配列にともなうユーラシアプレート内の変形運動が大きく寄与しているものと考えられる.

（受付：1985 年 11 月 16 日；受理 1988 年 4 月 28 日）